UNIVERSIDAD AUTONOMA DE MADRID

Facultad de Ciencias

Departamento de Biología Molecular

Epigenetic mechanisms involved in neuronal *Bdnf* gene expression in adult and aged mouse in response to cognitive stimulation

Tesis Doctoral

Ernest Palomer Vila

Madrid 2016

UNIVERSIDAD AUTONOMA DE MADRID

Facultad de Ciencias

Departamento de Biología Molecular

Epigenetic mechanisms involved in neuronal *Bdnf* gene expression in adult and aged mouse in response to cognitive stimulation

Tesis Doctoral

Ernest Palomer Vila

Madrid 2016

La realización de esta tesis doctoral ha sido posible gracias a la concesión de una Ayuda de Formación de Personal Investigador (FPI) del Ministerio de Ciencia e Innovación y el Ministerio de Economía y Competitividad. Su desarrollo ha tenido lugar en el laboratorio del Dr. Carlos G Dotti, en el Centro de Biología Molecular “Severo Ochoa” (CBMSO), centro mixto del Consejo Superior de Investigaciones Científicas (CSIC) y la Universidad Autónoma de Madrid (UAM).

El Dr. Carlos G. Dotti, profesor de investigación del CSIC y el Dr. Mauricio G. Martí, Investigador Adjunto Consejo Nacional de Investigaciones Científicas y Técnicas (CONICET), co-directrores de esta Tesis Doctoral, hacen constar:

Que el trabajo descrito en la presente memoria, titulado “Epigenetic mechanisms involved in neuronal *Bdnf* gene expression in adult and aged mouse in response to cognitive stimulation” ha sido realizado por Ernest Palomer Vila bajo su dirección y supervisión, dentro del programa de Doctorado en Biociencias Moleculares del Departamento de Biología Molecular de la Universidad Autónoma de Madrid.

Por reunir los requisitos de rigor científico, innovación y correcta aplicación metodológica, dan su Visto Bueno a la presentación de dicha Tesis Doctoral.

Carlos G. Dotti

Mauricio G. Martín

Madrid, a 21 de Diciembre de 2015

PRESENTACIÓN

En Septiembre de 2011 me incorporé al laboratorio del Dr. Carlos G. Dotti para desarrollar parte de su Plan Nacional titulado “Dysfunctional mechanisms in the aged brain”. En concreto me propusieron estudiar la regulación epigenética de genes de memoria en respuesta a estímulos nerviosos, tanto en el cerebro adulto como en el viejo. En este trabajo de Tesis nos propusimos caracterizar los mecanismos epigenéticos que controlan la transcripción de *Bdnf* en respuesta a LTD, y la posible relación de éstos con los déficits de aprendizaje y memoria que ocurren en el envejecimiento.

La regulación transcripcional de los genes de memoria de expresión temprana es un proceso esencial para la función cerebral, estando involucrada, entre otros procesos, en plasticidad sináptica, particularmente para mantener las fases tardías de la potenciación a largo plazo (LTP) y la depresión a largo plazo (LTD) ha sido descrita ampliamente. Trabajos realizados en animales sujetos a diferentes paradigmas de memoria han mostrado que existen mecanismos epigenéticos involucrados en la regulación de genesde memoria. Sin embargo poco se conoce sobre la contribución de los mecanismos epigenéticos en la expresión de estos genes en respuesta a estímulos puntuales, tanto en el cerebro adulto como en el viejo. En esta tesis describimos cómo la LTD, desencadenada por adición de bajas dosis de NMDA, induce la transcripción del gen *Bdnf* a partir de sus promotores I, II, IV y VI, mediante la desmetilación de H3K27Me3 y la fosforilación de H3K27Me3 en la Serina 28, que a su vez conlleva al desplazamiento de EZH2, la subunidad catalítica del Complejo Represor de Polycomb 2. La LTD no solo induce el desplazamiento de EZH2, sino también de otra enzima represora, la histona deacetilasa 4 (HDAC4), al tiempo que estimula la acetilación de H3K27 *via* pCREB/CBP. A diferencia de la situación descrita, típica del cerebro adulto, presentamos datos que muestran la alteración de la transducción normal de los estímulos neuronales al núcleo en el hipocampo envejecido. Esta ateración lleva a un estado basal de la cromatina diferente en los promotores de *Bdnf* del ratón viejo, acompañado de una incapacidad de remadelar la cromaitna y la transcripción de *Bdnf* en respueta a LTD. Una característica fisiológica del envejecimiento es la perdida de colesterol de la membrana plasmática neuronal. De hecho, la adición de colesterol a rebanadas hipocampales envejecidos recupera la regulación epigénetica y la expresión de *Bdnf* en respuesta a LTD, mientras que la reducción de colesterol en rodajas de hipocampo de adultos jóvenes resulta en deficits similares a las encontradas en los animales viejos. Apoyando nuestra hipótesis de que la desregulación epigéntica observada en animales viejos deriva de la pérdida de colesterol, la administración oral de Voricionazol, un inhibidor del enzima responsable de la pérdida de colesterol cerebral (Cyp46A1), rescata la pérdida de colesterol en el hipocampo y mejora las capacidades cognitivas de animales viejos, restituyendo además la regulación epigenetica de *Bdnf* y su transcripción en respuesta a LTD. Estos resultados desvelan uno de los mecanismos involucrados en los déficits cognitivos asociados al envejecimiento, y proponen a Cyp46A1 como una posible diana teraputica valiosa.

ABSTRACT

Transcription of immediate early memory genes is an essential process in brain function, regulating, among other processes, synaptic plasticity. It is well established the necessity of gene transcription in order to maintain the late phases of the long-term potentiation (LTP) and the long-term depression (LTD). Several works performed in animals subjected to different memory paradigms have shown that there are epigenetic mechanisms involved in memory genes regulation. However, little is known about the contribution of these epigenetics mechanisms in response to a single stimulus, in the adult and in the old brain. The aim of this thesis was to characterise such mechanisms in response to LTD, in order to better understand the regulation of *Bdnf* gene expression, and its possible relation with the aged associated learning and memory deficits. In this thesis we present that LTD stimulation triggered by low NMDA dose in young adult animals, induces the transcription of *Bdnf* gene from promoters I, II, IV and VI by H3K27Me3 demethylation and H3K27Me3 phosphorylation at Serine 28, leading to displacement of EZH2, the catalytic subunit of Polycomb Repressor Complex 2. LTD not only does induce EZH2 repressor detachment, but also the dissociation of another transcriptionally repressive enzyme such as histone deacetylase 4 (HDAC4). We also show that LTD enhances acetylation of histone H3K27 via pCREB/CBP. Differently from the described situation, typical of the mature brain, we present data showing that the normal singling transduction of the young upon LTD is impaired in the aged hippocampus, leading to a different basal chromatin state at *Bdnf* promoters in the old. The consequence of this impairment is the loss of *Bdnf* induction in the old when exposed to LTD, as a result of impaired HDAC4 dissociation, CBP recruitment and Histone H3K27 acetylation at *Bdnf* promoters. We also have observed that the loss of cholesterol at the neuronal plasma membrane, a physiological feature of the old, plays a role in these epigenetic deficits. In fact, cholesterol addition to old hippocampal slices rescued *Bdnf* epigenetic regulation and expression in response to LTD. Furthermore, cholesterol reduction in young adult hippocampal slices led to similar deficits to the ones found in the old animals. In further support of the cholesterol loss-epigenetic dysregulation in the old, oral administration of Voriconazole, an inhibitor of the enzyme responsible for cerebral cholesterol loss (Cyp46A1), rescued hippocampal cholesterol loss and enhanced cognitive abilities in the old animals, improving *Bdnf* epigenetic regulation and expression in response to LTD. These results unveil one of the mechanisms involved in the cognitive decline of the old and propose Cyp46A1 as valuable therapeutic possibility.

INDEX

INDEX Pages

INDEX Pages

INDEX Pages

INDEX Pages

FIGURE INDEX:

INDEX Pages

ABBREVIATIONS

- AMPA: α-amino-3-hydroxy-5-methylisoxazole-4-propionic acid
- AMPAR: AMPA receptor
- AP: alkaline phosphatase
- AP2: clathrin adaptor protein
- BDNF: Brain derived neurotropic factor
- CaMKII: Ca^{2+} /calmodulin-dependent protein kinase II
- CBP: CREB-binding protein
- CCIIh: CREB /CBP Interaction Inhibitor
- CDYL: chromodomain Y-like protein
- Chem-LTD: chemical LTD
- ChIP: Chromatin immunoprecipitation
- CNS: Central nervous system
- COase: cholesterol oxidase enzyme
- CREB: cAMP response element-binding protein
- Cyp46A1: cholesterol 24 hydroxylase
- Cyp51: sterol-14a-demethylase
- DNMT: DNA methyltransferase
- ERK1/2extra- cellular signal-regulated kinase 1/2
- EZH1/2: Enhancer of zeste homolog-1/2
- GluN: NMDA glutamate subtunit
- GSK3: glycogen synthase kinase-3
- HAT: Histone Acetyltransferase
- HDAC: histone deacetylase
- HMT: histone methyletransferase
- H3K4Me3: Histone H3 trimethylated at Lys 4 (K4)
- H3K27Me3: Histone H3 trimethylated at Lys 27 (K27)
- H3K27Ac: Histone H3 acetylated at Lys 27 (K27)
- H3K27Me3S28p Histone H3 trimethylated at Lys 27 (K27) and phosphorylated at Ser 28 (S28)
- IEGs: Immediate early genes
- JMJ: jumonji C (JmjC)-domain-containgin
- JMJD3: JmjC Domain-Containing Protein 3
- JNK1/2: c-Jun N-terminal kinase 1/2
- KAR: kainate receptor
- KDM: Histone methyl-lysines demethylases
- LFS: low-frequency stimulation
- LTP: Long Term Potentiation

- LTD: Long Term Depression
- MßCD-Ch: cholesterol complexes with methyl-ß-cyclodextrin
- MBD: methyl-binding domain
- MeCP2: methyl-CpG-binding protein 2
- MECS: maximal electroconvulsive seizure
- MDBP: methyl-DNA binding proteins
- mGluR: metabotropic glutamate receptor
- Msk-1/2: mitogen- and stress-activated kinases 1/2
- NAD: nicotinamide-adenine-dinucleotide
- NFkB: Nuclear Factor kappa B
- NMDA: *N*-methyl-d-aspartate
- NMDAR: NMDA receptor
- NSF: *N*-ethylmaleimide-sensitive factor
- p38-MAPK p38: mitogen-activated protein kinase
- PHD: Plant homeodomain
- PI3K: phosphatidylinositol 3-kinase
- PKA: protein kinase A
- PKB/AKT: Protein Kinase B
- PKC: protein kinase C
- PLC-gamma: phospholipase C gamma
- PP1: protein phosphatase 1
- PP2A: protein phosphatase 2A
- PP2B: protein phosphatase 2B
- PRC: Polycomb repressive complexes
- RNApolII :RNA polymerase II
- RTFs: regulatory transcription factors
- RTT: Rett syndrome
- SIRT: sirtuin
- STDP: spike-timing dependent plasticity
- TEZ: transposon exclusion zones
- TRD: transcription regulatory domain
- TrkB: tropomyosin-related kinase B
- TSS: transcriptional start sites
- UTR: un-translated regions
- UTX: Ubiquitously Transcribed X Chromosome Tetratricopeptide Repeat Protein
- vmPFC: ventromedial prefrontal cortex
- VPA: valproic acid

INTRODUCTION

Activity-regulated gene transcription is an essential process in brain function, regulating the strength of brain cells' connections, survival capacity and plasticity (Ghosh et al., 1994; Mao et al., 1999). Among the latter, activity regulates the transcription of, for example, genes induced during long-term potentiation (LTP) and long-term depression (LTD), the electrical grounds for learning and memory (Ahn et al., 1999; Nguyen et al., 1994). Although the last few years have highlighted the importance of epigenetics in the regulation of gene expression in response to external stimuli, little is known about the epigenetic mechanisms regulating learning and memory genes in response to a specific stimulus. During this thesis I have analysed the epigenetic mechanisms regulating the expression of the learning and memory gene *Bdnf* in response to a canonical cognitive stimulus: the NMDA-induced long-term depression.

1.-Learning and Memory: synaptic plasticity:

Learning may be described as the mechanism by which new information about the environment is acquired, and memory as the mechanism by which that knowledge is retained. It is convenient to categorize memory as being explicit, which is defined as that involved in the conscious recall of information about people, places and things, or implicit, which is characterized by the non conscious recall of tasks such as motor skills. Explicit memory depends on the integrity of temporal lobe structures such as the hippocampus, subiculum, and entorhinal cortex. Implicit memory includes simple associative forms of memory, such as classical conditioning, and non-associative forms, such as habituation, relaying on the integrity of the cerebellum and basal ganglia (Squire, 1992).

Although several areas of the brain play a part in consolidation of several forms of learning/memory, the hippocampus has been recognized to be playing a vital role in the formation of declarative memory (Scoville and Milner, 1957). It is widely accepted that memory formation is dependent on changes in synaptic efficiency allowing different degree of associations between neurons; indeed, activity-dependent synaptic plasticity at appropriate synapses during memory formation is believed to be both necessary and sufficient for storage of information. Cajal originally hypothesized that information storage relies on changes in strength of synaptic connections between neurons that are active (Ramón y Cajal, 1909). Hebb supported this hypothesis and proposed that if two neurons are active at the same time, the synaptic efficiency of the appropriate synapse will be strengthened (Hebb, 1949). Now a day we know that not only synaptic strengthening is a form of synaptic plasticity, but also synaptic weakening is. Both processes are thought to be involved in information storage, and therefore in learning, memory and other physiological processes. The two major forms of long-lasting synaptic plasticity in the mammalian brain — long-term potentiation (LTP) and long-term depression (LTD) — are

characterized by a long-lasting increase or decrease in synaptic strength, respectively.

1.2.-Long term depression:

LTD is an activity-dependent reduction in the efficacy of a neuronal synapse, a process lasting hours, or longer, after a stimulus. LTD occurs in many areas of the central nervous system (CNS) with varying mechanisms depending upon brain region and developmental progress (Massey and Bashir, 2007). Typically, LTD has two phases; the early-phase in which the depotentiation of the synaptic strength takes place, and the late-phase, which is the maintenance of the depressed currents. The early-phase of LTD is independent of macromolecules synthesis, whereas the late-phase, to be maintained, requires RNA transcription and protein synthesis (Goelet et al., 1986; Manahan-Vaughan et al., 2000). LTD can be induced by prolonged periods of low-frequency stimulation (LFS), by pairing baseline synaptic stimulation with depolarization (known as pairing), by appropriately timed back-propagating action potentials (a form of spike-timing dependent plasticity or STDP), or by application of an appropriate receptor agonist (known as chemical LTD or chem-LTD). Most synapses that undergo LTD respond to the neurotransmitter L-glutamate. L-glutamate acts on *N*-methyl-d-aspartate (NMDA) receptors (NMDARs), α-amino-3-hydroxy-5-methylisoxazole-4-propionic acid (AMPA) receptors (AMPARs), kainate receptors (KARs) and metabotropic glutamate receptors (mGluRs) (Collingridge et al., 2009, 2010). Here I will focus on the NMDAR-dependent LTD.

1.2.1.- NMDA receptors-dependent LTD:

NMDA receptors are tetramers of various GluN subunits (Collingridge et al., 2009). Normally they are composed by two GluN1 and two GluN2 subunits, although sometimes GluN3 replaces GluN2. The two GluN2 subunits can be identical (GluN2A, GluN2B, GluN2C or GluN2D), forming a diheteromer, or they can be different from each other, forming a triheteromer together with two identical GluN1 subunits (Collingridge et al., 2004). During LTD, the activation of NMDA receptors occurs at many different synapses (Fujii et al., 1991). As commented above, NMDA receptor activation leading to LTD can be induced by LFS or chemically by the brief application of an agonist, i.e. low dose of NMDA (NMDA-LTD). Although in general LFS-induced LTD and NMDA-LTD use common mechanisms, some differences between the two have been described (Kameyama et al., 1998; Morishita et al., 2001). In any event, numerous evidences point out that LTD involves AMPA receptor removal from synapses (Collingridge et al., 2004). In the canonical view, upon the LTD stimulus Ca^{2+} enters through the NMDAR and binds calmodulin. This binding leads to the activation of protein phosphatase 2B (PP2B), which

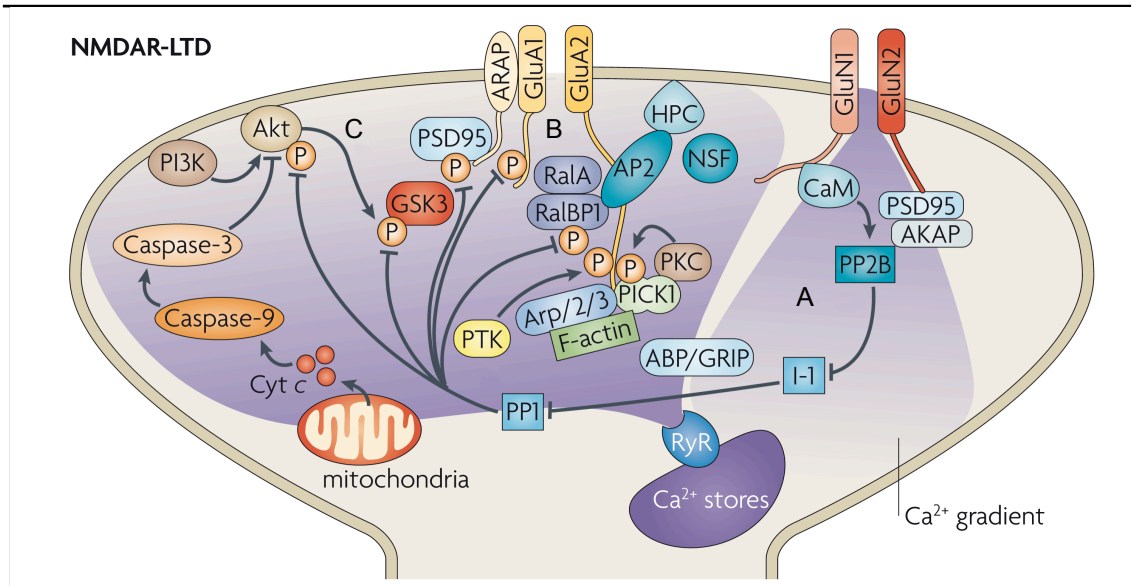

Figure I1: Signalling mechanisms involved in NMDAR-dependent LTD.
A) Calmodulin (CaM) detects Ca^{2+} that enters *via* NMDARs, leading to PP1 activation, which dephosphorylate various targets. B) GluA2-containing AMPARs are stabilised at synapses by *N*-ethylmaleimide-sensitive factor (NSF). When increase Ca^{2+} is sensed the adaptor protein 2 (AP2) is targeted to GluA2, displaceing NFS, and inictiateing the clatrin-mediated endocytosis of AMPARs. C) Glycogen synthase kinase-3β (GSK3β) is required for NMDAR-LTD during which it can be activated by PP1, and represde by Akt. AKAP, A-kinase anchor protein; ARAP, AMPAR-associated protein; I-1, inhibitor 1; PP2B, protein phosphatase 2B; RyR, ryanodine receptor. (Adapted from Collingridge et al. 2010)

dephosphorylates inhibitor-1, leading to the activation of the protein phosphatase 1 (PP1). When PP1 is activated, it dephosphorylates several substrates, including Ser845 on the AMPAR subunit GluA1, leading to AMPAR endocytosis and LTD (Collingridge et al., 2004). The first clue to understand the molecular mechanism that drives to AMPAR endocytosis in NMDAR-LTD was the disruption observed of GluA2- *N*-ethylmaleimide-sensitive factor (NSF) interaction, an ATPase involved in membrane fusion events. The loss of this interaction causes AMPAR internalization, mimicking the one that takes place in NMDAR-LTD (Nishimune et al., 1998). Later on, it was shown that clathrin-mediated endocytosis was involved, and that the clathrin adaptor protein AP2 binds GluA2 on the same site of NSF. These results suggested that AMPAR are stabilized at the membrane by NSF, and upon NMDAR-LTD stimulus AP2 replaces NSF to initiate AMPAR endocytosis (Lüscher et al., 1999) (Figure I1).

Although the above studies give the notion that NMDAR-LTD primarily involves the activation of phosphatases, several studies have implicated various serine/ threonine (Ser/Thr) protein kinases in this process as well. These include protein kinase A (PKA; Brandon et al., 1995), cyclin-dependent kinase 5 (Ohshima et al., 2005), p38 mitogen-activated protein kinase (p38-MAPK; Zhu et al., 2002), Ca^{2+} /calmodulin-dependent protein kinase II (CaMKII; Mayford et al., 1995; Pi et al., 2010), protein kinase C (PKC; Gean et al., 1995) and glycogen synthase kinase-3 (GSK3; Peineau et al., 2007; Fig. I1). A consensus now exists that both phosphatases and kinases activity are inter-related and important for the rapid, early phase of LTD. The late-phase of LTD requires, in addition,

protein synthesis and mRNA transcription (see below; Goelet et al., 1986; Manahan-Vaughan et al., 2000).

1.3.- Neuronal activity induces immediate early genes transcription:

The phrase 'Immediate early genes' (IEGs) was first used in virology to describe viral regulatory factors transcribed *de novo* by host cells within 2 minutes after viral integration (Jayaraman, 1972). It was shown 15 years later that the mRNAs of most of these genes were detected at their peaks between 30 minutes and 1 hour (Curran et al., 1985), setting up the general definition for IEGs. As commented above, late phases of LTP and LTD require gene transcription. Based on screens in control rats and rats that received maximal electroconvulsive seizure (MECS), the number of neuronal activity-induced IEGs was initially estimated to be around 500–1000 (Nedivi et al., 1993). Subsequently however, the number of activity-induced IEGs was found to be close to 30–40 (Lanahan and Worley, 1998). IEGs may be categorized into two functional classes: regulatory transcription factors (RTFs), which control transcription of other downstream genes, and effector IEGs, which directly influence cellular functions (Lanahan and Worley, 1998). By virtue of their ability to regulate transcription, RTFs are well situated to globally regulate cell function (Guzowski, 2002). In contrast, effector IEGs have a wide range of cellular functions, including those related to cell remodelling (*Bdnf*, *Narp*), intracellular signalling (*RheB*, *RGS-2*, and *Homer1a*), synaptic modification (*Arc*, *Homer1a*, *Narp*, *tissue plasminogen activator* or *Tpa* and *Bdnf*) and metabolism (*Cox-2*) (see Guzowski, 2002 and Lanahan and Worley, 1998 and references therein). In 2011 Saha et all. (2011) established a new categorization; rapid or delayed IEGs, depending on the presence of RNA polymerase II (RNApolII) in their chromatin, and therefore a fast triggered RNA transcription. They show that RNApolII is stalled just downstream of the transcription start site of *Arc*, allowing its near-instantaneous transcription (Saha et al., 2011).

2.-Epigenetics marks and gene regulation:

Waddington C. in 1957 was the first to use the term epigenetics to describe a mechanism or mechanisms that are 'on top of' or 'above' the level of the genes encoded by the DNA sequence (Waddington, 1957). These mechanisms, which can be influenced, among other stimulus, by environmental factors such as diet (Waterland and Jirtle, 2003) and experiential factors such as maternal care (Weaver et al., 2004), can ultimately control which or when, some genes will be expressed in cells, and even in whole organisms with the same genome, to become phenotypically distinct (Fraga et al., 2005). In molecular terms, epigenetics refers to the covalent modifications of chromatin that affect gene expression. In turn, these can be transient or long lasting modifications,

important to induce or perpetuate, respectively, changes in gene expression. The two major molecular epigenetic mechanisms are post-translational histone modifications and DNA methylation.

2.1. Histone modifications:

Histones are highly basic proteins that organize DNA into a chromatin unit, the nucleosome; 147 bp of DNA is wrapped tightly around an octamer of histone proteins (composed by two molecules of each one of the histones H2A, H2B, H3, and H4), and these nucleosomes are linked by histone H1 (Luger et al., 1997). The structure of the Histones is composed of a globular domain localized in the centre of the nucleosome and a N-terminal tail that contains multiple sites for potential modifications, including acetylation, phosphorylation, methylation, ubiquitination and ADP-ribosylation (Jenuwein and Allis, 2001; Strahl and Allis, 2000). These post-translational modifications are often called histone marks. Each of these marks is introduced or removed by specific enzymes; for instance, acetylation is catalysed by histone acetyltransferases and removed by histone deacetylases, methylation is catalysed by histone methyltransferases and removed by histone demethylases, and finally histone phosphorylation can be achieved by different nuclear kinases, such as mitogen- and stress-activated kinases 1 (Msk-1), and removed by different protein phosphatases, such as protein phosphatase 1 (PP1).

2.1.1.- Histone acetylation:

Histone acetylation takes place at lysine residues, specifically on their side chain amino group, neutralizing their positive charge, and decreasing the affinity between the histone tail and the DNA (Hong et al., 1993). Histone acetylation results in a chromatin relaxation, and allows the recruitment of transcription factors or RNA polymerase. Acetylated histone tails also serve as platforms for others co-activators to reach the chromatin. Histone acetylation is generally associated with transcriptional activation and is widely present in the active chromatin, the euchromatin (Tollefsbol, 2011).

Histone Acetyltransferases (HATs) catalyse the direct transfer of an acetyl group from acetylCoA to the NH^+ group of the lysine within the histone (Bannister and Kouzarides, 2011). HATs are evolutionarily conserved from yeast to humans and they are generally composed by multiple subunits, with the function of the catalytic subunit depending largely on the context of the other subunits in the complex (Lee and Workman, 2007). HATs can be grouped on the basis of their catalytic domains, Gcn5 and MYST HATs. Although these two families of HATs are the predominant ones, other proteins including p300/CBP (cAMP response element-binding protein (CREB)-binding protein), Taf1 and a number of nuclear receptor co-activators, have also been shown to possess intrinsic HAT activity.

However, they do not contain true consensus HAT domains and therefore represent the 'orphan class' of HAT enzymes (Lee and Workman, 2007).

As commented above, acetyl groups on histone tails can be removed by histone deacetylases (HDACs), therefore preventing the expression-prone status given by acetylation. Two categories of HDACs have been identified so far: zinc dependent HDACs and nicotinamide-adenine-dinucleotide (NAD)–dependent HDACs or sirtuins (SIRT). Depending on sequence similarity, the zinc-dependent HDAC family members are composed of class I (HDACs 1, 2, 3, and 8), classes IIa and IIb (HDACs 4, 5, 6, 7, 9, and 10), or class IV (HDAC 11). It is important to note that class I HDACs are found mostly within the nucleus, whereas class II members shuttle between the nucleus and cytoplasm (Gibson and Murphy, 2010). An exception is found with HDAC6, which is located only in the cytoplasm. The class III of HDACs or sirtuins constitutes a family of proteins highly conserved from prokaryotes to eukaryotes called the SIRT family (Grozinger et al., 2001).

2.1.2.- Histone methylation:

Histone methylation takes place on all basic residues: arginines, lysines and histidines (Byvoet et al., 1972; Fischle, 2008; Murray, 1964). Lysines can be mono-, di- or tri-methylated on their amine group, arginines can be mono-methylated, and symmetrically or asymmetrically di-methylated (Borun et al., 1972; Byvoet et al., 1972; Murray, 1964; Paik and Kim, 1969). Histidines are reported to be mono-methylated, although this methylation appears to be rare and has not been further characterized (Borun et al., 1972; Gershey et al., 1969). The more studied lysine and arginine methylations are the ones on Histones H3 and H4 (H3K4, H3K9, H3K27, H3K36, H3K79, H4K20, H3R2, H3R8, H3R17, H3R26 and H4R8). However, other residues of histones have been identified as methylated by proteomic studies (Tan et al., 2011). The effect of methylation on gene expression is context dependent; the location of residue methylated on a histone and its degree of methylation have been associated to different gene expression status. For example, H3K27Me3 is associated with repressed chromatin (Greer and Shi, 2012), while H3K4Me3 is generally associated with active transcription and elongation (Santos-Rosa et al., 2002). The same methylation status can be also associated with different transcriptional activity, for instance, H3K4Me2/Me3 when bound to PHD-domain-containing co-repressor protein inhibitor of growth factor family member 2 (ING2) is associated to transcriptional repression due to the stabilization of the HDAC1 complex (Shi et al., 2006). Therefore, histone methylation will lead to a different chromatin compaction status depending on which histone residue is methylated and depending on which proteins are associated to the methylated histone.

Histone methylation is carried out by histone methyletransferase (HMT) enzymes,

which work by adding methyl groups donated from S-adenosylmethionine to histones. Three different families of enzymes with HMT activity have been identified. The SET-domain containing proteins and DOT1-like proteins have been reported to methylate lysines, whereas arginines are methylated by protein arginine N-methyltransferase family (Greer and Shi, 2012). HMTs are recruited to specific histone targets by different mechanisms, namely: specific DNA sequences (Fritsch et al., 1999; Woo et al., 2010), long non-coding RNAs (Gupta et al., 2010a), small non-coding RNAs (Ogawa et al., 2008; Zilberman et al., 2003), and also DNA methylation state (Bartke et al., 2010). HMTs are usually found in complexes, for example HMTs Enhancer of zeste homolog-1/2 (EZH1/2) are the catalytic subunits of the Polycomb repressive complexes (PRC) (Lau and Cheung, 2011; Mousavi et al., 2012; Simon and Lange, 2008).

Similarly to acetylation, methyl groups can be removed by demethylases. Two families of methyl-lysines demethylases have been identified: the amine oxidases and the jumonji C (JmjC)-domain-containing, iron-dependent dioxygenases. Theses enzymes are highly conserved from yeast to humans. Histone demethylases recruitment is dependent on the stimuli; for example Mad1 recruits the histone demethylase RBP2 to the Myc target telomerase reverse transcriptase (hTERT) gene promoter to repress transcription *via* H3K4me3 demethylation (Zheng et al., 2010), or CBP recruits UTX to chromatin in order to demethylate H3K27Me3 and increase H3K27Ac in stage 4 embryos, not long after global transcriptional activation of the zygotic genome (Tie et al., 2012).

2.1.3.- Histone phosphorylation:

Histone phosphorylation takes place at serine, threonine and tyrosine residues of histone (Rossetto et al., 2012). Different histone phosphorylations are associated to a large range of functions, for example Histone H2A phosphorylation at residue T120 and S139 or Y142, from H2AX isoform, are associated to DNA repair (Cook et al., 2009; Rossetto et al., 2012) or phosphorylation of Histone H3 residues T6, S10 or S28 are associated to increased transcription (Clayton et al., 2000; Lau and Cheung, 2011; Lo et al., 2000; Metzger et al., 2010). While histone 3 phosphorylation is involved in chromatin relaxation and regulation of gene transcription, these modifications were originally identified to be associated with chromosome compaction during mitosis and meiosis. It has been shown that phosphorylation of the N-terminal tail of histone H2B is essential for apoptosis induced chromatin condensation (de la Barre et al., 2001). Kinases such ERK1/2, MSK1, p38, JNK1/2 and many others can phosphorylate histone residues in response to different stimuli (Choi et al., 2005; Gehani et al., 2010; Zhong et al., 2000). As commented above for Histone acetylation and methylation, Histone phosphorylation is a dynamic process since the phosphate groups from Histones can be removed by different

phosphatases that are in the nucleus, such as PP1 or PP2A (Koshibu et al., 2009; Nowak et al., 2003).

2.1.4.- Histone marks in neuroepigenetics:

A number of behavioural paradigms revealed changes in histone marks in several regions/genes, demonstrating that histone modifications are components of memory formation and/or consolidation. Thus, for example, it was shown that contextual fear conditioning enhances acetylation at several sites of histone H3 and H4 tails in the hippocampus, including H3K9, H3K14, H4K5, H4K8 and H4K12 (Peleg et al., 2010). This paradigm of associative learning also induces the increase of other activator marks such as H3K4 trimethylation or H3S10 phsphorylation, and modulates repressive marks, such as H3K9 dimethylation (Chwang et al., 2007; Gupta et al., 2010b). In agreement with these results, it was shown that interfering with the molecular machinery responsible for histone acetylation, phosphorylation or methylation impairs associative learning and LTP. Among the more notable experiments, it is worth mentioning that administration of HDACs inhibitors in mice resulted increased histone acetylation and enhanced LTP (Levenson et al., 2004) and that impaired memory formation was observed in *cbp*$^{+/-}$ mice (Alarcón et al., 2004). The central role of acetylation in memory was also proved genetically in mice lacking HDAC2, which displayed enhanced fear conditioning and hippocampal LTP while the overexpression of HDAC2 led to impaired memories and LTP (Guan et al., 2009).

2.2.- DNA methylation:

2.2.1.- DNA methylation molecular mechanisms:

DNA methylation is a direct modification of a cytosine side-chain by the addition of a -CH_3 group covalently. Methylation cannot take place at all cytosines; these residues have to be immediately followed by a guanine to be methylated. These CpG dinucleotides often occur in small clusters, known as CpG islands, and are poorly represented in the genome. DNA methylation is catalized by the DNA methyltransferases (DNMTs), which transfer the methyl group to cytosine residues, specifically at the 5th position of the pyrimidine ring (Bird, 2002; Miranda and Jones, 2007). Two different variants of DNMTs are identified: maintenance DNMTs and *de novo* DNMTs. DNMT1, the maintenance DNMT, methylates hemi-methylated DNA, whereas *de novo* DNMTs (DNMT3a and DNMT3b) methylate previously un-methylated CpG sites. Maintenance DNMT1 perpetuates methylation marks after cell division, regenerating methylation in the newly synthetized complementary DNA strand (Bestor et al., 1992; Hsieh, 1999; Okano et al., 1999). DNA methylation is stable, offering an ideal mechanism for the long-term cellular changes necessary to persist and

maintenance of memory, but it would also have to be dynamic (i.e. on/off) in order to enable neurons to respond to different stimulus. The DNA methylation off rate is controlled by DNA demethylation, a process seen for a long time as a passive and not exempt of controversy, especially for non-mitotic cells like neurons, mainly because the identity of DNA demethylases has remained elusive. However, there are increasing evidences that active methylation and dementylation are taking place in mature cells (Roth et al., 2009).

The predominant view in the literature is that DNA methylation is associated with gene repression, and in the majority of the cases large DNA methylation completely silences the associated genes. This type of gene silencing mechanism is achieved by recruiting methyl-DNA binding proteins (MDBP) at specifics sites of the genome. These proteins have the methyl-binding domain (MBD) and a transcription regulatory domain (TRD), which in turn recruits HDACs *via* adaptors/scaffold proteins (Clouaire and Stancheva, 2008). The HDACs remove acetyl groups form core histones, altering the chromatin structure locally, and leading to a more compact chromatin state and transcriptional suppression (see paragraph 2.1.1). Although DNA methylation is traditionally associated with gene repression, recent studies have identified other proteins recruited by MDBPs, which can also associate with transcriptional activation (Chahrour et al., 2008).

2.2.2.- DNA methylation in neuroepigenetics:

Several studies have investigated the capacity of DNA methylation to regulate synaptic plasticity and memory. It has been shown that DNMTs inhibitors affect DNA methylation in adult CNS, blocking LTP (Levenson and Sweatt, 2006; Miller et al., 2008) and hippocampal dependent memory formation in a contextual fear-conditioning paradigm (Lubin et al., 2008). Furthermore, it was shown that fear-conditioning can induce DNA methylation and transcriptional repression of Protein Phosphatase 1 (PP1) and, at the same time, demethylation and gene transcription of the synaptic plasticity gene *Reelin* (Miller and Sweatt, 2007), highlighting the complex interplay of DNA methylation marks during cognition. In concordance with this complexity, Miller et al showed that DNA methylation has circuit-specific importance, since DNMTs inhibition in prefrontal cortex impairs the recall of existing memories but not the formation of new ones (Miller et al., 2010). The genetic confirmation of the role of DNMTs in cognition was shown in conditional forebrain- and neuron-specific deflection of DNMT1 and DNMT3a. These mice had impaired performance on the Morris water-maze and the fear learning (Feng et al., 2010), implying that for this particular mnemonic paradigm, DNA methylation plays a pro-active role (see however *Bdnf* regulation by methylation, below).

2.3.-Bivalent genes:

Recent studies have shown that proteins of the Polycomb Repressive Complexes are required to silence an important subset of developmental regulator genes in both human and mouse embryonic stem (ES) cells, to ensure that expression occurs only at later stages, upon ES cell differentiation (Boyer et al., 2006; Lee et al., 2006). Genome-wide (Bernstein et al., 2006) and candidate-based chromatin studies (Azuara et al., 2006) indicate that the transcriptional start sites (TSSs) of these genes are frequently present in a bivalent state: *i.e.* the presence of histone modifications associated with gene activation (such as acetylated histone H3 and tri-methylated H3K4) and with PRC2- mediated gene repression (methylated H3K27). A characteristic observed for bivalent promoters in ES cells is that the presence of H3K4 methylation shows a strong positive correlation with the presence of CpG islands in the underlying DNA sequence, whereas the presence of H3K27-methylated regions showed a strikingly low density of transposon-derived sequences (transposon exclusion zones or TEZs) (Bernstein et al., 2006).

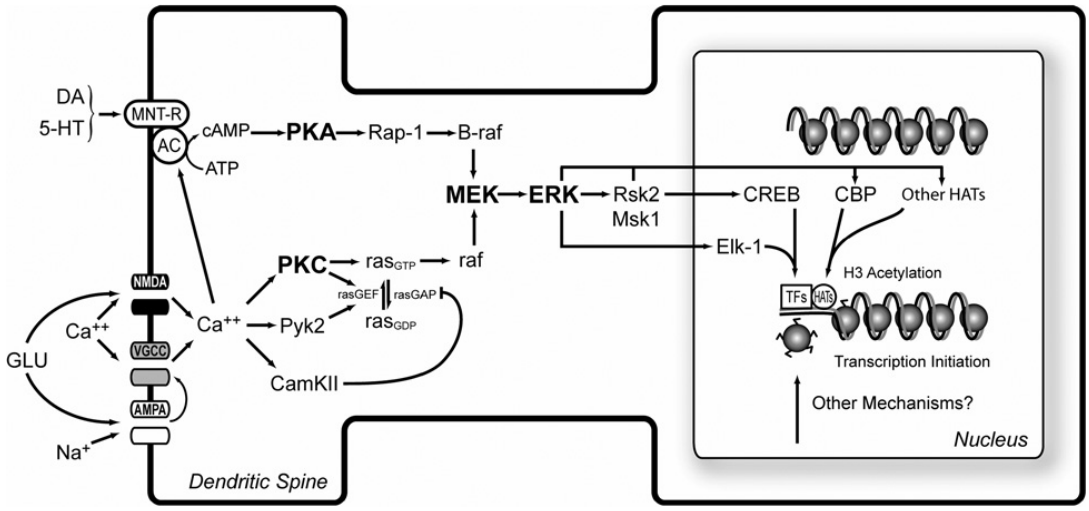

Figure I2: Hypothetic signal transduction mechanism operating to regulate chromatin structure in the hippocampus.
Different cell surface receptors signal to a complex intracellular downstream cascade, which leads to alterations in both transcription factors and chromatin structure. (From Levenson and Sweatt, 2006)

3.- Epigenetic regulation of learning/memory genes:

It is well established that learning and memory require immediate early genes transcription, and that their transcription is regulated epigenetically (see above). To achieve the transcriptional regulation, *via* chromatin remodelling, different pathways will operate after neuronal stimulation (Figure I2). From all IEGs reported, in this thesis I will focus on the *Bdnf* regulation.

3.1. *BDNF* as model gene:

The Brain-Derived Neurotrophic Factor (BDNF) is one of the earliest identified neurotrophins (Barde et al., 1982). BDNF was demonstrated to play several important roles in different biological processes, both during development and in the adult. In the nervous system, BDNF plays important roles in neuronal differentiation, survival, and synaptic plasticity (Dincheva et al., 2012; Ding et al., 2006; Ghosh et al., 1994; Lu et al., 2014). *BNDF* gene possesses a structural and functional complexity resulting from multiple promoters, leading to the expression of multiple transcripts, in turn susceptible of alternative splicing, and two different polyadenilation patterns, resulting in different precursors isoforms synthesis but only one mature BDNF.

3.2.-BDNF protein:

3.2.1.- BDNF structure and processing:

BDNF is encoded by the *BDNF* gene, which produces four different pre-pro-BDNFs depending on the TSS used and its translation start codon (Pruunsild et al., 2007). It has been proposed that different pre-domains will affect the intracellular BDNF trafficking, promoting the segregation of BDNF longer pre forms (Aid et al., 2007). Pro-BDNF is a 32 kDa precursor that undergoes glycosylation and glycosylsulfonation within the pro-domain. The precursor can undergo N-terminal cleavage to generate a mature BDNF of 14 kDa. In the brain it can experience three different paths; 1) it can be edited in the Golgi to be secreted as a mature form; 2) it can be secreted as a pro-BDNF which is then processed at the synaptic space to mature BDNF; or 3) it can be secreted as a pro-BDNF without further processing (Lu et al., 2005).

3.2.2.- BDNF Signal transduction:

Almost all roles of BDNF in the CNS depend on the interaction with two different receptors: p75 and the tropomyosin-related kinase B (TrkB) receptors. p75 is a member of the tumor necrosis factor receptor family and it has been postulated that pro-BDNF is the activating ligand. While the pro-BDNF/p75 association has been associated to LTD (Woo et al., 2005) and neuronal pruning (Deinhardt and Chao, 2014), the best characterized role is its involvement in the initiation of apoptosis (Kenchappa et al., 2010). Thus, it has been shown that proBDNF/p75 interaction induces the Jun kinase pathway, leading to apoptosis through p53 and caspases activation (Reichardt, 2006). This interaction also activates the small GTPase RhoA and its downstream Rho Kinases, which have been associated with neurite outgrowth inhibition (Sun et al., 2012). Different from pre-BDNF, mature BDNF binds to TrkB with high affinity, and this binding has been associated with

increased synaptic transmission and plasticity, neuronal proliferation and survival, and axonal sprouting (Deinhardt and Chao, 2014; Lu et al., 2005). If TrkB is not present, mature BDNF also can bind p75 (Deinhardt and Chao, 2014; Lu et al., 2005). BDNF/TrkB interaction leads to the activation of one or more of three major signalling pathways, involving phosphatidylinositol 3-kinase (PI3K), phospholipase C gamma (PLC-gamma) and extra- cellular signal-regulated kinase 1/2 (ERK1/2) (Huang and Reichardt, 2003). These mechanisms promote calcium entrance into the cell, leading to protein synthesis by transcriptional and translational mechanisms. This interaction also promotes neuronal survival *via* Protein Kinase B (PKB/AKT) signalling pathway, through PI3K (Koshimizu et al., 2010; Sossin and Barker, 2007).

3.3.- *BDNF* gene:

3.3.1.-Human *BDNF* gene

The human *BDNF* gene is located at chromosome 11, region p13-14: it consists of 11 exons, nine of which have their own regulatory promoter region, and it has the coding sequence residing in the last exon (Pruunsild et al., 2007, 2011)(Figure I3). Exon I also contains an in-frame ATG that can be translated alternatively to the one present in Exon IX, extending the pre-pro- region of BDNF by eight amino acids (Timmusk et al., 1993). This region has the archetypical GU-AG consensus signal intron-exon boundaries for alternative splicing (Modarresi et al., 2012; Pruunsild et al., 2007). Exon IX also has two different alternative spliced 3' un-translated regions (UTRs; Aid et al., 2007). Additionally, an interesting feature of the structure of the *BDNF* gene is the existence of a 200Kb antisense region that includes 10 exons transcribed from the same promoter with the

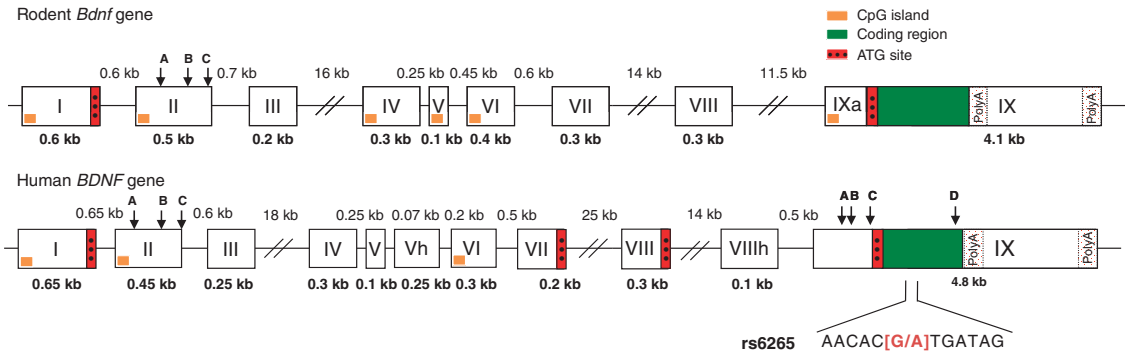

Figure I3: Structure of the human and rodent *BDNF* gene.
Exons are represented as boxes, and introns as the lines between boxes. Roman numerals indicate the number of the exons; Arabic numerals indicate the size of exons and introns. Red boxes represent the ATG codon, the initiation transcription marks; the green box at exon IX represents the pro-BDNF coding region, including the genetic variant implicated in Val66Met polymorphism and the two polyadenilation sites (PolyA). Yellow lines represent de CpG islands. Some exons, like exon II and IX, contain different transcript variants with alternative splice-donor sites (A, B, C, D). (From Boulle et al. 2012)

ability to synthesize a wide variety of anti-*BDNF* small non-coding RNAs (Kimura et al., 2006; Pruunsild et al., 2007, 2011). *In silico* analysis of the gene sequence revealed possible CpG islands at promoter I, II and IV of the human gene (Boulle et al., 2012; Figure I3).

3.3.2.-Structure of the rodent *Bdnf* gene:

The *Bdnf* gene is located at chromosome 2, region q3, and chromosome 3, region q35, in moues and rat respectively. The rodent *Bdnf* has 9 exons, eight of them have their own promoter region and are directly spliced to exon IX, which has the coding sequence (Aid et al., 2007). As it happens with human *BDNF*, Exon I of rodent gene has the ATG that can be alternatively translated (Timmusk et al., 1993). Exon II has three different isoforms due to its alternative splicing. Exon IX also has two different alternatively spliced 3' UTRs, as it happens in the human *BDNF* gene (Aid et al., 2007). Taking into account the gene architecture, there are, at least, 22 different *Bdnf* mRNAs isoforms. Antisense-*BDNF* transcripts are not expressed in rat and mouse (Aid et al., 2007). Five different CpG islands have been described at the rodent *Bdnf* gene, located around the transcription start sites of exons I, II, IV, V and VI (Lubin et al., 2008; Figure I3). Interestingly, transposon exclusion zones were found overlapping this four is promoters suggesting a possible bivalency of the these Bdnf promoters (Bernstein et al., 2006). Different DNA binding sites for distinct transcription factors have been characterized in different promoters (Marmigère et al., 2001; West et al., 2001).

3.3.3- *Bdnf* epigenetic regulation:

3.3.3.1.- *Bdnf* regulation by DNA methylation:

Several studies have focused on DNA methylation at *Bdnf* CpG islands. Experiments performed in cell lines treated with 5-azacitidyne, a DNMT inhibitor, revealed increased expression of exons I, IV, V, VIII and IX in C6 rat glioma cells, and exons I, III and IV in mouse neuroblastoma, Neuro2A, cells (Aid et al., 2007; Ishimaru et al., 2010). A similar regulation seems to occur *in vivo*; it was shown that zebularine, a DNMT inhibitor, infused to CA1 increases transcription of *Bdnf* exons I, IV, VI, and that increased mRNA levels correlate with decreased DNA methylation at the respective CpG islands (Lubin et al., 2008). Furthermore, it was reported that fear-conditioning induces demethylation of the CpG islands present at exons IV but no VI, resulting in increased transcription from exon IV. The behaviour-induced changes in DNA methylation at *Bdnf* CpG islands require NMDAR activation, since the pharmacological inhibition of the receptor by MK801 impairs

DNA demethylation and RNA transcription from promoter IV after fear conditioning (Lubin et al., 2008). In addition to these, physiological, *Bdnf* epigenetic regulatory processes, several groups have shown that aberrant regulation of *Bdnf* gene can play a role in the neural phenotype of Rett syndrome (RTT) mouse model, a severe progressive neurological disorder characterized by autistic behaviour, mental retardation and motor dysfunction. RTT is associated with mutations in methyl-CpG-binding protein 2 (MeCP2), which has been shown to selectively regulate *Bdnf* in response to neuronal activity (Chen et al., 2003; Martinowich et al., 2003; Zhou et al., 2006). In fact, it has been shown that membrane depolarization induces calcium-mediated MeCP2 phosphorylation, which in turn decreases MeCP2 binding to methylated CpGs, facilitating *Bdnf* transcription (Chen et al., 2003; Martinowich et al., 2003). In contraposition, more recent data presented by Li et al. showed that impairing MeCP2 activity-induced phosphorylation enhances synaptogenesis, LTP and spatial memory (Li et al., 2011). All in all, the studies on DNA methylation suggest that this epigenetic mechanism plays a role on *Bdnf* gene expression.

3.3.3.2.- *Bdnf* regulation by Histone acetylation:

There are emerging evidences that histone acetylation is a key event controlling *Bdnf* transcription upon neuronal stimulus. Proper histone acetylation levels have been shown to affect LTP and long-term memories (Alarcón et al., 2004). It has been reported that increased acetylation of histone H4 at *Bdnf* promoters I and IV in prefrontal cortex contributes to improve the extinction of conditioned fear in mice (Bredy et al., 2007). Moreover, the HDAC inhibitor valproic acid (VPA) enhanced not only the extinction of cued fear memory but also its acquisition and consolidation (Bredy and Barad, 2008). Interestingly, a single exposure to prolonged stress before fear conditioning in rats increased acetylation of histones H3 and H4 at the *Bdnf* promoters I and IV and heightened the hippocampal levels of *Bdnf* transcription, thus strengthening the subsequent consolidation of fear memories (Takei et al., 2011). In further agreement, it was shown that contextual fear conditioning in mice results in increased H3 acetylation at the *Bdnf* promoter IV (Lubin et al., 2008). Several other studies have reported the positive correlation between histone acetylation with *Bdnf* expression through the use of mood/cognitive-enhancer or anti-depressants drugs used in the clinics. Thus, chronic treatment with imipramine, an antidepressant drug, restored hippocampal *Bdnf* expression through hyper-acetylation of promoters IV and VI and selective downregulation of HDAC5 in chronic social defeat stress mice, which normally present lower *Bdnf* expression (Tsankova et al., 2006). The administration of fluoxetine, another antidepressant that specifically inhibits serotonin reuptake, promoted acetylation at *Bdnf* promoter IV and

reversed depression-like behaviour in depressive-induced mice model (Onishchenko et al., 2008). Interestingly, neither imipramine nor fluoxetine did alter the repressive histone methylation marks in these two studies. Trichostatin A, an HDAC inhibitor, but also fluoxetine, have been shown to reactivate visual cortical plasticity in adult rats, inducing a transient increased transcription of *Bdnf* through histone hyperacetylation at its promoters (Maya Vetencourt et al., 2011). The impact of acetylation on *Bdnf* has been also shown in studies focusing on the mechanisms of action of drugs of social abuse. Cocaine-induced neuronal plasticity has been implicated in the activation of *Bdnf* promoter IV by increased acetylation and phosphor-CREB recruitment in rat prefrontal cortex. In contrast, cocaine abstinence increases histone H3 acetylation and induces *Bdnf* exon I transcription in ventral tegmental area (Schmidt et al., 2012). Epigenetic activation of *Bdnf* promoter I in the ventromedial prefrontal cortex (vmPFC) through acetylation of histone H3 has been associated with the successful extinction of aversive memories of morphine withdrawal (Wang et al., 2012).

3.3.3.3.- *Bdnf* and Histone methylation:

Several groups reported changes in histone methylation and therefore changes in *Bdnf* transcription *in vivo*. Onishchenko and colleagues showed that the induction of a depression-like behaviour in mice, by perinatal exposure to methylmercury, decreases *Bdnf* total mRNA in dentate gyrus, and that this reduction was due to increased histone H3 Lys 27 trimethylation at *Bdnf* promoter IV (Onishchenko et al., 2008). Other groups also showed similar effects on *Bdnf* transcription by other adverse environmental conditions, such as defeat stress or light deprivation. For instance, defeat stress induces the downregulation of *Bdnf* transcripts IV and VI accompanied by increased H3K27 dimethylation at these promoters (Tsankova et al., 2006) and one week of light deprivation in male rats decreases *Bdnf* transcripts of exons I, II, IV and VI in visual cortex by increasing H3K27 trimethylation (Karpova et al., 2010). On the contrary, positive environmental conditions, such as environmental enrichment, increase *Bdnf* total mRNA expression, which is accompanied by decreased repressive methylations (H3K9Me3 and H3K27Me3) and increased levels of the activating methyl mark H3K4Me3 (Kuzumaki et al., 2011).

3.3.4.-Post-transcriptional regulation of *Bdnf* mRNAs trafficking:

Localized delivery of mRNAs to dendrites in response to a cognitive stimulus is thought to be a critical event in synaptic plasticity, assuring the rapid synthesis, through the dendritic translation machinery, of the essential factors required in the cognitive process; dendritic transport of *Bdnf* mRNAs fits into this premise (Bramham and Wells,

2007; Tongiorgi et al., 1997). In fact, the *Bdnf* gene complex structure allows diversity in expression, not only for the temporal neuronal response to different stimulus, but also for the differential spatial distribution of *Bdnf* transcripts (Aid et al., 2007; An et al., 2008; Chiaruttini et al., 2008, 2009; Pruunsild et al., 2007). Studies in neuronal cultures show that *Bdnf* transcripts targeting to dendrites might be promoted by a constitutively active element in the protein-coding region, while multiple 5' or 3' UTRs, with either inhibitory or permissive signals for dendritic targeting, control the transcript selective trafficking (Chiaruttini et al., 2009). The dendritic targeting of *Bdnf* mRNAs is driven by the protein-coding sequence and is mediated by the RNA-binding protein Tarnslin. This interaction is blocked by the C196A (or Val66Met) mutation, compromising mRNA trafficking to distal dendrites, and therefore the correct spatial segregation of *Bdnf* mRNA variants (Chiaruttini et al., 2009).

Different groups have shown that *Bdnf* splice variants containing the 5´exons II and VI are transported to distal dendrites whereas the transcripts containing 5´exons I and IV are required in the soma or in proximal dendrites. (Baj et al., 2011; Chiaruttini et al., 2008, 2009). By use of overexpression and silencing of specific *Bdnf* mRNA isoforms, Baj and colleagues found that dendritic BDNF (from exons II and VI) plays a role in secondary dendrites' plasticity in response to external stimuli. Furthermore, the expression of individual *Bdnf* splice variants was shown to be relevant for the spatially restricted activation of TrkB receptors: i.e. overexpression of exon I or IV transcripts led to phosphorylation of 80–100% of TrkB receptors within the first 45 μm from the soma whereas overexpressing exon II or VI *Bdnf* variants led to 80%TrkB phosphorylation at 80 μm from the soma and beyond. Thus, the spatial segregation of *Bdnf* transcripts enables this neurotrophic factor to differentially shape distinct dendritic compartments (Baj et al., 2011).

Bdnf mRNAs trafficking is further regulated by the two different 3' UTR, the short or long one. *Bdnf* mRNAs containing the short 3' UTR have been shown to be located somatically, where they are constitutively translated in order to maintain the basal levels of BDNF protein. In contrary, the long 3' UTR containing transcripts are targeted to distal dendrites and they are translated upon neuronal stimulus (An et al., 2008; Lau et al., 2010). Moreover, different neuronal stimuli, such as KCl-induced depolarization in rat hippocampal neurons, change the somatic targeting of the short 3'UTR targeting to distal dendrites (Oe and Yoneda, 2010).

4.- Physiological relevance: Learning, memory and neuroepigenetics in ageing:

Ageing is characterized by a progressive decline in cognitive capacities that can, in part, be explained by changes in neuronal plasticity or cellular alterations that directly affect plasticity mechanisms (Burke and Barnes, 2006).

4.1.- Learning and memory in ageing:

At the beginning of the second half of 20th century, several studies attributed cognitive impairments in the aged brain to neuronal loss, reaching up to 60% loss in cortical neurons, and also in the hippocampus (Ball, 1977; Brody, 1955; Coleman et al., 1987). It was not until late 80´s, when new stereological principle were developed, that it was shown that in normal ageing there is no significant cell death in the hippocampus or neocortex (Pakkenberg and Gundersen, 1997; Rasmussen et al., 1996; West et al., 1994). Different studies in dendritic extent have confirmed that, in general, there is no regression of dendrites with age in the hippocampus (Flood et al., 1987; Hanks and Flood, 1991). Pyramidal neurons, on the other hand, show decreased dendritic branching with age, both in apical and basal dendrites, in superficial cortical layers (Grill and Riddle, 2002). Spine density age-associated alterations are also region-specific. For instance, no differences in spine density was found at the CA1 or dentate gyrus while significant reduction of spine density is found in the subiculum (Curcio and Hinds, 1983; Uemura, 1985). Apparently there are no major changes in brain anatomy in the old, but several studies show that spatial memory, which is essential for most episodic memories, declines with ageing in humans, monkeys, dogs, rats and mice (Bach et al., 1999; Head et al., 1995; Newman and Kaszniak, 2000; Rapp et al., 1997; Rosenzweig and Barnes, 2003). Because the hippocampus is particularly susceptible to ageing, it is not surprising that task performances that require information processing are declined with ageing.

4.2.- Neuroepigenetics in ageing:

Several recent reports indicate that epigenetic mechanisms are affected in the aged brain and contribute to the aged brain phenotype (Morse et al., 2015; Penner et al., 2010, 2011). Thus, RNA microarray-based screening revealed the significant down-regulation of *zif268/early growth response 1 (Egr1)*, *Arc*, *Narp* and *Homer1* in the hippocampus of old rats (Blalock et al., 2003; Rowe et al., 2007). Also, Hattiangady and colleagues found that *Bdnf* is also downregulated in the hippocampus of middle-aged and aged rats (Hattiangady et al., 2005). We now know that the reduced IEG transcription can occur by an increase in repressive marks (H3K9Me2-Me3 or H3K27Me3), a decrease in activator marks (H3K9Ac, H3K14Ac, H4K12Ac or H4K20Me1), and/or decreased marks linked to transcriptional elongation processes (H3K36Me3) (Peleg et al., 2010; Tang et al., 2011;

Walker et al., 2013; Wang et al., 2010). Furthermore, it has been shown that not only histone marks are differently present in the chromatin of the old brain, but also HDACs undergo age-associated changes (Baltan, 2012; Chouliaras et al., 2013). On the other hand, a number of studies suggest that the state of chromatin of the old can still be modulated by different paradigms, turning a repressed transcriptional state into a more active state and facilitating IEG transcription (Morse et al., 2015; Peleg et al., 2010; Reolon et al., 2011). In this regard, Morse and colleagues have recently published that environmental enrichment enhances memory in old mice by increasing H3K4Me3 at *Bdnf* promoter IV and the subsequent increased transcription of total *Bdnf* (Morse et al., 2015). Furthermore, Peleg and colleagues showed that H4K12Ac increase was a key difference between young and old animals in response to fear conditioning, and that by treating old mice with SAHA, an HDAC inhibitor, they could enhance memory in the old mice. These authors attributed the improved memory effect to an increase in H3K12Ac after fear-conditioning resulting in increased IEG transcription (Peleg et al., 2010).

4.3.- LTD in ageing: the role of cholesterol:

In all sub-regions of the hippocampus, most electrical properties remain constant over lifespan (Barnes, 1994). However CA1 pyramidal neurons show an increased Ca^{2+} conductance, possibly due to increased density of L-type Ca^{2+} channels that might contribute to plasticity deficits associated with ageing (Foster and Norris, 1997; Thibault and Landfield, 1996). While increased Ca^{2+} could lead to facilitated LTD in the aged (Norris et al., 1996), several works reported deficits of NMDA-LTD in ageing (Billard and Rouaud, 2007; Martin et al., 2014a; Yang et al., 2013; Figure I4). Furthermore, hippocampal neurons maintained for long period in culture, until showing aging signs, present reduced AMPA mobility and endocytosis, and a poor LTD response to the addition of NMDA (Martin et al., 2014a). In this study it was shown that reduced AMPA mobility, endocytosis and LTD could be rescued by the addition of cholesterol, both *in vitro* and *in vivo* (Martin et al., 2014a; Figure I4).

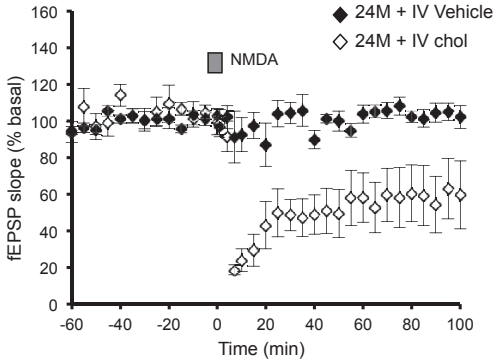

Figure I4: Impaired LTD in the old can be rescued by the addition of cholesterol.
Intraventricular infusion of cholesterol in old mice restored NMDA-LTD. Field excitatory postsynaptic potentials (fEPSPs) were recorded from hippocampal slices of 24- month-old mice infused with cholesterol (◊) or vehicle (♦) in the lateral ventricle for 14 days. A significant NMDA-LTD was obtained in slices prepared from cholesterol-infused mice, but no LTD was observed in the vehicle-treated group. (From Martín et al. 2014a)

The important role of cholesterol in the cognitive deficits of the old was also suggested by other lines of work. Thus, it was shown that synaptic plasticity of CNS is limited by the reduced availability of cholesterol provided by glial cells in mature brains (Goritz et al., 2005; Mauch et al., 2001). Also, age-dependent loss of cholesterol was reported in the human brain (Söderberg et al., 1990; Svennerholm et al., 1991, 1994, 1997) and in the rodent hippocampus, *in vivo* and *in vitro* (Martin et al., 2008, 2014a; Sodero et al., 2011). At present, the precise causes for the age-associated cholesterol loss are not known. However, this may be the consequence of the cooperation between three different mechanisms: increased catabolism, reduced synthesis and reduced transference from astrocytes (Martin et al., 2014b). Increased catabolism is the consequence of the transcriptional activation of the brain-specific cholesterol-hydroxylating enzyme Cyp46A1 (Ohyama et al., 2006; Sodero et al., 2012), increasing cholesterol solubility and removal from membranes for its subsequent extrusion from the brain. This possibility is supported by the observations that Cyp46A1 transcription *in vitro* is induced by oxidative stress by-products but not by sterol levels (Ohyama et al., 2006) and also by the observation that enzyme's activity increases in high stress situations, such as during cortical injury, induced autoimmune encephalomyelitis and in Alzheimer's disease (Bogdanovic et al., 2001; Cartagena et al., 2008; Teunissen et al., 2007). Age-dependent reduced synthesis was observed in neurons together with impaired delivery of newly synthesized cholesterol from glial cells (Thelen et al., 2006). Irrespective of the real contribution of each of these processes, the final outcome is that old neuronal cells contain reduced cholesterol levels and that this is in part responsible for impaired LTD.

OBJECTIVES

The general Objectives planned for this Thesis were:

1.- To determine the epigenetic mechanisms involved in *Bdnf* expression after NMDA receptor stimulation by chemical LTD.
2.- To determine the relationship between cholesterol reduction and immediate early genes transcription associated to the cognitive deficits in the old.

The work performed to reach the above objectives consisted in the following two phases.

Phase 1:

1.1.- Analysis of the transcriptional response of *Bdnf* transcripts containing exons I, II, IV, or VI to a pure cognition-related chemical stimulus as NMDA induced LTD.
1.2.- Analysis of different activation and repressive histone marks and associated chromatin remodelling enzymes at *Bdnf* promoters I, II, IV and VI in basal conditions and after NMDA-LTD stimulation.
1.3.- Dissection of the biochemical pathway connecting NMDA receptor stimulation (NMDA-LTD) to the epigenetic remodelling involved in *Bdnf* expression.

Phase 2:

2.1.- Analysis of the basal state of the different epigenetic marks on *Bdnf* promoters in the aged hippocampus.
2.2.- Analysis of *Bdnf* epigenetic regulation and transcription in the old in response to NMDA-LTD.
2.3.- Analysis of the relationship between cholesterol reduction with age and *Bdnf* expression by NMDA-LTD.
2.4.- Test a pharmacological approach to increase cholesterol levels in the old in order to enhance memory and rescue epigenetic regulation and IEGs transcription.

METHODS

1.- Primary hippocampal neurons:

Primary cultures of hippocampal neurons were prepared from embryonic day 18 (E18) Wistar rats as described in Kaech et al. (Kaech and Banker, 2006). For our experiments hippocampal neurons were kept in culture for 15 days *in vitro* (15 DIV), when they have reached full maturation.

Hippocampi were dissected and placed into ice-cold Hank's solution with 7 mM HEPES and 0,45% glucose. The tissue was then treated with 0,005% trypsin (trypsin 0,05% EDTA; (Invitrogen; Life Technologies Co.) and incubated at 37º C for 16 min and then treated with DNase (72 µg mL^{-1}; Sigma-Aldrich) for 1 min at 37º C. Hippocampi were washed three times with Hank's solution. Cells were dissociated in 5 mL of plating medium (Minimum Essential Medium (MEM) supplemented with 10% horse serum and 20% glucose) and cells were counted in a Neubauer Chamber. Cells were plated into pre-coated dishes with poly D-lysine (Sigma-Aldrich) (750.000 cells in a 10 cm dish and 270.000 in a 6 cm dish) and placed into a humidified incubator containing 95% air and 5% CO_2. The plating medium was replaced with equilibrated neurobasal media supplemented with B27 and GlutaMAX (Gibco; Life Technologies Co.). On DIV 7 the culture medium was replaced with medium without GlutaMAX. Cultures were used at 15 DIV.

2.- Hippocampal Slices:

Hippocampal slices were prepared from C57BL/J mouse (8 month the adult mice and 20 month old the old mice). Hippocampi were extracted in dissection solution (10 mM D-glucose, 4 mM KCl, 26 mM $NaHCO_3$, 233.7 mM sucrose, 5mM $MgCl_2$, 1:1000 Phenol Red), oxygen saturated with carbogen (95 % O_2 / 5% CO_2), and sliced in an automatic tissue chopper (McIlwain Tissue Chopper, Standard Table, 220V, Ted Pella Inc.) to obtain 400µm hippocampal slices. Then, slices were kept in artificial cerebrospinal fluid (ACSF; 119 mM NaCl, 2.5 mM KCl, 1 mM NaH_2PO_4, 11 mM glucose, 1.2 mM $MgCl_2$, 2.5 mM $CaCl_2$; osmolarity was adjusted to 290 Osm; ACSF was oxygen saturated with carbogen) for 1 hour. Finally the experiments were performed in ACSF.

3.- Cell Cultures:

HEK293T cells (ATCC) and Mouse Embrionic Fibroblasts (MEFs) WT and p38 KO (Porras et al., 2004) (kindly provided by Dr. A. R. Nebreda; Institute for Research in Biomedicine (IRB Barcelona), Barcelona, Spain) were grown with Dulbecco's modified Eagle's medium (DMEM) supplemented with 10% FBS and antibiotics (100 units/mL penicillin and 100 mg/mL streptomycin). DMEM was supplemented with 2 mM L-glutamine for MEFs culture. Cells were incubated at 37ºC in a humidified atmosphere of 5% CO_2.

4.- Drug treatments:

Stock solutions of CBP-CREB Interaction Inhibitor (250 mM (CCIIh); Millipore ref. 217505), KDM6A/B inhibitor (GSK-J4; 100 mM; Tocris Bioscience ref. 4594), p-38 MAK inhibitor (SB203580; 100mM; Axon Medchem ref. Axon 1363), Forskolin (50 mM, Tocris Bioscience ref. 1099) and Rolipram (100µM, Tocris Bioscience ref. 0905) were prepared in dimethyl sulfoxide (Sigma). Stock solutions of CaMKII inhibitor (KN93 phosphate; 20 mM; Tocris ref. 5215), mitogen- and stress-activated kinases 1/2 (Msk1/2) inhibitor (H89 dihydrochloride; 25 mM; Tocris ref. 2910), Portein Kinase C (PKC) inhibitor (Chelerytrine chloride; 10 mM; Tocris ref. 1330) and NMDA (20mM; Sigma-Aldrich ref. M3262) was prepared in Milli-Q water. Hippocampal neurons were treated with 5 µM CCIIh (1 hour), 10 µM GSK-J4 (1 hour), 10µM SB203580 (1 hour), 30 µM KN93 (20 min), 50 µM H89 (20 min) or 10 µM Chelerytrine (20 min) prior to NMDA-LTD induction. Stock solution of Cholesterol Oxidase (COase; 500 U/mL; Millipore ref. 228250) was prepared in water. MßCD-Ch solution was prepared freshly at use concentration, containing 30 µM of Cholesterol Water soluble (Sigma-Aldrich ref. C4951) with 5 µM Cholesterol (Sigma-Aldrich ref. C3045). Hippocampal slices were treated with COase 10 U/mL for 30 min or with MßCD-Ch for 1 hour prior to NMDA-LTD induction. For all biochemical experiments LTD was induced by 20 µM NMDA (Sigma-Aldrich ref. M3262) for 5 minutes, medium was then replaced and samples collected 5 or 25 minutes after LTD induction. Samples without LTD induction were used as a control. The experiments conducted in primary hippocampal neurons were performed at 37ºC, the ones conducted in hippocampal slices were performed at 25ºC. For Voriconazole treatments see below (Animals oral treatment paragraph 17.1).

5.- Relative RT-PCR:

Hippocampal slices on primary neurons were homogenized with Trizol Reagent (Ambion / RNA Life Technologies Co.) and the RNA was extracted with Direct-zolTM RNA minipreps (Zimo research ref. R2052) following manufactures instructions. RNA was quantified by absorbance at 260 nm using a Nanodrop ND-100 (Thermoscientific; Themo Fisher Scientific Inc.). Retrotranscription to first strand cDNA was performed using RevertAid H Minus First Strand cDNA Synthesis kit (Thermoscientific; Themo Fisher Scientific Inc.). Briefly, 5 ng of synthesized cDNA was used to perform the qPCR using GoTaq® qPCR Master Mix (Promega Co., Madison, WI, USA) in ABI PRISM 7900HT SDS (Applied Biosystems; Life Technologies Co.). The primers purchased to Sigma-Aldrich (Supplementary Table 1) were used at 0.5µM final concentration. Three housekeeping genes *Gapdh*, *GusB* and *Pgk1* were used as endogenous controls.

6.- Chromatin immunoprecipitation (ChIP):

ChIP experiments were performed as described by Millanes-Romero *et al.* (Millanes-Romero et al., 2013). Briefly hippocampal slices were crosslinked with 1% formaldehyde for 15 min at RT. Primary hippocampal neurons were crosslinked with 1% formaldehyde for 10 min at 30ºC. Crosslinking was stopped by adding glycine to a final concentration of 0.125 M for 2 min at RT. Samples were washed three times with cold PBS and homogenized in cold Soft Lysis Buffer (50 mM Tris [pH 8.0], 10 mM EDTA, 0.1% NP-40 and 10% glycerol) plus inhibitors (protease inhibitor (cOmplete, EDTA-free; Roche), phosphatase inhibitor cocktail 2 (Sigma-Aldrich) and NaBut [5mM] (Sigma-Aldrich)). Finally, lysates were centrifuged at 3.000 rpm at 4 ºC for 15 minutes. Nuclei enriched pellets were lysed with SDS Lysis Buffer (1% SDS, 10mM EDTA and 50mM Tris [pH 8.0]) plus inhibitors and extracts were sonicated with Bioruptor® Plus 300 to generate 400 to 700 bp DNA fragments. Samples were centrifuged at 13.000 rpm, 4ºC, 10 min to remove insoluble material, and the supernatant containing DNA–protein complexes was collected. Additionally, protein quantification from sonicated chromatin was performed using Pierce® BCA protein assay kit (Thermoscientific; Themo Fisher Scientific Inc.). The chromatin was diluted 1/10 with Dilution Buffer (0.01% SDS, 1.1% Triton X-100, 1.2 mM EDTA pH8, 16.7 mM Tris pH 8 and 167 mM NaCl) and pre-cleared with 50 µL protein A/G agarose beads (Santa Cruz Biotechnology, Inc.) and 40 µg of normal IgG (Santa Cruz Biotechnology, Inc.) for each 500 µg of protein. Samples were placed in a rotor for 1–3 h at 4ºC. The mixture was centrifuged and the supernatant was collected. 100 µg of protein were used for each ChIP assay, reserving 10µg as the input. The antibodies (Supplementary Table 2) were added to the chromatin lysate, incubated on a rotor O/N at 4ºC. Immune complexes were precipitated by the addition protein A/G agarose beads. As a negative control, non-immune rabbit IgG (Santa Cruz Biotechnology, Inc.) was used in place of specific antibodies. Immuneprecipitated complexes were washed three times with the following buffers: Low-Salt Wash Buffer (0.1% SDS, 1% Triton X-100, 2 mM EDTA pH8, 20 mM Tris pH 8 and 150 mM NaCl), High-Salt Wash Buffer (0.1% SDS, 1% Triton X-100, 2 mM EDTA pH8, 20 mM Tris pH 8 and 500 mM NaCl), and LiCl Wash Buffer (250 mM LiCl, 1% NP-40, 1% NaDOC, 1mM EDTA and 10 mM Tris pH8). Immune complexes were eluted in 100 µL 1% SDS and 100 mM $NaHCO_3$ at 37ºC for 30 min. DNA-protein cross-links were reversed by adding NaCl to a final concentration of 200mM O/N at 60ºC. Protein digestion was preformed 1h at 37ºC by adding Proteinase K 0.04 mg/mL (Promega ref. MC5005), 50 mM EDTA pH8 and 500 mM Tris pH6.5 at final concentration. Finally, DNA was purified with QIAquick Gel Extraction Kit following the manufacturer procedures (Qiagen, Hilden, Germany) and eluted in 140 µL DNA/RNAse free MilliQ

water. 4µL of purified DNA was used to perform a qPCR, using the listed primers on Supplementary Table 1.

7.- Protein identification by Western Blot:

Hippocampal slices or primary hippocampal neurons were lysed on ice with a solution containing 1M Tris-HCl, 1% Nonidet P-40, 150 mM NaCl, 5 mM EDTA, 1 mM sodium orthovanadate, 1 mM dithiotreitol, pH 7.4, protease inhibitor cocktail (Roche) and phosphatase inhibitor cocktail 2 (Sigma-Aldrich). Protein concentration was determined by Pierce® BCA protein assay kit (Thermoscientific). Protein samples were electrophoretically resolved within reduced and denaturing gels: 8% for CREB, 10% for CaMKIIα and 15% for Histones, and afterwards transferred to nitrocellulose membranes using iBlot Gel Transfer System (Invitrogen). Membranes were blocked for 1 hour in Tween 20-Tris buffer solution (TTBS: 0.1% v/v Tween 20, 100 mM Tris-HCl, 150 mM NaCl, pH 7.5), containing 5% BSA (Sigma-Aldrich), and incubated overnight at 4°C with the antibodies (Supplementary Table 2), diluted in 5% BSA in TTBS. Peroxidase-conjugated polyclonal goat anti-rabbit (Dako ref. P0448) or peroxidase-conjugated polyclonal rabbit anti-mouse (Dako ref. P0260) were used as secondary antibodies at 1:5000 for 1 h at RT in TTBS containing 5% BSA. Bands were visualized with Super Signal (Thermoscientific) in an ImageQuant LAS 4000 Mini (GE Healtcare Life Sciences). Bands were quantified with ImageJ.

8.- p38 antobody validation for ChIP:

Wild type and p38 KO MEFs were traded with 100 mM NaCl for 45 minutes in order to induce hyperosmotic stress, a treatment known to activate p38 and promote its recruitment to different genes promoters (Ferreiro et al., 2010). In Figure R7 (see pag. 66) we show p38 is recruited to *Cox2* promoter upon hyperosmotic stimulation in WT MEFs and that this recruitment does not take place in p38 KO MEFs. These results suggest that the antibody used is ChIP grade for p38 (Supplementary Table 2).

9.- H3K27Me3S28p antibody crossreactivity:

Inreasing amounts of Histone H3 peptides containing different marks (Diagenode: H3K9Me3S28p ref. C16000128, H3K27 unmodified ref.C16000998, H3K27Me3 ref. C16000069, H3K27Me3S28p ref. C16000091) mixtures were loaded onto a nitrocellulose membrane using a dot-blot (Bio-Rad, ref. 1706545). Membrane were blocked 1h with 5% BSA in TTBS and incubated O/N with H3K27Me3S28p antibody (Supplementary Table 2). Peroxidase-conjugated polyclonal goat anti-rabbit (Dako ref. P0448) was used as secondary antibody at 1:5000 for 1 h at RT in TTBS containing 5% BSA. Dots were

visualized with Super Signal (Thermoscientific) in an ImageQuant LAS 4000 Mini (GE Healtcare Life Sciences).

10.- Histone H3 peptides dephosphorylation:

20 µL of Histone H3 peptides H3K27Me3 and H3K27Me3S28p 10 µM (Diagenode, H3K27Me3 ref. C16000069, H3K27Me3S28p ref. C16000091) were incubated for 1hour at 37ºC with 4 units of Alkaline Phosphatase (CIP; New England BioLabs ref. M0290S) and in a buffer containing 50 mM HEPES (pH 7.9) and MgCl 10 mM. 20 µL of Histone H3 peptides H3K27Me3 and H3K27Me3S28p 10 µM control non dephosphorylated peptides were incubated in a buffer containing 50 mM HEPES (pH 7.9) and MgCl 10 mM plus phosphatase inhibitors. After treatment mixtures were loaded onto a nitrocellulose membrane using a dot-blot (Bio-Rad, ref. 1706545). Membrane were blocked 1h with 5% BSA in TTBS and incubated O/N with H3K27Me or H3K27Me3S28p antibodies (Supplementary Table 2). Peroxidase-conjugated polyclonal goat anti-rabbit (Dako ref. P0448) was used as secondary antibody at 1:5000 for 1 h at RT in TTBS containing 5% BSA. Dots were visualized with Super Signal (Thermoscientific) in an ImageQuant LAS 4000 Mini (GE Healtcare Life Sciences).

11.- Chromatin dephosphorylation:

Samples were collected and sonicated in Sof Lysis Buffer and SDS Lysis buffer with protease inhibitors and without EDTA, and finally chromatin was adjusted at 1µg/µL with SDS Lysis Buffer without EDTA. Samples were incubated for 1hour at 37ºC with 4 units of Alkaline Phosphatase *per* µg of chromatin (CIP; New England BioLabs ref. M0290S) and MgCl 10 mM. After 1 hour phosphatase inhibitor was added. Control non-de-phosphorylated samples were incubated 1 hour at 37ºC with MgCl 10 mM and phosphatase inhibitors. After de-phosphorylation treatment we followed ChIP protocol by diluting samples 1/10 with Dilution Buffer.

12.- Lentiviral production and neuronal infection:

Packaging plamids and Sh-RNA plamid against JMJD3 or srcamble were purchased from Origene. Lentiviral particles were produced in HEK293T according to Origene instructions. Neurons were infected at 11 DIV and medium was fully changed with neuronal conditioned medium at 12 DIV. Experiments were performed at 15 DIV.

13- JMJD3 antibody validation for ChIP:

In the Figure R9 we show the experiments designed to assess the specificity of the antibody used. In the panel A we show that treatment of hippocampal neurons in culture

with a lentivirus expressing a shRNA to knock down JMJD3 leads to a 50% reduction in the amount of the specific mRNA compared to cultures infected with leniviral particles expressing a scrambled shRNA. In the panel B, the Western blot show that JMJD3 knock down resulted in a 75% reduction of JMJD3 compared to scrambled-shRNA treated controls. The ChIP experiments performed with the Abcam, ab38113 antibody (Supplementary Table 2) show that the enrichment of JMJD3 at the *Bdnf* promoters is lost in cultures where JMJD3 was knocked down. These results suggest that the antibody used is ChIP grade for JMJD3.

14.- *In vitro* JMJD3 demethylase activity assay:

Histone demethylase assay was performed as described by Hong et al. (Hong et al., 2007) with minor modifications. Briefly, 10 μM of H3K27Me3 (Diagenode) peptide were incubated with 0 or 14 pmol of the active human recombinant JMJD3 (Sigma-Aldrich, ref. SRP0162) in the demethylase assay buffer [50 mM HEPES (pH 7.9), 50 mM KCl, 50 mM $(NH_4)_2Fe(SO_4)_2 \cdot 6(H_2O)$, 1 mM α-ketoglutarate, and 2 mM ascorbic acid]. 10 μM H3K27Me3S28p peptide (Diganeode) were incubated with increasing concentrations (0, 3.5, 7 and 14 pmol) of the active human recombinant JMJD3 in the demethylase assay buffer. Demethylation assay mixtures were kept for 5 h at 37°C with soft agitation (400 rpms). Assay mixtures were loaded onto a nitrocellulose membrane using a dot-blot (Bio-Rad, ref. 1706545). Membrane were blocked 1h with 5% BSA in TTBS and incubated O/N with specific antibodies (Supplementary Table 2). Peroxidase-conjugated polyclonal goat anti-rabbit (Dako ref. P0448) was used as secondary antibody at 1:5000 for 1 h at RT in TTBS containing 5% BSA. Dots were visualized with Super Signal (Thermoscientific) in an ImageQuant LAS 4000 Mini (GE Healtcare Life Sciences). Dots were quantified with ImageJ.

15.- Immunoprecipitation:

HEK293T cells were transfected with Lipofectamine 2000 according to the manufacturer instructions (Life technologies, ref. 11668) using a plasmid that drive the expression of 6xMyc-JMJD3-FLAG (Addgene, ref. 17440; Hong et al., 2007) and a plasmid that drive the expression of CBP when co-transfectred with a Tet-Off containing plasmid (kindly provided by Dr A. Barco; Instituto de Neurociencias, Universidad Miguel Hernández-Consejo Superior de Investigaciones Científicas, Alicante, Spain; Valor et al., 2011). HEK293T were treated with Forskolin (50μM) and Rolipram (0.1 μM) for 15 min and crosslinked with dithiobis(succinimidyl-propionate) (DSP) 5 mM (Life technologies ref. 22585) for 30 min at RT, and reaction was stopped by adding Tris pH7.5 at final concentration 20 mM for 15 min. Cells were washed two times with cold PBS and

homogenized in STEN plus inhibitors and sonicated until clarification. Samples were pre-cleared with 40 µL protein A/G agarose beads and 10 µg of normal IgG for each 200 µg of protein. Samples were placed in a rotor for 1–3 h at 4ºC. The mixture was centrifuged and the supernatant was collected. 200 µg of protein were used for each IP assay. The antibodies (Supplementary Table 2) were added to the lysate, incubated on a rotor O/N at 4ºC. Immune complexes were precipitated by the addition protein A/G agarose beads. As a negative control, non-immune mouse IgG was used in place of specific antibodies. Immuneprecipitated complexes were washed five times with STEN Buffer and one time with PBS. Complexes were eluted with Laemmli Buffer 2X (120 mM Tris pH 6.8, 4% SDS, 20% glycerol, 2% ß-mercaptoethanol and 0,02% bromophenol blue) for 10 min at 95ºC and proteins were identified by Western Blot.

16.- Cholesterol quantification:

Hippocampal slices were washed in cold PBS and then homogenized in a lysis buffer containing 25 mM MES, 2 mM EDTA and cocktails of protease and phosphatase inhibitors from Roche. The protein amount was quantified by Pierce® BCA Assay Kit (Thermo Scientific) and the cholesterol content measured per µg of protein using the Amplex® Red Cholesterol Assay Kit (Invitrogen).

17.- Animal treatment and behaviour experiments:

17.1.- Oral Treatment with Voriconazole:

Voriconazole (from HangZhou Dayangchem Co., CAS No:137234-62-9) was solubilized using hydroxyl propyl-b-cyclodextrin (Sigma): 15g of hydroxyl propyl-b-cyclodextrin were dissolved in 100ml of saline solution (0.9% NaCl) and heated to 80°C in a water bath with stirring. Then, 1.5g Voriconazole was slowly added to the cyclodextrin solution with stirring at 80°C until complete dissolution. This stock solution (15 mg voriconazole/ml cyclodextrin/saline) was conserved at 4°C protected from the light. On the first day of experimentation, an aliquot of this solution was diluted in drinking water to a final concentration of 0.68 mg/ml Voriconazole. Considering that a mouse drinks 3 ml water per day, the dose corresponds to 2.04 mg/day. The average weight of a mouse is 34 g, resulting therefore in a dose 60 mg/kg b.w. Water with this concentration of Voriconazole was used as the hydration source in 19 month-old mice during 45 days. Vehicle, 19 month-old mice received the same amount of hydroxyl propyl-b-cyclodextrin than Voriconazoles during 45 days. Bottles containing the Voriconazole or Vehicle water were changed weekly.

17.2.- Water Maze Learning: Spatial training

The water maze was a white circular pool (1.5 m diameter, 45 cm high) filled with water diameter containing water made opaque with white non-toxic paint, at 24 ± 1 ºC. An invisible escape platform (10 cm diameter) was placed at a fixed location equidistant from the sidewall and middle of the pool, and submerged 1 cm below the water surface. The behaviour of the animal (latency, distance, swim speed, and navigation path) was monitored by a video camera, mounted in the ceiling above the centre of the pool, and a computerized tracking system (Ethovision 1.90, Noldus IT, The Netherlands). Mice received four trials of 90 s maximum, separated by a 45- to 60-min inter-trial interval every day for four consecutive days. If the animal failed to escape within 90 s, it was gently guided to the platform by the experimenter and allowed to remain on it for 30 s. During the training procedure, the location of the platform remained constant in one virtual quadrant of the maze, and the starting position for each trial was varied among four equally spaced positions around the perimeter of the maze. On day 5, we conducted a probe trial in which the escape platform was removed from the pool and the mouse was allowed to swim for 60 sec. The trial began with the mouse in the quadrant opposite to the trained platform location. The time spent in each quadrant was recorded. During the visible platform task, the platform was cued with a black flag.

17.3.- Novel-Object Location

Mice were first habituated individually to an empty open-field box (35 x 35 x 15 high cm) for 30 min, during 2 consecutive days. A sample trial (object exposure) consisted of placing a mouse into the test box, which contained 2 identical objects, small plastic toys (10 x15 high cm) that were placed in a symmetrical position about 5 cm away from walls, and the animal was allowed to explore them for 5 min. The objects were always thoroughly cleaned between sessions using a 0.1% acetic acid solution. Spatial memory was evaluated after a 30 min delay during a 3 min test. A preference index, a ratio of the amount of time spent exploring the novel object over the total time spent exploring both objects, was used to measure recognition memory. Exploration was defined as follows: directing the nose to the object at a distance of no more than 2 cm and/or touching the object with the nose. Novel and familiar object location was counterbalanced across animals. This task depends on the hippocampal function (Galani et al., 1998).

17.4.- Fear conditioning

Training and testing took place in a rodent observation cage (30 × 37 × 25 cm) that was placed in a sound-attenuating chamber. In the training (conditioning), the mouse was exposed to the conditioning context (180 sec) followed by a tone (CS, 20 sec, 2 kHz, 85

dB). After termination of the tone, a footshock (US, 0.75 mA, 2 sec) was delivered through a stainless steel grid floor. Mice received three footshocks with an inter-trial interval of 60 s. Mice were removed from the fear conditioning box 30 sec after shock termination and returned to their home cages. Testing: In the contextual fear conditioning version, mice were placed back into the original training context for 8 min, during which no footshock was delivered. In the auditory-cued fear conditioning version, animals were placed into a novel context (same cages, but with different walls, floor, and background odour), and, after a 3 min baseline period, they were continuously reexposed to the tone (same characteristics as at conditioning) for 5 min, but in the absence of shocks. The animals' behaviour was video recorded and later scored by an observer blind to the treatment condition. Using a time-sampling procedure every 2 s, each mouse was scored blindly as either freezing or active at the instant the sample was taken. Freezing was defined as behavioural immobility except for movement needed for respiration.

18.- Animal handling:

All the experiments were performed in accordance with European Union guidelines (2010/63/UE) regarding the use of laboratory animals.

19.- Statistical analysis:

All values are presented as mean ± SEM. In Chapter 1, Mann-Whitney U test or Kruskal-Wallis followed by Mann-Whitney U test multiple comparisons with Bonferroni adjustment were used for statistical analysis. In Chapter 2, data normality and variances were tested by Shapiro–Wilk test and Levene test respectively. Mann–Whitney U-test, Kruskal-Wallis or Friedman were used for nonparametric data, and one-sample t-test, Student's t-test or ANOVA for parametric data, assuming or not equal variances. All the analysis was performed using SPSS6 (SPSS6 Statistics, IBM.). For values and statistical analysis see Supplementary tables 3-32. In the figures asterisks indicate P values as follows: *< 0.05; **< 0.01; ***< 0.001.

RESULTS

CHAPTER I: Epigenetic regulation of *Bdnf* transcription upon LTD.

1.1.- Transcriptional analysis of *Bdnf* promoters.

We first determined whether or not the mild synaptic stimulation triggered by low doses of N-methyl-D-aspartate (NMDA) is able to induce expression changes of *Bdnf* promoters. Hippocampal neurons maintained in culture for 2 weeks were exposed during 5 min to 20μM NMDA, a stimulus known to lead to LTD (Ehlers, 2000; Fernández-Monreal et al., 2012; Lee et al., 1998; Lin et al., 2000). The expression levels of exons I, II, IV and VI were then determined by qPCR at different time points after stimulation. Fig. R1 A-B shows that a significant increase was observed for transcripts II and VI at 10min after NMDA addition. The amount of these mRNAs reached a peak at 30 min after stimulation and returned to basal levels at later time-points: 60 min for mRNA VI and 180 min for mRNA II. The expression of exons I and IV however, presented a different behavior since a significant increase of these mRNAs was observed only after 30 min upon stimulation. The levels of mRNA I remained at maximum along the entire length of time analyzed (180min) while the levels of mRNA IV returned to basal at 180min after NMDA application.

These results reveal that chemically induced LTD (NMDA-LTD) triggers two different responses of these *Bdnf* promoters, a fast response of promoters II and VI driving a transient expression of *Bdnf* exons II and VI and a slower response of promoters I and IV, leading to a more stable expression of exons I and IV.

1.2.- Epigenetic marks found at *Bdnf* promoters in mature neurons.

As commented in the Introduction, the structure and genetic environment of *Bdnf* promoters I, II, IV and VI suggest that *Bdnf* could be a bivalent gene, and that its promoters are potential sites to be controlled by repressive (PRC) and activating (H3K4Me3) marks. Hence we next assessed if activator trimethyl-H3K4 (H3K4Me3) and repressor trimethyl-H3K27 (H3K27Me3) are present at *Bdnf* promoters under non-stimulated conditions. In addition, we also searched for the presence of acetyl-H3K27 (H3K27Ac) as an activation form of the H3K27. Chromatin immunoprecipitation (ChIP) assays followed by promoter-specific qPCR performed in non-stimulated hippocampal neurons revealed that these three histone marks are present in all the four *Bdnf* promoters (Figure R2 A-C).

The amount of each histone mark at *Bdnf* promoters was compared to the amount bound to the promoters of two control genes, *ßActin* and *hoxA1*. In fact, the constitutively active *ßActin* presents high levels of activator marks H3K27Ac and H3K4Me3 (Fig. R2 A, B) and low levels of the repressive H3K27Me3 mark (Fig. R2C). In contraposition, the

constitutively repressed *hoxA1* showed high levels of the repressive H3K27Me3, low amounts of H3K4Me3 and undetectable H3K27Ac (Fig. R2 A-C).

To further substantiate that *Bdnf* promoters I, II, IV and VI are repressed by PRC in non stimulated neurons, we determined the level of association to Enhancer of zeste homologue 2 (EZH2), the catalytic subunit of the Polycomb Repressive Complex 2 (PRC2), to these promoters. ChIP experiments revealed the presence of EZH2 associated to the four *Bdnf* promoters (Fig. R2D) at levels that are comparable to the levels bound to

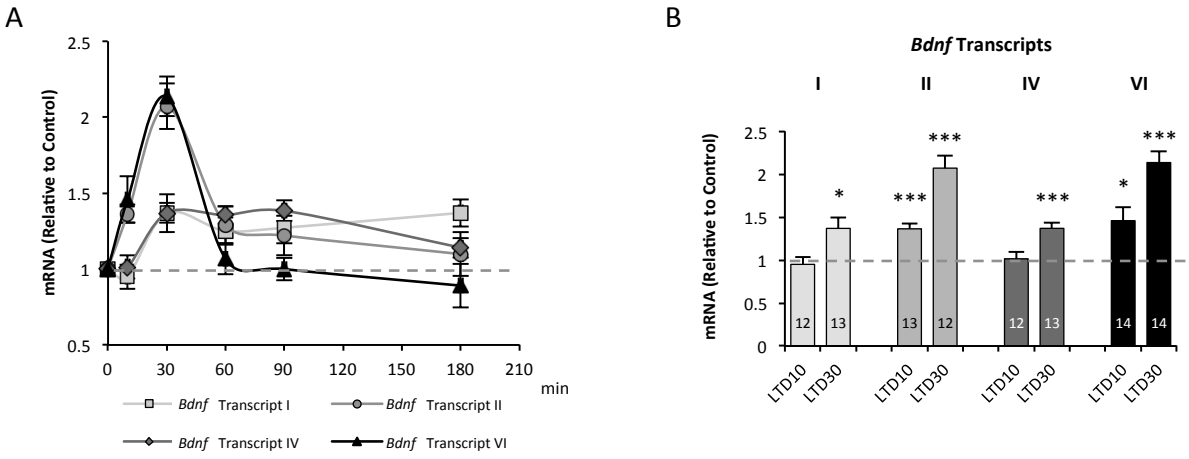

Figure R1: **Response of *Bdnf* promoters to NMDA stimulation in mature hippocampal neurons.**

A) RT-qPCR analysis of the levels of *Bdnf* mRNAs transcribed from promoters I, II, IV and VI after NMDA stimulation. B) The bar plot shows the relative amount of each transcript compared to non stimulated controls at 10 or 30 min after NMDA addition. Data are represented as mean ± SEM (*p<0.05; **p<0.01, ***p<0.001). For statistical analysis see Supp. Table 3.

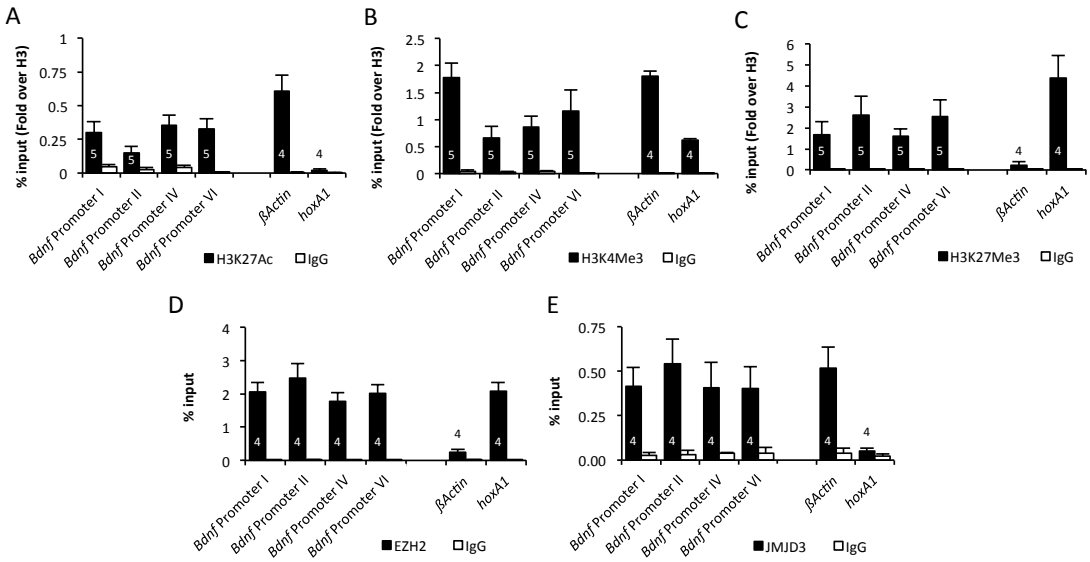

Figure R2**: Epigenetic marks found at *Bdnf* promoters in mature neurons**

A-E) ChIP-qPCR analysis of epigenetic marks and regulatory proteins bound at *Bdnf* promoters in basal conditions: (A) H3K27Ac, (B) H3K4Me3, (C) H3K27Me3, (D) EZH2 and (E) JMJD3. The plots also show the levels of the respective marks found at the promoter region of two control genes: a constitutively transcribed *ßActin* and a repressed gene *hoxA1*. For values see Supp. Table 4.

the PRC2 repressed gene *hoxA1*. Strikingly, a similar ChIP experiment revealed that, different from *hoxA1*, high levels of the H3K27Me3-demethylase Jumonji domain containing-3 (JMJD3) were present at these *Bdnf* promoters suggesting that these promoters are ready to be de-repressed by H3K27Me3 demethylation (Fig. R2E).

1.3.- NMDA leads to epigenetic remodeling at *Bdnf* promoters.

To test if NMDA-LTD induces quantitative changes in the different histone marks at our target promoters, similar ChIP experiments were performed in 2 week-old hippocampal neurons in culture 10 minutes after NMDA stimulation. Figure R3A shows the result of this study: the activation marks H3K4Me3 and H3K27Ac, as well as the JMJD3 demethylase, all increased by the LTD stimulus at promoters II and VI. Furthermore, NMDA treatment resulted in lower levels of the repressor EZH2 at promoters II and VI and reduction of the repressive H3K27Me3 mark at promoter VI. These results may explain the enhanced expression of these transcripts after NMDA stimulation. On the other hand, no change in the levels of these marks were detected at promoter I after stimulation, according to the later expression time of this transcript (30 min, see Fig. R1A). However, in promoter IV, which also undergoes a delayed increased expression (see Fig. R1A), significant decreased levels of repressor EZH2 were accompanied by recruitment of the H3K27Me3 demethylase JMJD3 and decreased amount of H3K27Me3, which would imply derepression at this early time. However, different from promoters II and VI, no increase of the activator marks H3K4Me3 and H3K27Ac was observed at this promoter

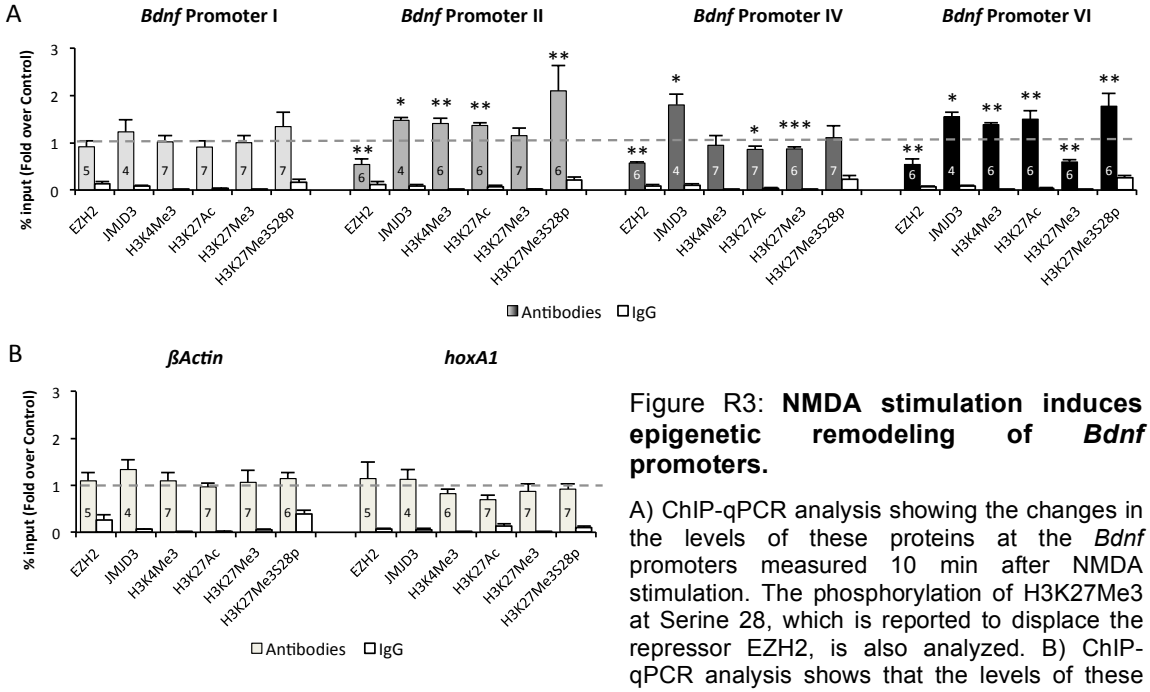

Figure R3: **NMDA stimulation induces epigenetic remodeling of *Bdnf* promoters.**

A) ChIP-qPCR analysis showing the changes in the levels of these proteins at the *Bdnf* promoters measured 10 min after NMDA stimulation. The phosphorylation of H3K27Me3 at Serine 28, which is reported to displace the repressor EZH2, is also analyzed. B) ChIP-qPCR analysis shows that the levels of these proteins do not change 10 min after NMDA stimulation at control *ßActin* and *hoxA1* promoters. Data are represented as mean ± SEM (*p<0.05; **p<0.01, ***p<0.001). For statistical analysis see Supp. Table 5.

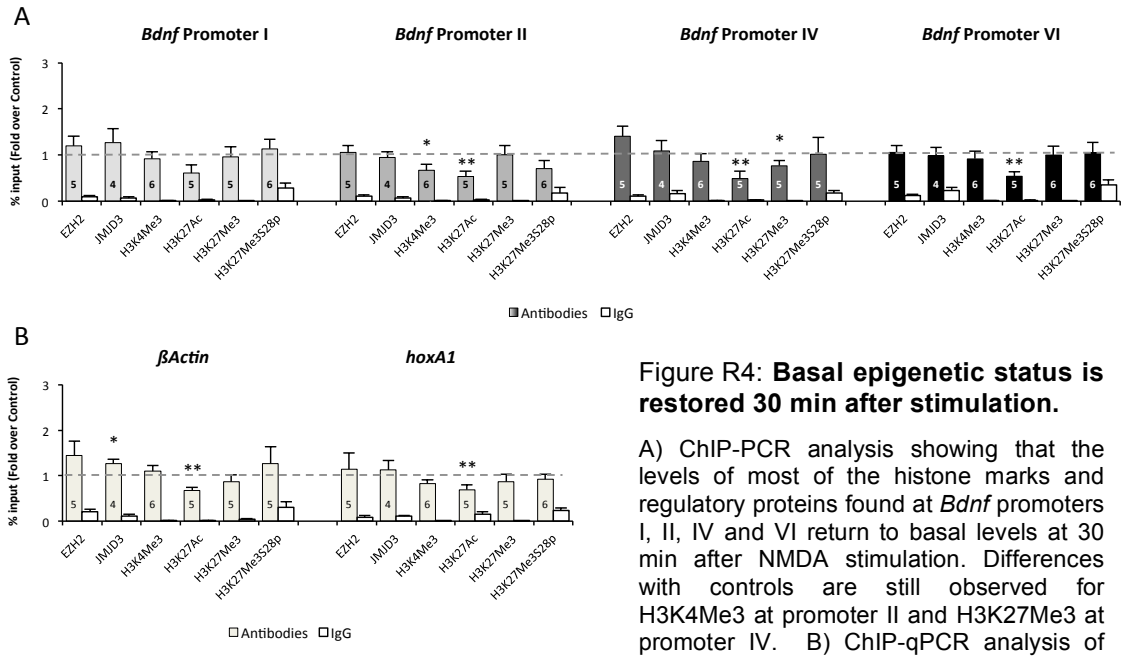

Figure R4: **Basal epigenetic status is restored 30 min after stimulation.**

A) ChIP-PCR analysis showing that the levels of most of the histone marks and regulatory proteins found at *Bdnf* promoters I, II, IV and VI return to basal levels at 30 min after NMDA stimulation. Differences with controls are still observed for H3K4Me3 at promoter II and H3K27Me3 at promoter IV. B) ChIP-qPCR analysis of these proteins 30 min after NMDA stimulation at *ßActin* and *hoxA1* control promoters. Levels of H3K27Ac that are lower than in non stimulated cells were found at all promoters suggesting a that H3K27 deacetylation could be a general effect observed at 30 min after NMDA addition. Data are represented as mean ± SEM (*p<0.05; **p<0.01). For statistical analysis see Supp. Table 6.

implying that both, increase of activation marks and decreased repressive marks, are required for fast transcriptional induction.

As expected, we did not observe changes in the levels of these epigenetic marks in the promoter regions of the control genes *ßActin* and *hoxA1*, which are not regulated by NMDA (Fig. R3B).

ChIP experiments performed 30 min after NMDA stimulation showed that the levels of all histone marks and their upstream regulators were restored to basal conditions. Significantly, lower levels of H3K27Ac, compared to non-stimulated controls, were observed at promoters II, IV and VI (Fig. R4A), suggesting that H3K27Ac deacetylation is involved in the silencing of these promoters after stimulus. However, the possibility of a general effect triggered after NMDA-LTD could not be discarded since reduced levels of H3K27Ac were also observed at the control genes 30 min after NMDA application (Fig. R4B).

1.4.- Derepression of *Bdnf* requires H3K27Me3S28 phosphorylation.

It has been reported that p38 MAPK and mainly its downstream kinases, mitogen- and stress-activated kinases (Msk1 and Msk2), lead to gene activation through H3K27Me3 phosphorylation at Serine 28, and the consequent displacement of the EZH2 and promoter derepression (Gehani et al., 2010). That was proposed as a mechanism required to activate a subset of Polycomb group of proteins (PcG) target genes by biological stimuli in developing cells (Gehani et al., 2010). ChIP experiments revealed that

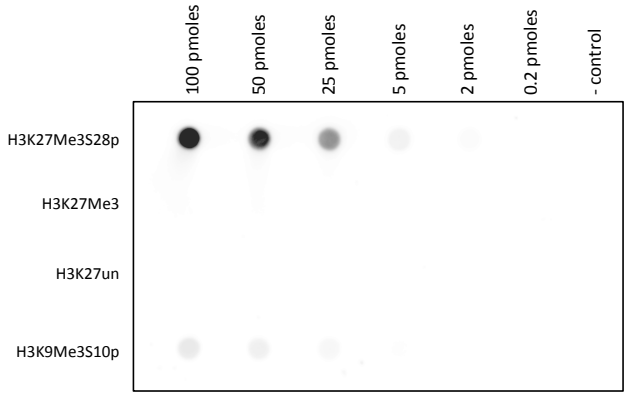

Figure R5: **H3K27Me3S28p antibody corsreactivity.**

H3K27Me3S28p Rabbit antibody cross reactivity: Increasing concentrations of histone H3 peptides containing marks (H3K27Me3S28p, H3K27Me3, H3K9Me3S10p or unmodified H3) were loaded onto a Dot Blot and incubated wit the antibody against H3K27Me3S28p. The experiment shows a weak cross reactivity to H3K9Me3S10p.

H3K27Me3S28 phosphorylation occurs at *Bdnf* promoters II and VI after 10 min of NMDA stimulation (Figure R3A), suggesting that a mechanism similar to the one reported in developing cells may participate during NMDA-induced *Bdnf* expression in mature neurons. In the Figure R5 we show that the antibody used in our experiments does not cross react with H3K9Me3S10p as previously reported for other rabbit polyclonal antibodies for H3K27Me3S28p (Gehani et al., 2010; Rothbart et al., 2015).

To assess if the p38 MAPK pathway may be involved in H3K27Me3S28 phosphorylation in mature neurons, we treated NMDA-stimulated hippocampal neurons with the p38 specific inhibitor SB-203580 (Kramer et al., 1996; Powell et al., 2003; Saklatvala et al., 1996). The qPCR analysis revealed that this treatment prevented NMDA-induced increase of transcripts II and VI (Fig. R6A). Moreover, ChIP experiments showed that p38 MAPK inhibition abolished NMDA-induced H3K27Me3S28 phosphorylation at promoters II and VI (Fig. R6B). According to these results, ChIP assays performed using a ChIP tested antibody against p38 (Fig R7A) showed that LTD-induced recruitment of p38 to promoters II and VI at 10 min after stimulation (Fig. R7B-C).

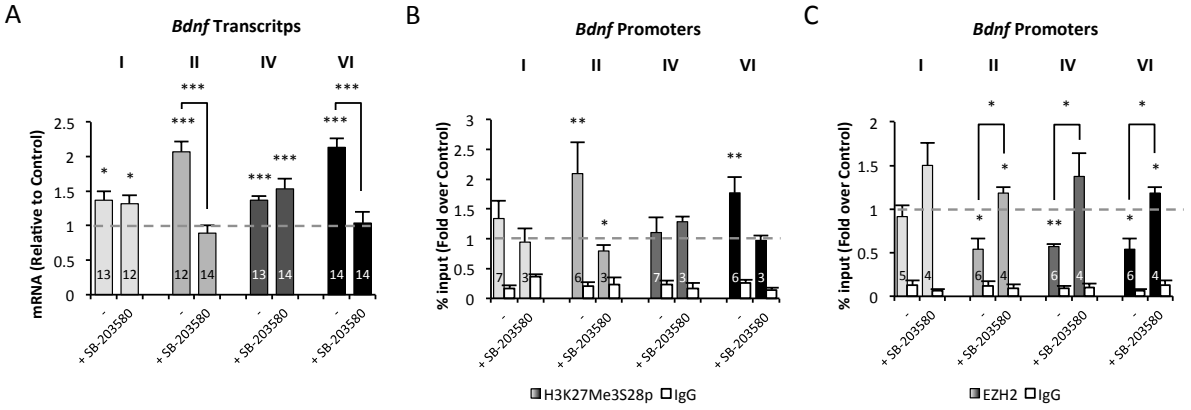

Figure R6: **LTD induced derepression and transcription of *Bdnf* promoters II and VI requires EZH2 displacement *via* p38 pathway activation.**

A) RT-qPCR analysis of the *Bdnf* transcripts shows that treatment with the p38 inhibitor SB-203580 blocks the increase of mRNAs transcribed from promoters II and VI at 30 min after NMDA stimulation. B-C) ChIP-qPCR analysis performed 10 min after stimulation shows that SB-203580 impairs H3K27Me3S28 phosphorylation at promoters II and VI (B). Interestingly, SB-203580 blocked EZH2 displacement from the four promoters studied suggesting a role for EZH2 in the transcriptional control of these regions (C). Data are represented as mean ± SEM (*p<0.05; **p<0.01; ***p<0.001). For statistical analysis see Supp. Table 7.

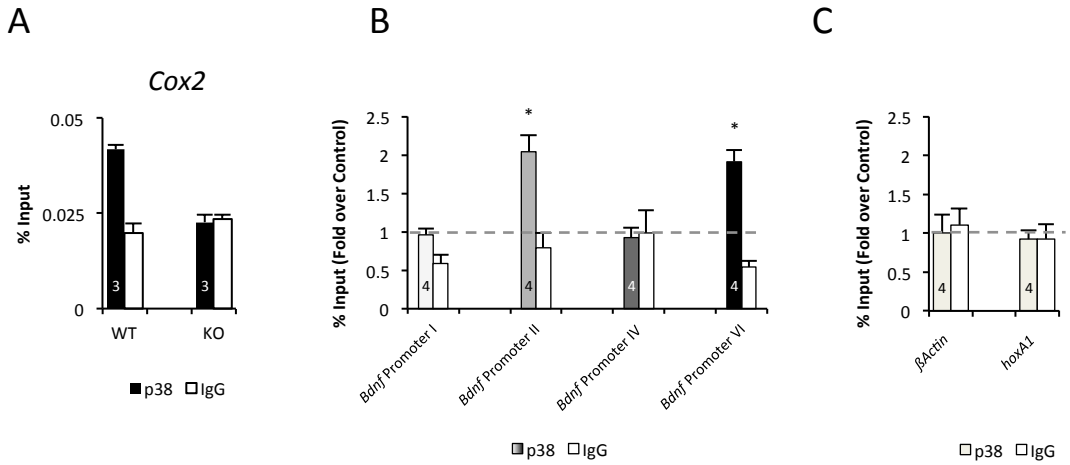

Figure R7: **p38 is recruited to *Bdnf* promoters II and VI after LTD.**

A) p38 antibody validation for ChIP : WT or p38-KO MEFs were treated with 100 mM NaCl for 45 min in order to induce p38 recruitment to *Cox2* promoter. The ChIP experiments show that p38 is detected, above of non specific signal, only in the WT cells. B) ChIP assays performed in neuronal cultures show that LTD induction triggers the recruitment of p38 to promoters II and VI at 10 min after stimulation. C) p38 is not recruited to the promoter region of control genes *ßactin* and *hoxA1* after LTD induction. Data are represented as mean ± SEM. (*p<0.05). For statistical analysis see Supp. Table 8.

In further support that phosphorylation of H3K27Me3S28 is required for Polycomb removal, p38 inhibition precluded EZH2 displacement from *Bdnf* promoters II and VI after NMDA stimulation (Fig R6C). Differently from these promoters, the expression of exons I and IV was not affected by the treatment with the inhibitor (Figs. R6A and R6B), further strengthening our early assumption that promoters I and IV are controlled by mechanisms different from the ones controlling promoters II and VI. Although the SB-203580 also blocked the release of EZH2 from promoters I and IV (change not significant in the case of promoter I), increases in H3K27Me3S28p were not observed in these two promoters after NMDA stimulation, further strengthening the notion that both derepression and activation are required for NMDA-induced *Bdnf* expression.

Altogether, these data show that the p38 pathway is involved in H3K27Me3S28 phosphorylation and required for the displacement of EZH2 from promoters II and VI after NMDA treatment. Gehani *et al*. (2010) (Gehani et al., 2010) have demonstrated that Msk1/2 kinases are required for H3K27Me3S28 phosphorylation in human developing fibroblasts. Furthermore, by *in vitro* experiments these authors have shown that Msk2 kinase phosphorylates H3K27Me3S28 more efficiently than p38. Hence, it appears reasonable to conclude that p38 could lead to H3K27Me3S28 phosphorylation by a dual, direct and indirect (*via* its downstream kinases Msk2) mechanism. Moreover, the results presented here also suggest that the EZH2 displacement could be involved, but is not sufficient, to induce the derepression of promoters I and IV.

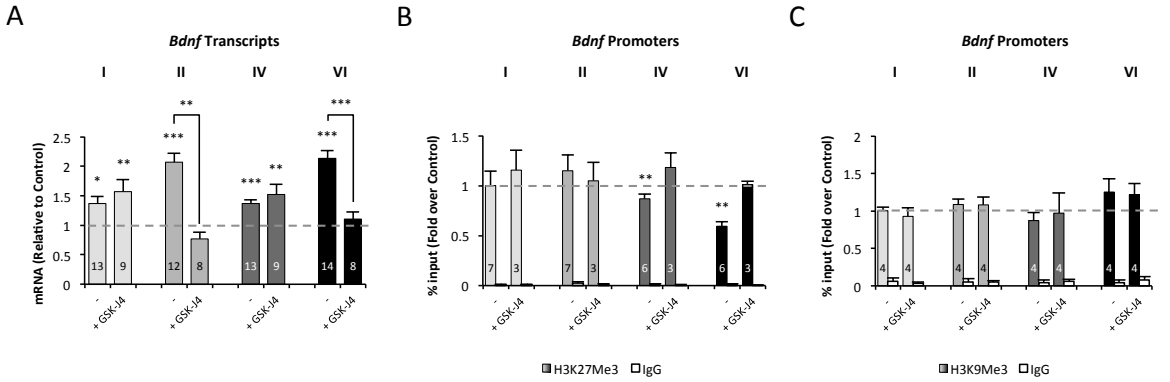

Figure R8: **JMJD3 is involved in H3K27Me3 demethylation and *Bdnf* induction after LTD.**

A) The RT-qPCR analysis show that the H3K27Me3 demethylases inhibitor GSK-J4 impairs the NMDA-triggered increase of *Bdnf* mRNAs II and VI observed 30 min after stimulation. B) ChIP-qPCR studies confirm that H3K27Me3 demethylation observed at *Bdnf* promoters IV and VI is blocked by GSK-J4. C) ChIP experiments showing that demethylation of the repressive mark H3K9Me3 is not involved in the transcriptional induction of *Bdnf* promoters I, II, IV and VI by NMDA-LTD. According to this conclusion, the treatment with the KDM inhibitor GSK-J4 has no effect on the levels of H3K9Me3 bound to these promoters in stimulated neuron. Data are represented as mean ± SEM (*p<0.05; **p<0.01; ***p<0.001). For statistical analysis see Supp. Table 9.

1.5.- JMJD3 recruitment to *Bdnf* is required for activation by LTD.

Our previous ChIP experiments showed that JMJD3 demethylase is recruited to promoters II, IV and VI after LTD induction (Fig. R3A). To test if JMJD3 demethylase activity is in fact playing a role for the transcriptional induction of these *Bdnf* promoters by LTD, ChIP and qPCR were performed in hippocampal neurons treated with the Jumonji H3K27Me3 demethylase inhibitor GSK-J4 (Kruidenier et al., 2012) at the time of stimulation. The qPCR experiment revealed that GSK-J4 inhibited the transcriptional activation of promoters II and VI but had no effect on promoters I and IV (Fig. R8A). The ChIP experiments confirmed that GSK-J4 treatment impaired the decrease of H3K27Me3 observed after NMDA on promoters IV and VI (Fig. R8B). The absence of changes in the levels of H3K27Me3 at promoter II at 10 min after stimulation suggests either that H3K27Me3 demethylation at this promoter occurs at a lower extent than at promoter VI or that it is not detected at 10 min after stimulation. Again, the increase of mRNAs containing exons I and IV was unaffected by the treatment, further supporting the notion that these promoters are controlled by a different regulatory mechanisms. As a matter of fact, even if the GSK-J4 prevented H3K27Me3 demethylation at promoter IV (Fig. R8B), it did not block its activation (Fig. R8A).

The GSK-J4 inhibitor is able to block the catalytic activity of the KDM6 demethylase proteins but also blocks the activity of demethylases from the KDM2, KDM3, KDM4 and KDM5 subfamilies (Heinemann et al., 2014). KDM3 and KDM4 proteins demethylate the repressor mark H3K9Me3, meaning that inhibition of these proteins by GSK-J4 could block induction of the *Bdnf* promoters after LTD, however by ChIP experiments we found

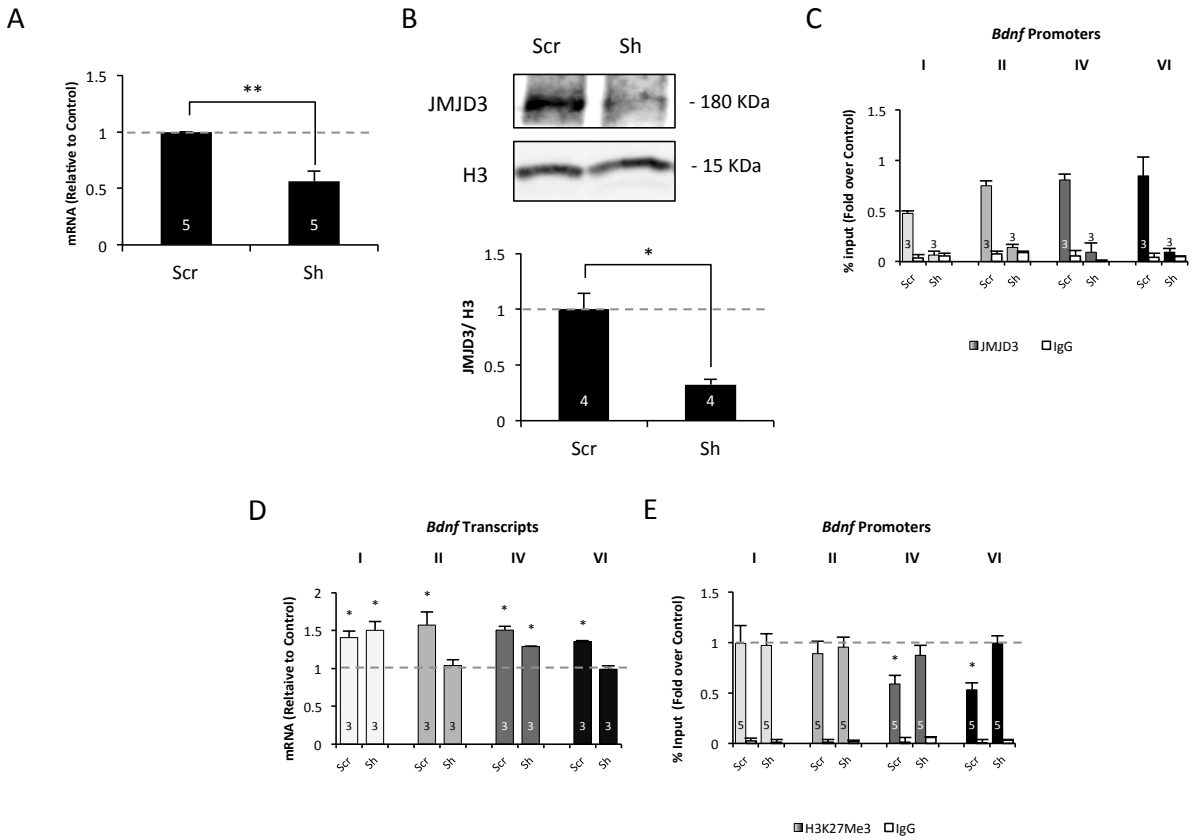

Figure R9: **Genetic validation of JMJD3 involvment in H3K27Me3 demethylation and *Bdnf* induction after LTD.**

A) Quantification by qPCR show that the treatment of hippocampal neurons in culture with a lentivirus expressing a shRNA to knock down JMJD3 (Sh) led to a 50% reduction in the amount of the specific mRNA compared to cultures infected with leniviral particles expressing a scrambled shRNA (Scr). B) Western blot showing that JMJD3 knock down resulted in a 75% reduction of JMJD3 compared to scrambled-shRNA treated controls. C) The ChIP experiments performed with the Abcam, ab38113 antibody show that the enrichment of JMJD3 at the *Bdnf* promoters is lost in cultures where JMJD3 was knocked down. D) The qPCR analysis show that JMJD3 knock down blocked the increase of the *Bdnf* transcripts II and VI triggered 30 minutes after LTD. E) The ChIP results show that the H3K27Me3 demethylation observed at promoters IV and VI in control neuronal cultures (Scr) at 10 min after NMDA addition was blocked by JMJD3 knock down (Sh). Data are represented as mean ± SEM (*p<0.05; **p<0.01). For statistical analysis see Supp. Table 10.

that no H3K9Me3 demethylation is observed at any of the four *Bdnf* promoters at 10 min after NMDA application (Fig R8C)

To further prove that JMJD3 is involved in H3K27Me3 demethylation and *Bdnf* induction after NMDA-LTD, hippocampal neurons were infected with lentiviral particles expressing an shRNA to knock down JMJD3, validating JMJD3 antibody for CIP (Fig. R9A-C). In agreement with the pharmacological results, the qPCR analysis show that JMJD3 knock down blocked the NMDA-mediated *Bdnf* induction of transcripts II and VI (Fig. R9D). The ChIP results have shown that the H3K27Me3 demetylation was also blocked by JMJD3 knock down (Fig. R9E). All together these results confirm that JMJD3 is involved in H3K27Me3 demethylation after NMDA-LTD.

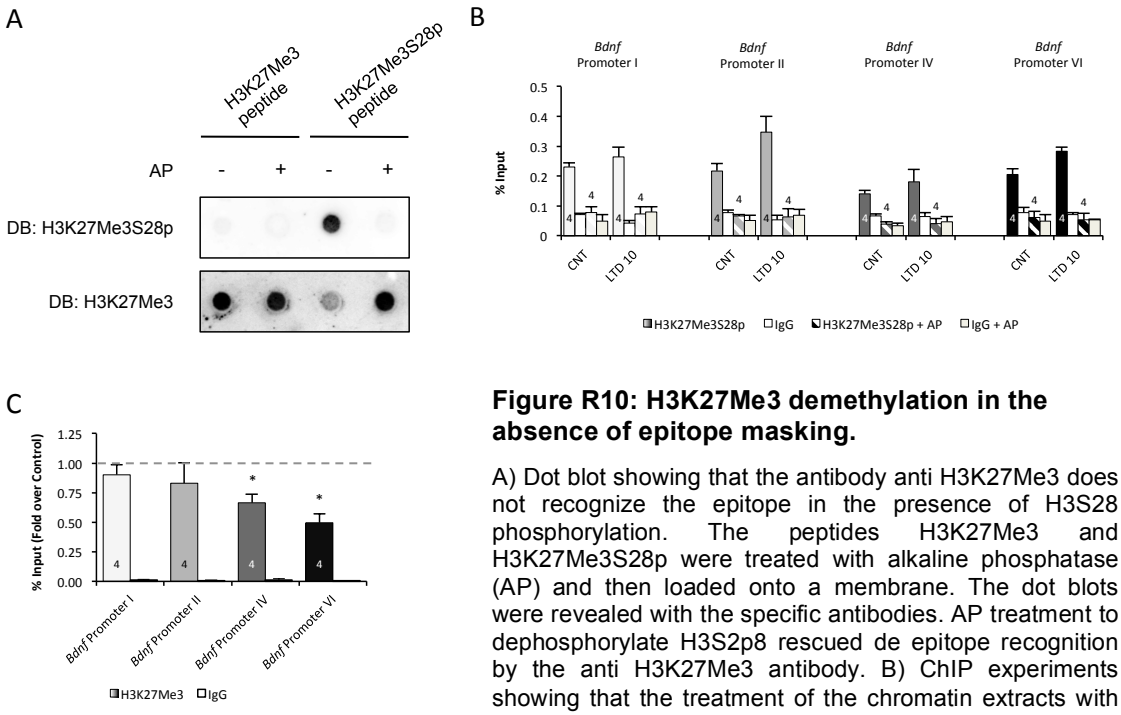

Figure R10: H3K27Me3 demethylation in the absence of epitope masking.

A) Dot blot showing that the antibody anti H3K27Me3 does not recognize the epitope in the presence of H3S28 phosphorylation. The peptides H3K27Me3 and H3K27Me3S28p were treated with alkaline phosphatase (AP) and then loaded onto a membrane. The dot blots were revealed with the specific antibodies. AP treatment to dephosphorylate H3S2p8 rescued de epitope recognition by the anti H3K27Me3 antibody. B) ChIP experiments showing that the treatment of the chromatin extracts with AP completely removed the phosphate groups from H3K27Me3S28p since only background levels (similar to levels obtained with IgG) of this mark were identified at the four *Bdnf* promoters treated. C) The ChIP experiments show that the levels of H3K27Me3 bound to promoters IV and VI decrease at 10 min after LTD induction in AP treated samples. Data are represented as mean ± SEM (*p<0.05). For statistical analysis see Supp. Table 11.

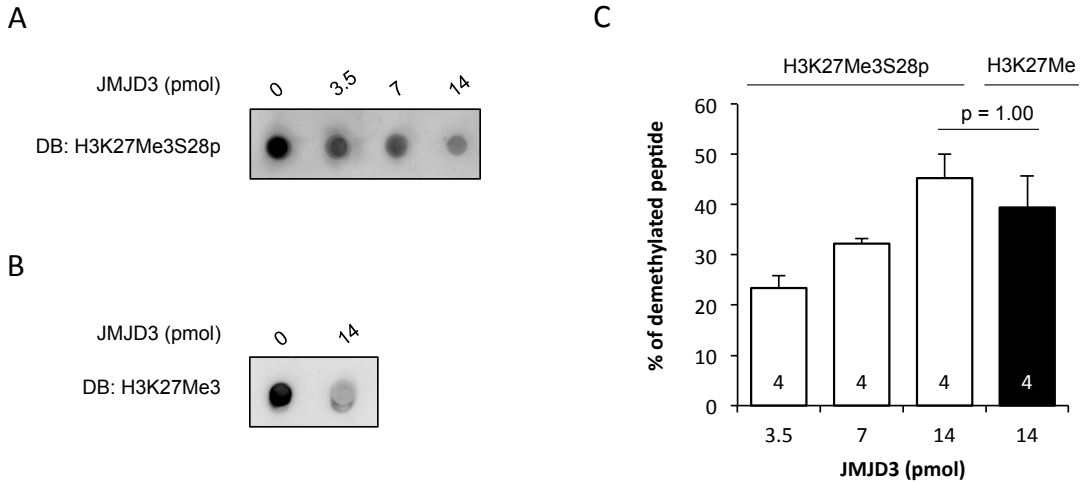

Figure R11: JMJD3 is able to demethylate H3K27Me3S28p *in vitro*.

A) Dot blot revealed for H3K27Me3S28p indicate that the recombinant JMJD3 catalytic domain is able to demethylate the phosphorylated peptide H3K27Me3S28p *in vitro*. B) Control demethylation recombinant JMJD3 catalytic domain assay on H3K27Me3 peptide. C) Quantification of dot blots as shown in A and B. For statistical analysis see Supp. Table 12.

It has been described that H3K27Me3 phosphorylation at Serine 28 masks the recognition of H3K27Me3 by different specific antibodies (Gehani et al., 2010; Rothbart et al., 2015), an event also observed by us (Fig. R10A). It means that the decreases observed in the levels of H3K27Me3 at *Bdnf* promoters after stimulation could be attributed to epitope masking rather than true demethylation. However, experiments

based on extracts obtained from neuronal cultures treated with alkaline phosphatase to remove the phosphate group from H3K27Me3S28p (Fig. R10B) followed by ChIP with H3K27Me3 antibodies, still revealed demethylation. This ChIP shows a significant decrease of H3K27Me3 at promoters IV and VI in phosphatase-treated samples indicating that H3K27Me3 demethylation does occur in an epitope unmasked situation (Fig. R10C). Moreover, *in vitro* assays using the human recombinant catalytic domain of JMJD3, suggest that JMJD3 is able to demethylate the phosphorylated peptide H3K27Me3S28p (Fig. R11A-C). If this is the case *in vivo*, epitope masking would have the opposite effect because H3K27Me3S28p demethylation will not be detected, and demethylation may be underestimated.

Thus, in this likely three-way scenario where H3K27Me3S28 phosphorylation, H3K27Me3S28p demethylation and H3K27Me3 demethylation occur it becomes difficult to assess the contribution of epitope masking to H3K27Me3 demethylation. However, our observations indicate that epitope masking would not be a major determinant of decreased methylation under LTD because demethylation is prevented by inhibiting demethylase activity with GSK-J4 or by JMJD3 knock-down (Fig. R8 and Fig. R9). Consistently, in the absence of epitope masking LTD still induces demethylation (Fig. R10). In further support that epitope masking is not the main cause of reduced methylation in LTD, we did not observe a decrease of H3K27Me3 at *Bdnf* promoter II in neuronal cells in which this promoter presented increased H3K27Me3S28p (Fig. R3A).

1.6.- *Bdnf* induction requires CREB-p/CBP/ JMJD3.

Several signaling pathways lead to the activation of cAMP response element-binding protein (CREB) kinases, which phosphorylate CREB on the transcriptional regulatory residue Ser133 (Gonzalez and Montminy, 1989; Sheng et al., 1990, 1991). Upon phosphorylation at Ser133, CREB translocates to the nucleus and recruits the transcriptional co-activator CREB-binding protein (CBP), a histone acetyl transferase that promotes histone acetylation and assembly of transcriptional complexes (Vo and Goodman, 2001). We speculated that a similar mechanism could explain the H3K27 acetylation induced by NMDA stimulation (Fig. R3A). Consistent with this possibility, NMDA-LTD triggers a transient CREB phosphorylation at Serine 133 (CREB-pS133) 10 min after stimulation (Fig. R11A). To determine the pathway by which NMDA stimulation, i.e. Ca^{2+}/calmodulin-dependent protein kinase II (CamKII) or Protein Kinase C (PKC), leads to CREB phopsphorylation, hippocampal neurons were treated with the CamKII inhibitor KN93 or the PKC inhibitor Chelerytrine before NMDA stimulation. The levels of pS133-CREB were then determined by Western blot at 10 min after LTD induction. Both KN93 and Chelerytrine blocked CREB phosphorylation at 10 min after NMDA stimulation

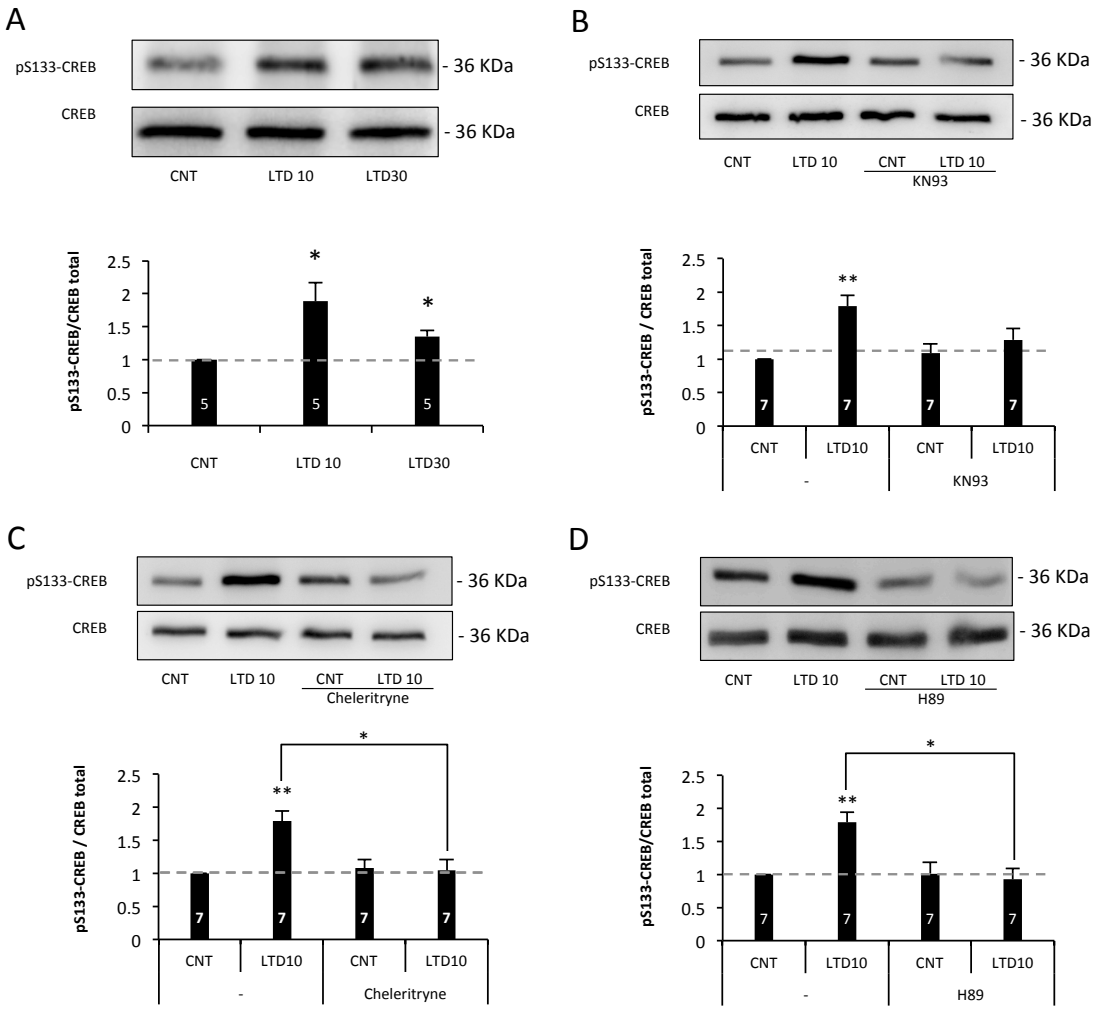

Figure R12: **NMDA stimulation triggers CREB phosphorylation at Ser133 in mature hippocampal neurons *via* CamKII-PKC/MSK1 kinases.**

A) Western blot studies show the CREB phosphorylation at its Ser133 in basal control conditions (CNT), at 10 min (LTD 10) and at 30 min (LTD 30) after NMDA stimulation. B-D) Western blots and it quantification showing that the S133-CREB phosphorylation observed in neuronal cultures at 10 min after LTD induction (LTD10) is blocked by treatment with the CamKII inhibitor KN93 (B), the PKC inhibitor Chelerytrine (C) and the Msk1 inhibitor H89 (D). Data are represented as mean ± SEM. (*p<0.05; **p<0.01). For statistical analysis see Supp. Table 13.

(Fig. R11B-C), suggesting that the NMDA-LTD paradigm used in our study may require synergic activities between PKC and CamKII, like previously reported during LTP. In fact, it was shown that PKC potentiates NMDA receptor gating in turn enhancing Ca^{2+} influx and intracellular Ca^{2+}/camodulin, which could trigger CaMKII autophosphorylation (Gardoni et al., 1999; Strack and Colbran, 1998; Yan et al., 2011). To further dissect the pathway leading to S133-CREB phosphorylation, we analyzed the contribution of Msk1, a downstream kinase common to PKC and CamKII pathways. To address this possibility, hippocampal neurons were incubated with the Msk1 inhibitor H89 before NMDA stimulation. As shown in Figure R11D, the treatment with H89 blocked CREB phosphorylation at 10 min after NMDA stimulation indicating that Msk1 triggers CREB phosphorylation at Ser 133. We can conclude that our NMDA-dependent paradigm of LTD

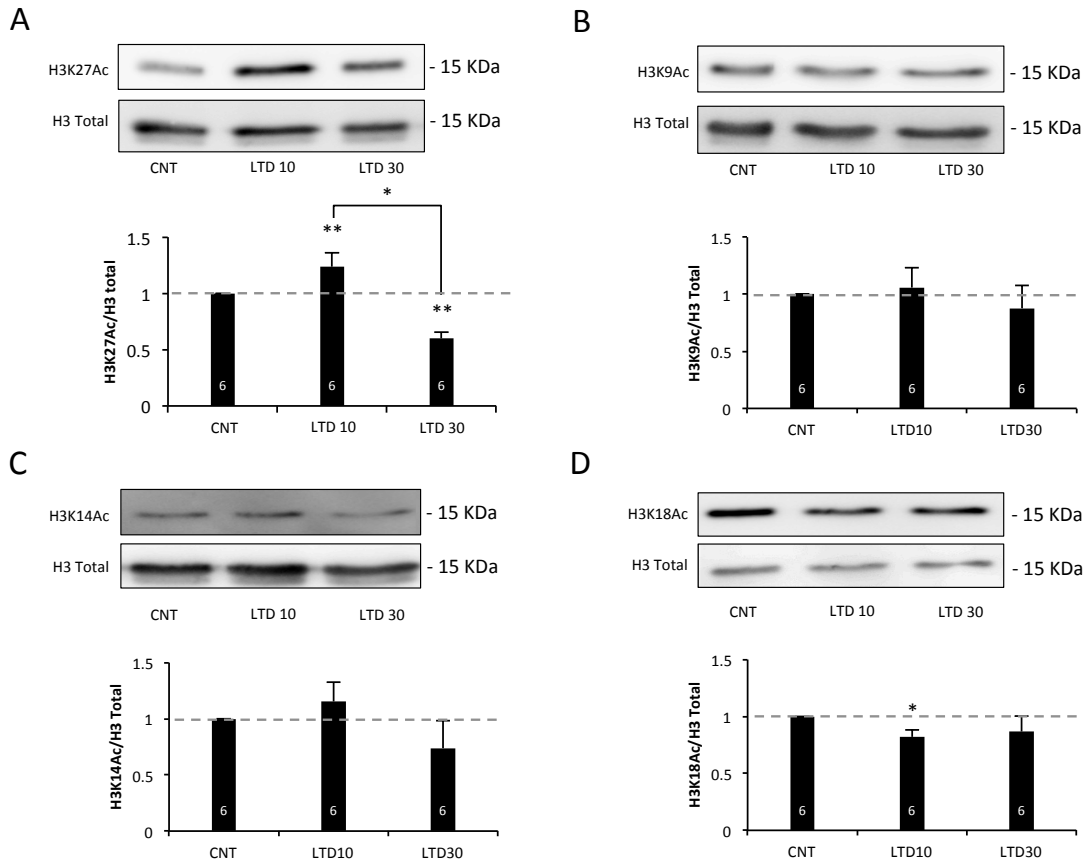

Figure R13: **NMDA stimulation triggers Histone H3 acetylation at Lysine 27, but not at Lysines 9, 14 or 18 in mature hippocampal neurons.**

A-D) Western blots analysis of histone H3 acetylation at different Lysine residues in basal conditions, at 10 min and at 30 min after NMDA stimulation; H3K27Ac (A), H3K9Ac (B), H3K14Ac (C) and H3K18Ac (D). The bar plots show the quantification of the western blots. Each acetylated form was corrected for total levels of H3 histone. Data are represented as mean ± SEM (*p<0.05; **p<0.01). For statistical analysis see Supp. Table 14.

leads to S133-CREB phosphorylation *via* CamKII-PKC/Msk1 kinases. However, since H89 also inhibits PKA with a similar potency (Lochner and Moolman, 2006), we could not exclude a role of PKA in the phosphorylation of CREB by NMDA.

Coherent with the CREB activation, NMDA triggers a transient and a significant increase in the acetylation of H3K27 10 min after treatment (Fig. R13A). Such increased acetylation of H3 was not observed at other lysine residues, H3K9, H3K14 or H3K18, after NMDA addition (Fig. R13B-D). To directly assess the functional association with CREB activation, we treated hippocampal neurons with CREB-pS133/CBP Interaction Inhibitor (CCIIh) to impair CREB-pS133/CBP binding (Best et al., 2004; Li and Xiao, 2009). This treatment blocked the transcriptional activation of promoters II and VI and impaired H3K27 acetylation at these promoters (Fig. R14A and R14B). These results confirm that CREB-p/CBP is required for H3K27 acetylation at promoters II and VI and for the activation of these promoters after NMDA-LTD. The activation of promoters I and IV was unaffected by the inhibitor. In fact, no changes of H3K27Ac were observed at promoters I and IV at 10

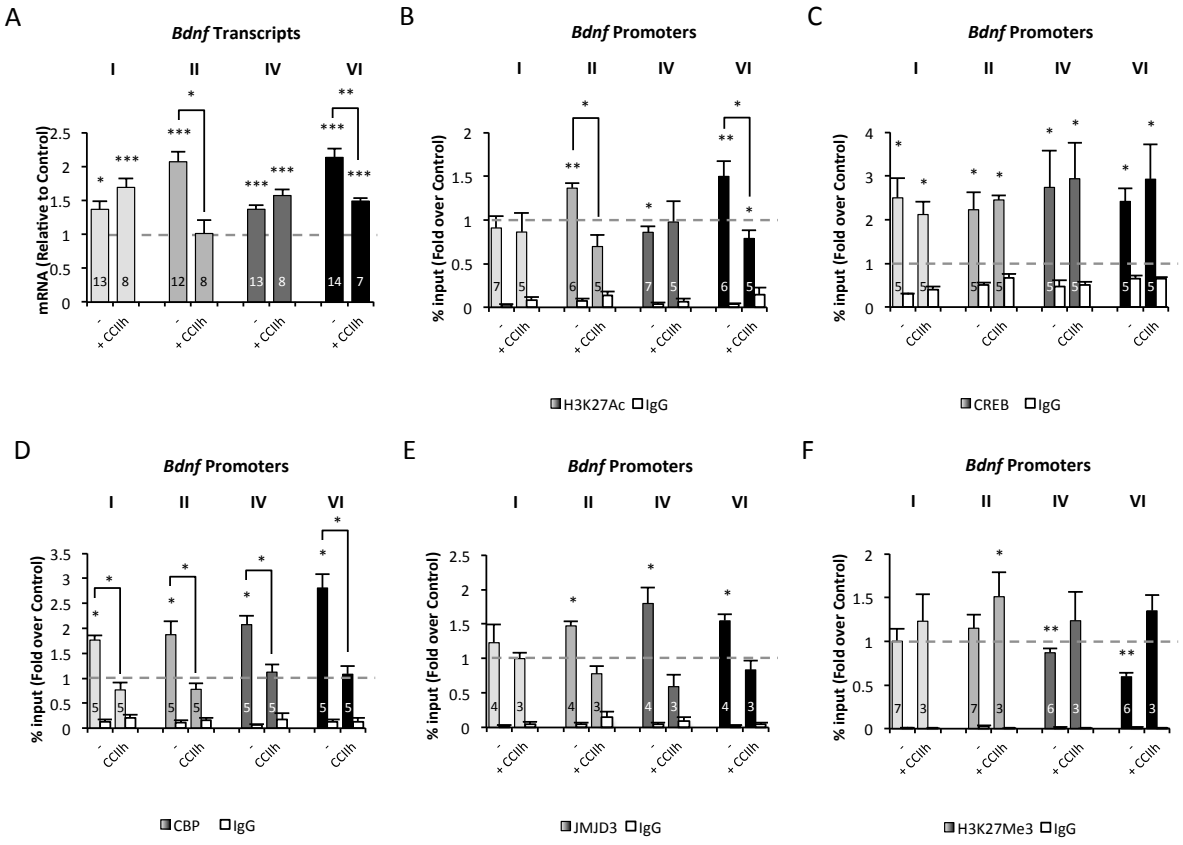

Figure R14: **CREB-CBP/JMJD3 interaction is required to fully activate and transcribe *Bdnf* promoters II and VI.**

A) RT-qPCR showing that the increased expression of *Bdnf* mRNAs II and VI observed 30 min after NMDA stimulation is impaired when CREB-CBP interaction is blocked by CCIIh. B-F) ChIP-qPCR analysis show that treatment with CCIIh: blocked H3K27 acetylation at promoters II and VI (B), it does not block CREB binding to *Bdnf* promoters (C), it prevents CBP recruitment to promoters I, II, IV and VI (D) it prevents JMJD3 recruitment at promoters II, IV and VI (E) and H3K27Me3 demethylation at promoters IV and VI (F). Data are represented as mean ± SEM SEM (*p<0.05; **p<0.01; ***p<0.001). For statistical analysis see Supp. Table 15.

min after induction (Fig. R3A). ChIP experiments also revealed that active CREB is bound to the *Bdnf* promoters either in the presence or absence of the inhibitor in NMDA stimulated neurons. However, treatment with the CREB/CBP inhibitor CCIIh blocked the recruitment of CBP to these promoters (Fig. R14C and R14D).

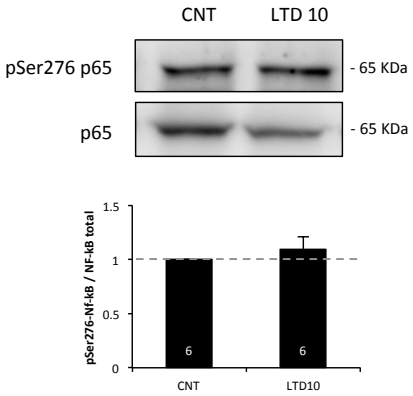

Figure R15: **p65-Serine 276 is not phosphorylated at 10 min after NMDA-LTD.**

Western blot and its quantification show that stimulation of hippocampal neurons in culture with 20µM NMDA is not able to trigger phosphorylation of p65Ser273 at 10 min after stimulation (LTD10). CNT: control non-stimulated neurons. Data are represented as mean ± SEM. For statistical analysis see Supp. Table 16.

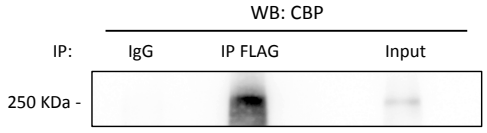

Figure R16: **CBP coimmunoprecipitates with JMJD3.**

Detection of CBP by Western blot in samples where JMJD3-FLAG or IgG (negative control) were immunoprecipitated from total protein extracts prepared from HEK transfected cells expressing both proteins and treated with Forskolin and Rolipram in order to induce CREB activation. The coimmunoprecipitation of CBP and JMJD3 confirms the interaction of these proteins.

The CCIIh inhibitor blocks the interaction between the KID domain of CREB and the KIX domain of CBP. This KIX domain in CBP also interacts with the p65 subunit of the transcriptional activator Nuclear Factor kappa B (NFkB), implying that the interaction CBP-p65 is also disrupted by CCIIh (Best et al., 2004). Although a role of NFkB has been described in the activation of *Bdnf* promoters I and IV but not in the activation of promoters II and VI (Lipsky et al., 2001; Lubin and Sweatt, 2007; Tian et al., 2010a), the possibility exists that the observed effect of CCIIh could be due to inhibition of the recruitment of CBP by NFkB to promoters II and VI.

Zhong *et al*. (Zhong et al., 1998) have shown that the activation of p65 by phosphorylation at its Serine 276 is strictly required for the interaction with CBP: in Figure R15 we show that application of 20μM NMDA to hippocampal neurons in culture was not able to trigger phosphorylation of p65-Ser273 at 10 min after stimulation, indicating that p65 is not involved in the recruitment of CBP to *Bdnf* promoters at least at this time point after NMDA stimulation.

The interaction of CBP with the demethylase UTX from the Lysine-specific demethylase 6 (KDM6) family has been described (Tie et al., 2012), opening the possibility that CREB-p/CBP complex would be also involved in the recruitment of the demethylase JMJD3 (also a member of the KDM6 family) to the *Bdnf* promoters after stimulation. The ChIP experiments confirmed that the recruitment of JMJD3 to promoters II, IV and VI is impaired by CCIIh (Fig. R14E). In addition, CCIIh blocked the H3K27Me3 demethylation induced by NMDA at promoters IV and VI (Fig. R14F). Note that CCIIh treatment also resulted in significantly higher levels of H3K27Me3 at promoter II after stimulation (Fig. R14F). These results support our previous conclusion that H3K27Me3 demethylation is required for induction of promoter II (Fig. R3A), but it occurs at lower levels than at promoters IV and VI. The direct interaction CBP-JMJD3 was further confirmed by coimmunoprecipitation (Fig. R16).

From these results we conclude that the mechanism of *Bdnf* induction triggered by NMDA involves CREB-p mediated recruitment of CBP and JMJD3 to all *Bdnf* promoters, yet rapid transcription from promoters II and VI requires H3K27Me3 demethylation followed by H3K27 acetylation.

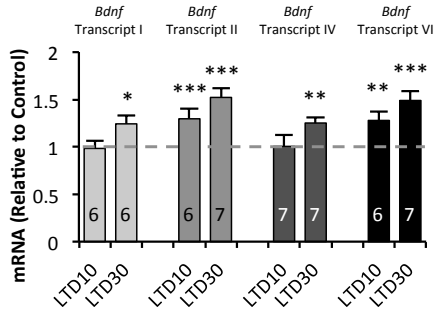

Figure R17: **Response of *Bdnf* promoters to NMDA stimulation in hippocampal slices.**

According to the data *in vitro*, RT-qPCR analysis performed in acute hippocampal slices from adult mice show that NMDA stimulation triggers the increase of the *Bdnf* mRNAs transcribed from promoters II and VI 10 min after LTD, and from promoters I, II IV and VI at 30 min after stimulation. Data are represented as mean ± SEM. For statistical analysis see Supp. Table 17.

1.7.- Validation in acute hippocampal slices.

Our results indicate that *Bdnf* promoters II and VI are subjected to EZH2 repression and that, after specific neuronal stimuli, the increased transcriptional activity is due to the release of the repressor EZH2 as a consequence of H3K27Me3Ser28 phosphorylation, H3K27Me3 demethylation and H3K27 acetylation. Because our data were obtained in neurons grown *in vitro*, we decided to test our model in neurons that had developed and matured in a physiological environment. To explore whether our conclusions obtained *in vitro* also occur *in vivo*, we analyzed the effect of NMDA-LTD on the expression levels and epigenetic marks found at *Bdnf* promoters in hippocampal slices prepared from adult mice. Similar to what occurs *in vitro*, NMDA addition to hippocampal slices resulted in increased levels of mRNA species II and VI at 10 min, and in increased levels of the four species at 30 min after stimulation (Fig. R17). The data shown in the Figure R17 represent the mRNA levels relative to unstimulated controls. Likewise *in vitro*, higher increases were observed for mRNAs transcribed from promoters II and VI (Fig. R17). Also paralleling the data in cultures, the repressive H3K27Me3 and EZH2 marks were detected at these four *Bdnf* promoters in adult mice hippocampus (Figs. R18A and R18B). High amounts of JMJD3 demethylase were also found at these promoters (Fig. R18C), suggesting that transcriptional activity requires H3K27Me3 demethylation. As expected, the presence of activation marks H3K4Me3 and H3K27Ac were also observed at promoters I, II, IV and VI at the same proportions than in neuronal cultures (Figs. R18D and R18E). However in hippocampal slices, the amount of H3K27Ac found at promoter II was comparable to the levels found at the repressed gene *hoxA1*, suggesting a low basal transcriptional activity for this promoter.

The ChIP experiments performed in hippocampal slices revealed that LTD induces phosphorylation of H3K27Me3S28p and displacement of EZH2 not only at promoters II and VI but also at promoters I and IV (Fig. R19A). These results strengthen the conclusion previously obtained from *in vitro* data that phosphorylation of H3K27Me3S28 displaces EZH2 repressor from all the four promoters (see Fig. R6C). In hippocampal slices, H3K27Me3 demethylation was also evident at promoter II (Fig. R19A), explaining the

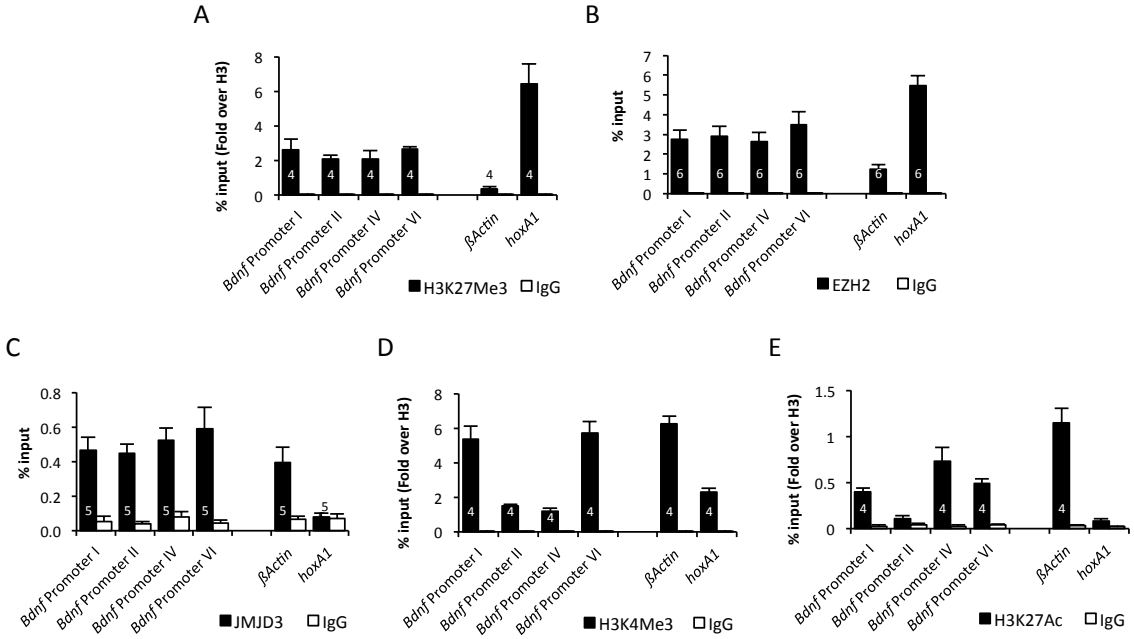

Figure R18**: Epigenetic marks found at *Bdnf* promoters in adult hippocampus.**

ChIP-qPCR analysis performed in adult mice hippocampus. The presence of activator and repressor histone marks and chromatin remodeling enzymes, indicate that *Bdnf* promoters I, II, IV and VI are bivalent in adult mice: (A) H3K27Me3, (B) EZH2, (C) JMJD3, (D) H3K4Me3 and (E) H3K27Ac. The levels of these proteins at promoter regions of the control genes *ßActin* and *hoxA1* are also shown in the plots. Data are represented as mean ± SEM. For values see Supp. Table 18.

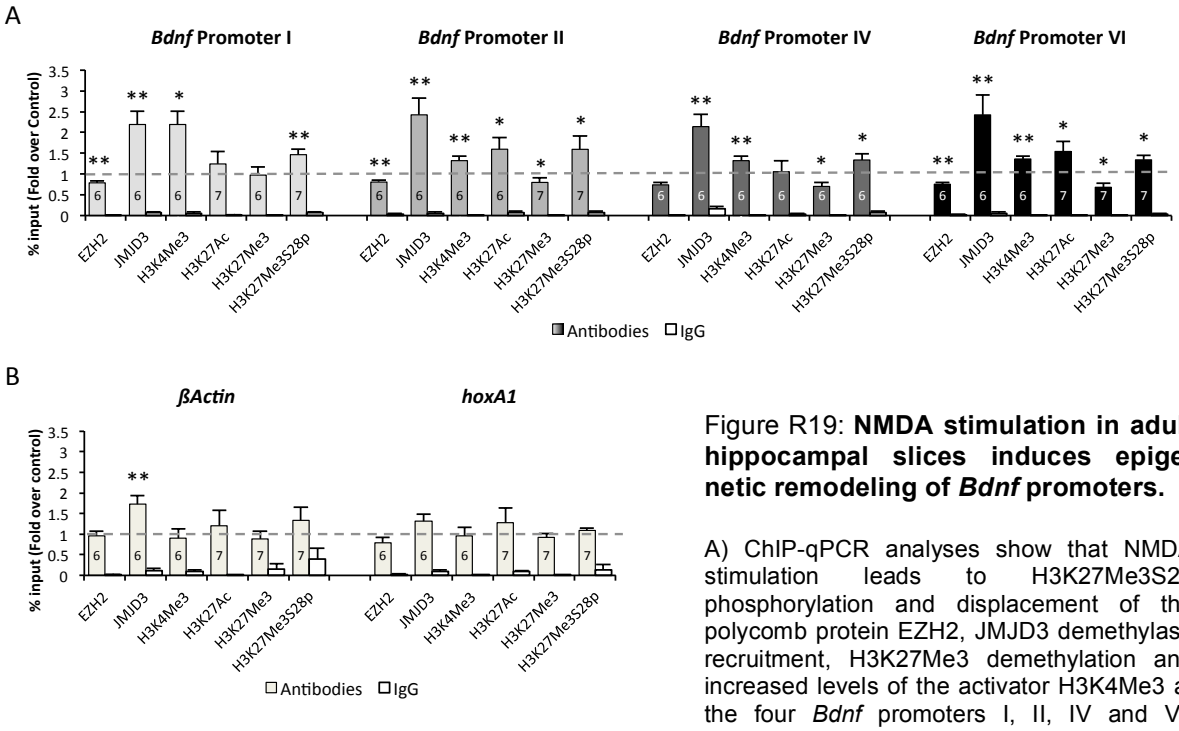

Figure R19: **NMDA stimulation in adult hippocampal slices induces epigenetic remodeling of *Bdnf* promoters.**

A) ChIP-qPCR analyses show that NMDA stimulation leads to H3K27Me3S28 phosphorylation and displacement of the polycomb protein EZH2, JMJD3 demethylase recruitment, H3K27Me3 demethylation and increased levels of the activator H3K4Me3 at the four *Bdnf* promoters I, II, IV and VI. H3K27 acetylation was observed only at promoters II and VI suggesting that this mark is responsible for the fast induction of these two promoters. B) ChIP-qPCR analyses at promoter regions of the control genes *ßActin* and *hoxA1* after NMDA stimulation. The data show that, except for the increased levels of JMJD3 observed at the *ßActin* promoter, none of the other marks present changes after NMDA stimulation. Data are represented as mean ± SEM (*p<0.05; **p<0.01, ***p<0.001). For statistical analysis see Supp. Table 19.

effect of GSK-J4 on this promoter *in vitro* (see Fig. R8B). Interestingly, increases of the activation mark H3K4Me3 was observed for all the four promoters in hippocampal slices (Fig. R19A). Similar to *in vitro* grown hippocampal neurons, H3K27 acetylation in hippocampal slices was only evident at promoters II and VI (Fig. R19A), suggesting that H3K27 acetylation may be the relevant modulator for the fast induction of these two promoters after stimulation. Except for an increase in JMJD3 interaction with *ßActin* promoter, for which we do not have an explanation, no other changes in the levels of these marks were observed at the promoters of the control genes (Fig. R19B).

All in all, the results obtained in hippocampal slices reinforce the notion that these four promoters of *Bdnf* are controlled by PRC2 repressor and suggest that fast (10min) response of promoters II and VI would be due to H3K27 acetylation.

CHAPTER II: Cholesterol role in aged-associated cognitive decline and synaptic plasticity.

2.1.- Epigenetic marks at *Bdnf* promoters in aged hippocampus.

Of the four *Bdnf* promoters studied in the first chapter, we focused on the regulation of promoters II and VI, as the mRNA species transcribed from these promoters are transported to distal dendrites and are thought to play a role in TrkB/BDNF-mediated dendritic architectural and functional plasticity in response to external stimuli (Baj et al., 2011; Chiaruttini et al., 2008; Pattabiraman et al., 2005), a process known to decline with ageing.

Firstly we analysed the relative amount of *Bdnf* mRNAs containing exons II and VI in the hippocampus of old mice, compared to adult hippocampus. In agreement with previous reports (Perovic et al., 2013), we also found reduced *Bdnf* expression of transcripts II and VI in the old hippocampus (Fig. R20). In order to determine if age-

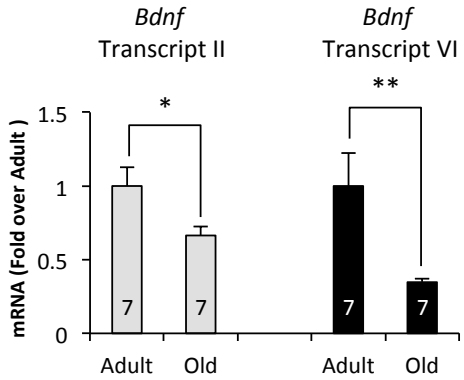

Figure R20: ***Bdnf* transcripts containing exons II and VI are reduced in ageing.**

RT-qPCR analysis of the levels of *Bdnf* mRNAs transcribed from promoters II and VI in adult (8 month) and old (20 month) hippocampus of mice. Data are represented as mean ± SEM (*p<0.05; **p<0.01). For statistical analysis see Supp. Table 20.

associated reduced expression of *Bdnf* was due to increased repression or decreased activation of its promoters, we analysed the basal levels of histone H3 marks. We found that the old hippocampus present higher H3K27Me3 and also higher H3K27Me3S28p marks (Fig. R21A-B). The existence of increased levels of H3K27ME3S28p implies reduced EZH2 binding to these promoters, suggesting therefore that age-associated reduced *Bdnf* expression levels are not due to increased repression but to a decreased activation of *Bdnf* promoters.

We next analysed the levels of histone H3 Lys 27 acetylation and CBP at *Bdnf* promoters II and VI. This study revealed decreased levels of both in the old hippocampus (Fig. R21C-D), reinforcing our previous assumption that reduced *Bdnf* expression in the old is predominantly due to an activation deficit. As a matter of fact, reduced CBP implies reduced levels of JMJD3 bound to *Bdnf* promoters, and therefore increased H3K27Me3 mark at its promoters.

In view that the hippocampus of old mice presents lower levels of the acetylated mark, we next wondered if it presents also higher levels of deacetylases bound to its promoters.

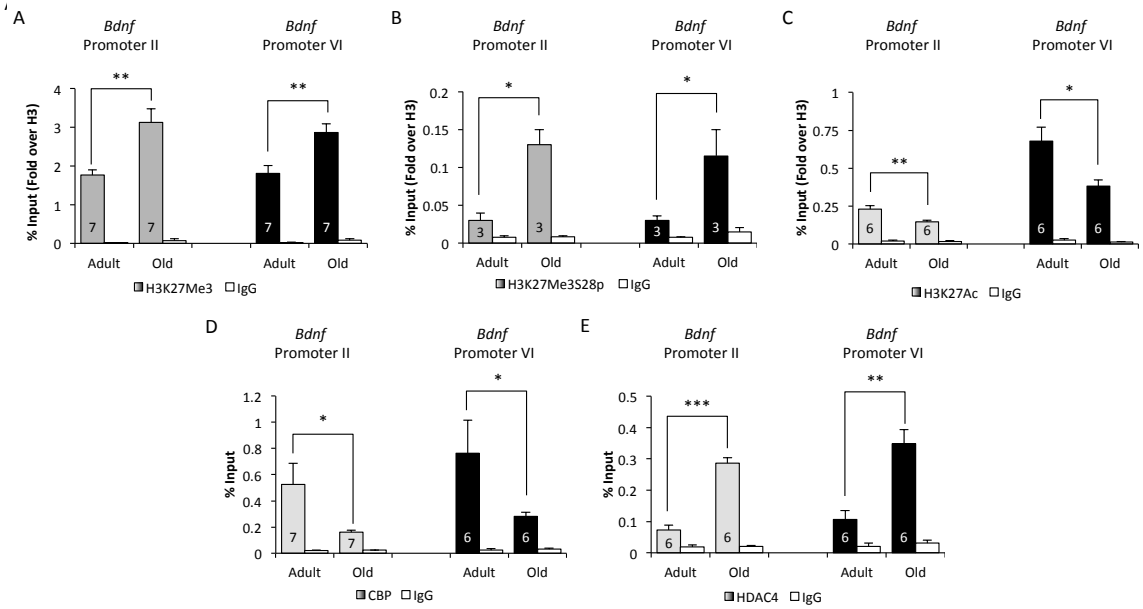

Figure R21: **Epigenetic marks found at *Bdnf* promoters in the old hippocampus**

ChIP-qPCR analysis of the differential epigenetic marks and regulatory proteins bound at *Bdnf* promoters in basal conditions during ageing: (A) H3K27Me3, (B) H3K27Me3S28p, (C) H3K27Ac, (D) CBP and (E) HDAC4. Data are represented as mean ± SEM (*p<0.05; **p<0.01, ***p<0.001). For statistical analysis see Supp. Table 21.

Among all the histone deacetylases (HDACs), we focused on the HDAC class IIb, more specifically on HDAC4 since it is known that its activity is regulated by Ca^{2+} and it has been implicated in *Bdnf* regulation (Backs et al., 2006; Koppel and Timmusk, 2013; McKinsey et al., 2000). As expected, we found higher levels of HDAC4 bound to *Bdnf* promoters II and VI (Fig. R21E).

All in all, the above series of experiments suggest the existence of reduced expression of *Bdnf* in the old could be due to decreased transduction of the transcriptional activation signalling to the nucleus.

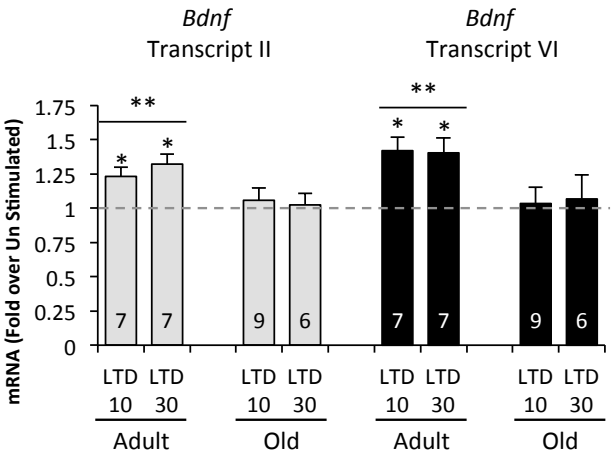

Figure R22: **Impaired *Bdnf* transcription after LTD in hippocampal slices from old mice.**

RT-qPCR analysis of the levels of *Bdnf* mRNAs transcribed from promoters II and VI after NMDA stimulation in adult and old hippocampal slices. Data are represented as mean ± SEM (*p<0.05; **p<0.01). For statistical analysis see Supp. Table 22.

2.2.- Aged-impaired *Bdnf* transcription in response to LTD.

As commented in the introduction, ageing is characterized by a progressive cognitive decline and synaptic plasticity impairment, and it is accompanied by reduced transcription of IEGs (see Introduction paragraph 4). Thus we studied the ability of NMDA-LTD stimulus to induce *Bdnf* transcription in old hippocampal slices; Figure R22 shows that LTD fails to induce *Bdnf* transcription in the old. Taking into account that the old presents lower levels of CBP and higher levels of HDAC4 bound to *Bdnf* promoters at basal state (Fig. R22), and also previous data showing LTD membrane signalling defects in old mice hippocampi (Martin et al., 2014a), we proceeded with the analysis of CREB and CaMKII activation. Figure R23A shows that induction of LTD in hippocampal slices from old mice does not result in CREB phosphorylation, an event required for CBP binding and histone acetylation (Hu et al., 1999; Vo and Goodman, 2001). A similar reduced activation in response to LTD was observed for CaMKII (Fig. R23B), the activity of which is required for

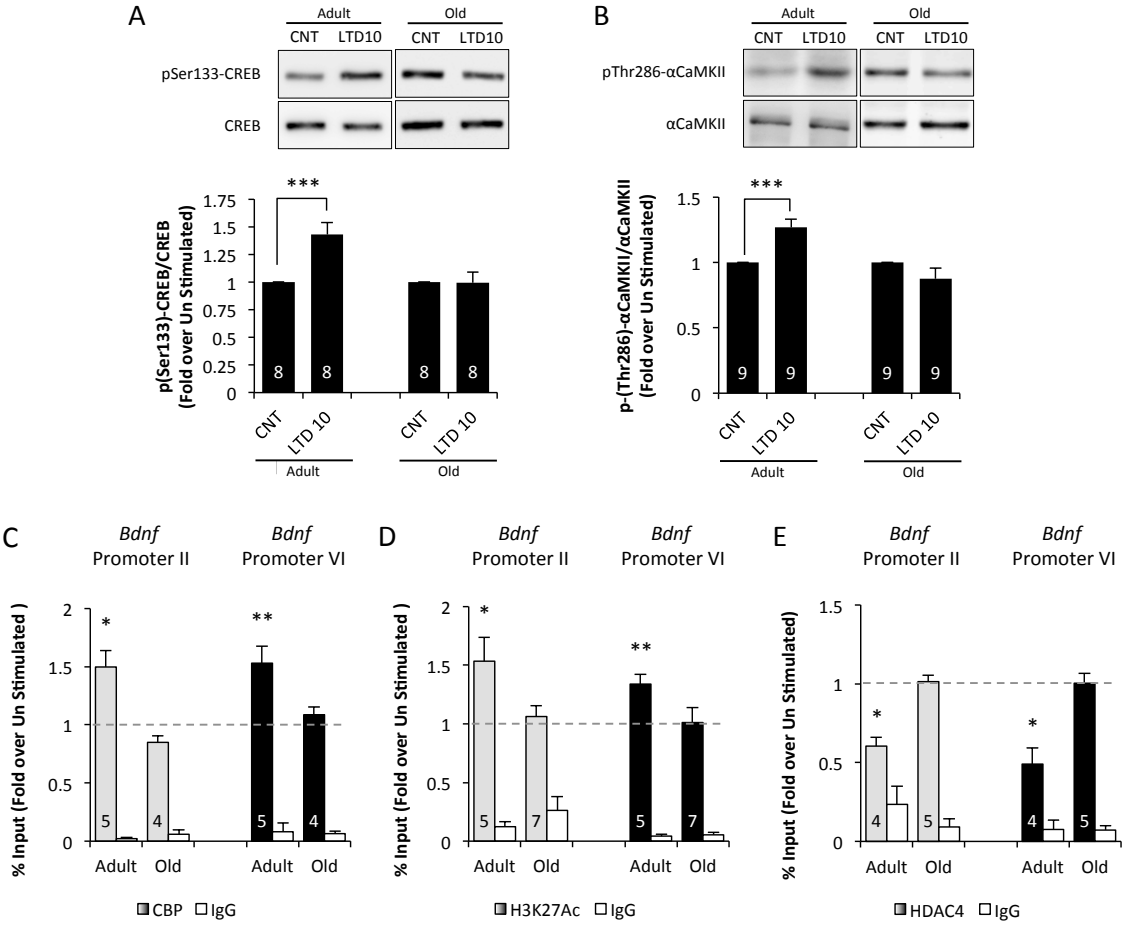

Figure R23: **Impaired nuclear activating signal and chromatin remodelling upon LTD in hippocampal slices from old mice.**

A-B) Western blot analysis of (A) CREB and (B) αCaMKII activation 10 minutes after LTD in hippocampal slices of adult and old mice. C-E) ChIP-qPCR analysis of H3K27Ac and regulatory proteins bound at *Bdnf* promoters 10 minutes after LTD induction in hippocampal slices from adult and old mice: (C) CBP, (D) H3K27Ac and (E) HDAC4. Data are represented as mean ± SEM (*p<0.05; **p<0.01, ***p<0.001). For statistical analysis see Supp. Table 23.

the functional repressive phosphorylation and nuclear export of HDAC4 (Backs et al., 2006; McKinsey et al., 2000). In order to determine whether reduced LTD activation of kinases in old hippocampi had an effect on chromatin remodelling, therefore resulting in impaired *Bdnf* transcription, we performed ChIP experiments. According to the transcriptional and kinase activation results, ChIP performed in extracts obtained 10 min after NMDA stimulation showed impaired recruitment of the histone acetyl transferase CBP and preventing the H3K27 acetylation at these *Bdnf* promoters in the slices from old mice compared to slices from adult, middle age, mice (Fig. R23C-D). Furthermore, ChIP experiment revealed that NMDA stimulation failed to trigger a significant displacement of the histone deacetylase HDAC4 from the *Bdnf* promoters in hippocampal slices from old mice compared to the effect in slices from middle age mice (Fig. R23E). Altogether, the above data are consistent with the view that LTD is ineffective to trigger the transcriptional induction from *Bdnf* promoters II and VI in the hippocampus of old mice. These data suggest that defects exist in the signalling pathways linking the activation of NMDA receptors in LTD to the downstream kinases leading to the epigenetic remodelling required for *Bdnf* transcription.

2.3.- Cholesterol is sufficient to rescue LTD-induced *Bdnf* transcription.

We then wanted to determine whether the loss of cholesterol that occurs with aging (Svennerholm et al., 1991, 1994, 1997, Martín et al 2008, see also Fig. R24A) is involved in the membrane signalling defects, preventing the proper transcriptional induction of the *Bdnf* promoters under LTD. Hippocampal slices of old mice were incubated in a cholesterol-rich solution, using a protocol known to restore the cholesterol concentration on the plasma membrane found in adult animals (Fig. R24B; Martin et al., 2014a).

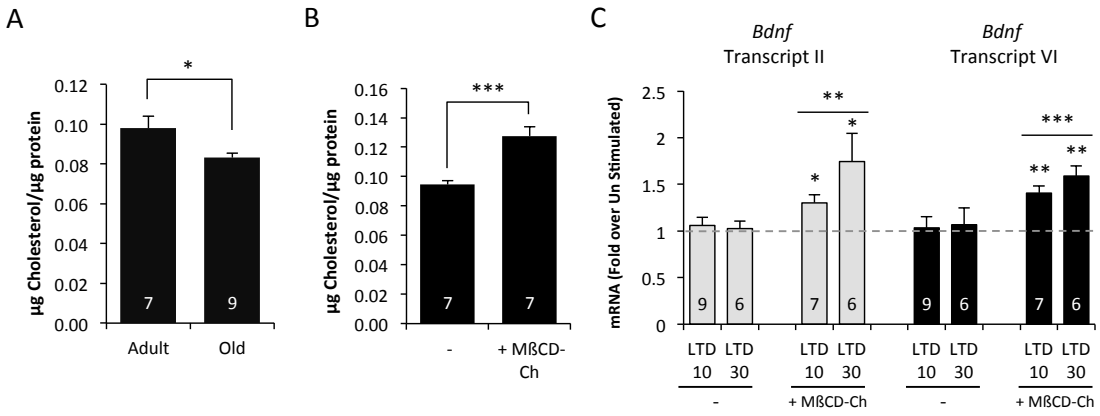

Figure R24: **Restoring age-associated cholesterol loss is sufficient to rescue *Bdnf* transcription.**

A-B) cholesterol quantification of adult and old mouse hippocampus (A) and of quantification old hippocampal slices treated with MßCD-Ch (B). RT-qPCR analysis of the levels of *Bdnf* mRNAs transcribed from promoters II and VI after NMDA stimulation in old hippocampal slices compared to old hippocampal slices treated with MßCD-Ch. Data are represented as mean ± SEM (*p<0.05; **p<0.01; ***p<0.001). For statistical analysis see Supp. Table 24.

Consistent with a possible cause-effect association, addition of cholesterol to hippocampal

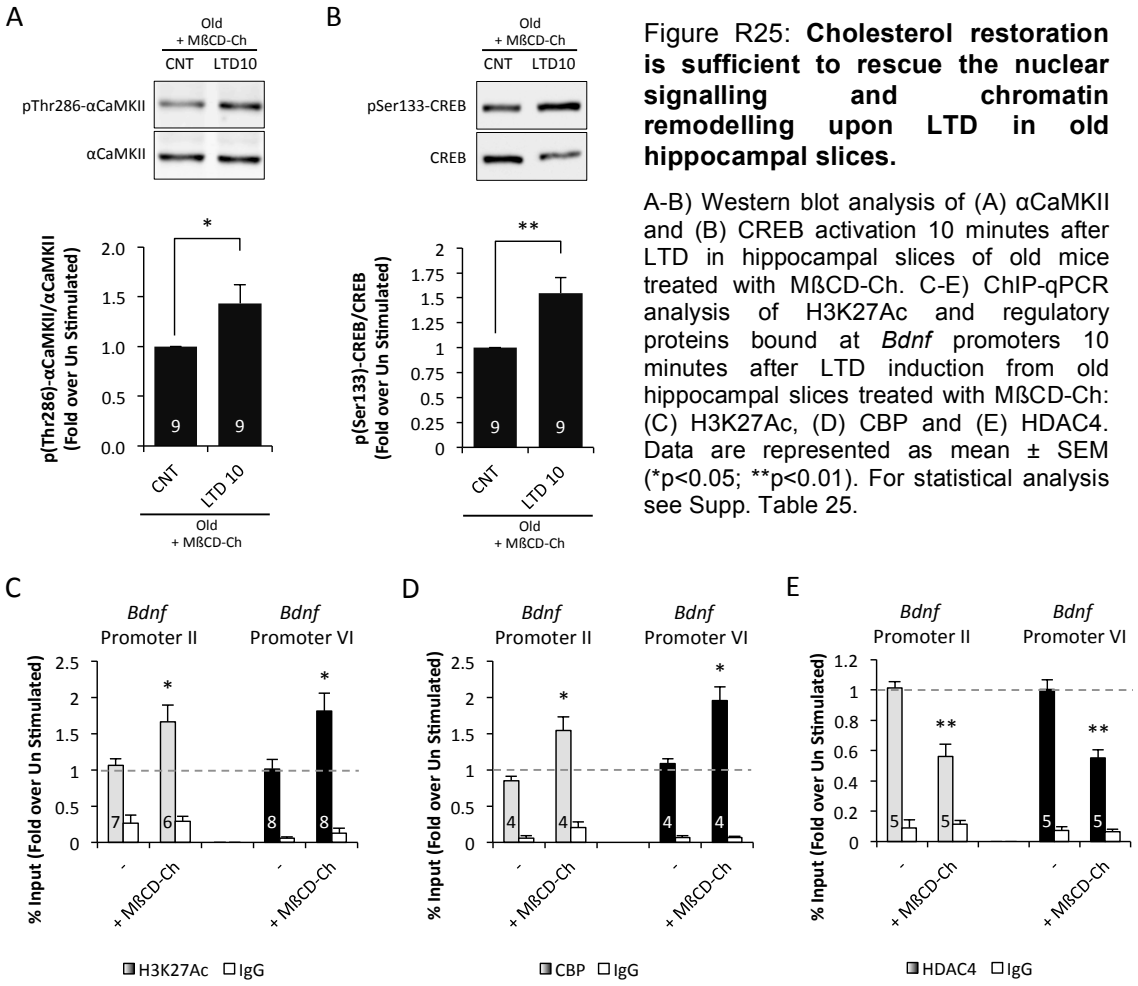

Figure R25: **Cholesterol restoration is sufficient to rescue the nuclear signalling and chromatin remodelling upon LTD in old hippocampal slices.**

A-B) Western blot analysis of (A) αCaMKII and (B) CREB activation 10 minutes after LTD in hippocampal slices of old mice treated with MßCD-Ch. C-E) ChIP-qPCR analysis of H3K27Ac and regulatory proteins bound at *Bdnf* promoters 10 minutes after LTD induction from old hippocampal slices treated with MßCD-Ch: (C) H3K27Ac, (D) CBP and (E) HDAC4. Data are represented as mean ± SEM (*p<0.05; **p<0.01). For statistical analysis see Supp. Table 25.

slices from old mice rescued *Bdnf* transcription in response to NMDA stimulus at 10 and 30 minutes (Fig R24C). To further validate cholesterol sufficiency, we studied kinases activation and chromatin remodelling in response to LTD. Figures R25A and R25B shows that in cholesterol enriched old hippocampal slices NMDA stimulus triggers CaMKII and CREB phosphorylation, as in young adult slices (see Figures R23A and R23B). Furthermore, NMDA addition was able to trigger chromatin remodelling 10 minutes after LTD in old slices where cholesterol levels were restored; increased levels of histone H3K27Ac were accompanied by CBP recruitment and HDAC4 detachment of *Bdnf* promoters in response to LTD (Fig. R25C-E). The above results strongly suggest that reduced cholesterol levels impair LTD downstream signalling and *Bdnf* transcription, and reinforce our assumption that the lack of pro-transcriptional signal transduction upon NMDA activation in the old brain might reside on the lipidic composition of the membrane.

2.4.- LTD-induced *Bdnf* transcription requires the appropriate neuronal cholesterol content.

To further test that a low cholesterol environment has negative consequences on the expression of the *Bdnf* gene, the levels of endogenous cholesterol were lowered in

hippocampal slices of adult middle age animals, by transient application of cholesterol oxidase enzyme, which it has been show to reduce cholesterol levels (Fig. R26A; Brachet et al., 2015). This treatment impaired *Bdnf* transcription 10 and 30 minutes after LTD

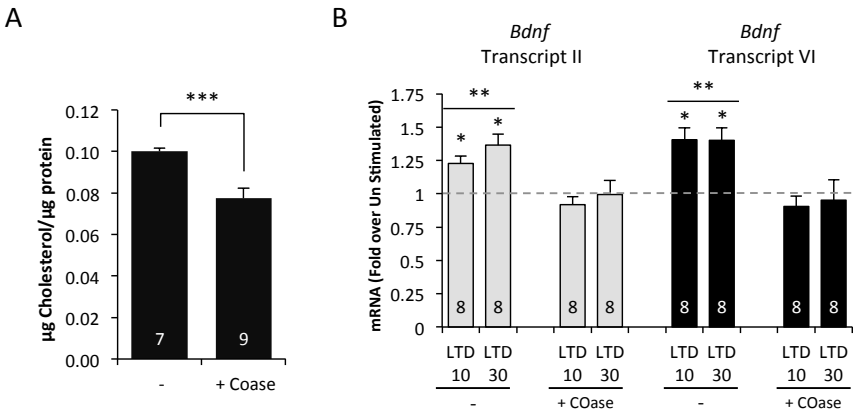

Figure R26: **Reduced cholesterol levels impair *Bdnf* transcription after LTD in adult hippocampal slices.**
A) Cholesterol quantification of adult hippocampal slices treated with COase. B) RT-qPCR analysis of the levels of *Bdnf* mRNAs transcribed from promoters II and VI after NMDA stimulation in adult hippocampal slices compared to adult hippocampal slices treated with COase. Data are represented as mean ± SEM (*p<0.05; **p<0.01; ***p<0.001). For statistical analysis see Supp. Table 26.

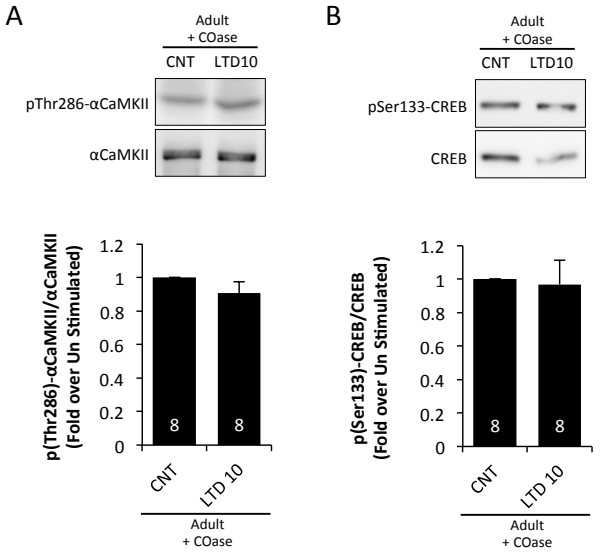

Figure R27: **Reduced cholesterol levels impair the nuclear signalling and chromatin remodelling upon LTD in adult hippocampal slices.**

A-B) Western blot analysis of (A) αCaMKII and (B) CREB activation 10 minutes after LTD in hippocampal slices of adult mice treated with COase. C-E) ChIP-qPCR analysis of H3K27Ac and regulatory proteins bound at *Bdnf* promoters 10 minutes after LTD induction from adult hippocampal slices treated with COase: (C) CBP, (D) H3K27Ac and (E) HDAC4. Data are represented as mean ± SEM (*p<0.05; **p<0.01). For statistical analysis see Supp. Table 27.

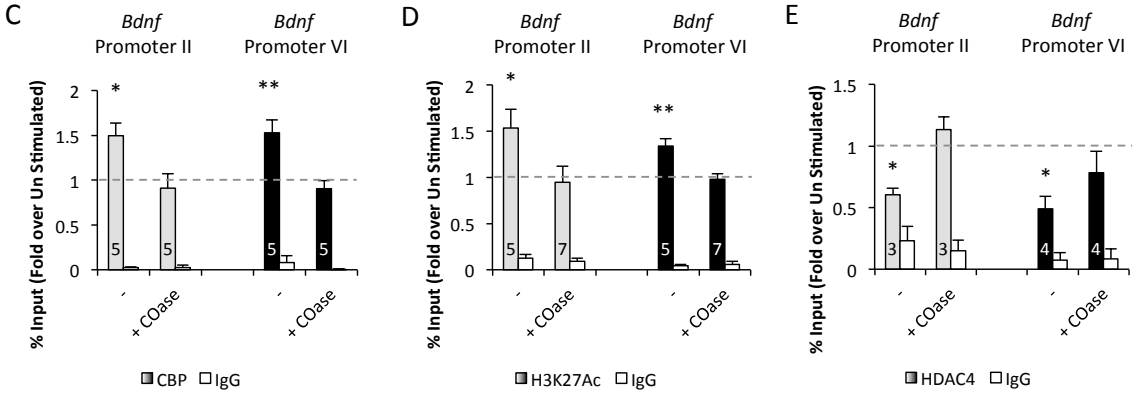

induction (Fig. R26B). According to our hypothesis, low cholesterol levels also disrupted the signalling downstream LTD. Figures R27A and R27B show that in the low cholesterol scenario LTD fails to activate CREB and CaMKII. Therefore, the chromatin remodelling events that lead to *Bdnf* transcription were impaired; COase treated hippocampal slices presented reduced CBP recruitment and H3K27 histone acetylation and, on the opposite side, showed no detachment of HDAC4 from *Bdnf* promoters 10 minutes after LTD (Fig. R27C-E). These results show that appropriate cholesterol levels are required to activate the mechanisms leading to *Bdnf* transcription upon neuronal stimuli, and strengthen the idea that low cholesterol content in the aged brain is responsible, at least in part, for the decreased IEG transcription, synaptic plasticity impairment and cognition decline.

2.5.- Oral administration of the Cyp46A1 inhibitor Voriconazole to old mice rescues epigenetic control of *Bdnf* transcription and enhances cognition.

We next tested if preventing the loss of cholesterol in the old might be able to rescue the transcriptional induction of *Bdnf* in response to LTD and, more generally, we tested if it can result in beneficial effects at the cognitive level in living animals. To restore cholesterol levels in the old, we inhibited the main cholesterol catabolic enzyme of the brain, cholesterol 24 hydroxylase (or CYP46A1; Russell et al., 2009). This was accomplished by administering to old mice Voriconazole, a drug used in the clinics to treat resistant fungal infections (Dolton and McLachlan, 2014). Different from fungi where Voriconazole inhibits the enzyme sterol-14a-demethylase (Cyp51) involved in the synthesis of ergosterol, in mammalian cells Voriconazole binds and inhibits Cyp46A1, both *in vitro* and *in vivo*.

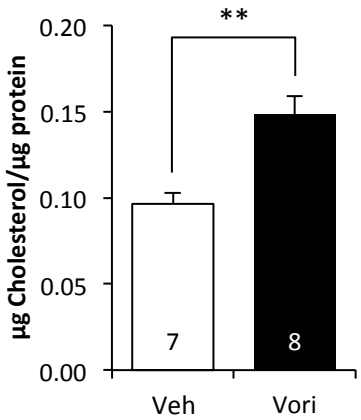

Importantly, it was also shown that Voriconazole crosses the blood brain barrier when administered intraperitoneally and inhibits brain Cyp46A1 (Shafaati et al., 2009).

The Voriconazole treatment consisted in the oral administration of a Voriconazole solution (60 mg/kg b.w./day) to 19 month-old mice during 45 days. Analysis of cholesterol concentration in the hippocampus of Voriconazole and vehicle treated

Figure R28: **Oral administration of Voriconazole reduces the age-associated cholesterol loss.**

Cholesterol quantification of hippocampus of Voriconazole- (Vori) and vehicle- (Veh) treated old mice for 45 days. Data are represented as mean ± SEM (*p<0.05; **p<0.01). For statistical analysis see Supp. Table 28.

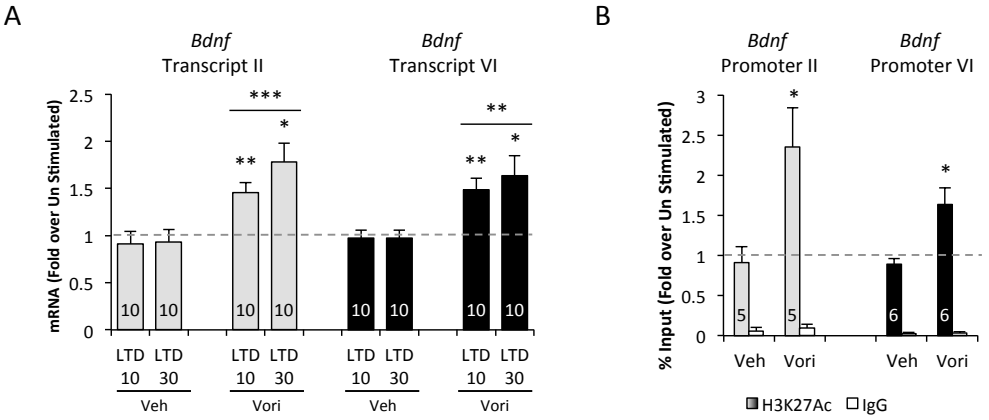

Figure R29: **Oral administration of Voriconazole reduces *Bdnf* transcription and chromatin remodelling.**

Ex vivo analysis of oral administration of Voriconazole (Vori) and Vehicle (Veh): (A) RT-qPCR analysis of *Bdnf* mRNAs levels transcribed from promoters II and VI after LTD and (B) ChIP-qPCR analysis of H3K27Ac 10 minutes after NMDA stimulation. Data are represented as mean ± SEM (*p<0.05; **p<0.01; ***p<0.001). For statistical analysis see Supp. Table 29.

animals revealed that the treatment reduced the age-associated cholesterol loss by 51% (Fig. R28). We observed that Voriconazole treatment rescued *Bdnf* transcription 10 and 30 min after LTD induction, while no transcriptional induction was observed in slices prepared from vehicle treated mice (Fig. R29A). The ChIP experiments performed in hippocampal slices from Voriconazole treated animas also showed an increase in histone H3K27 acetylation at *Bdnf* promoters II and VI facilitating *Bdnf* transcription. (Fig. R29B). On the contrary, no differences were found in vehicle-treated animals (Fig. R29B). These experiments support the notion that appropriate cholesterol levels are necessary to induce IEG transcription by a LTD stimulus. In further support, Voriconazole treatment also

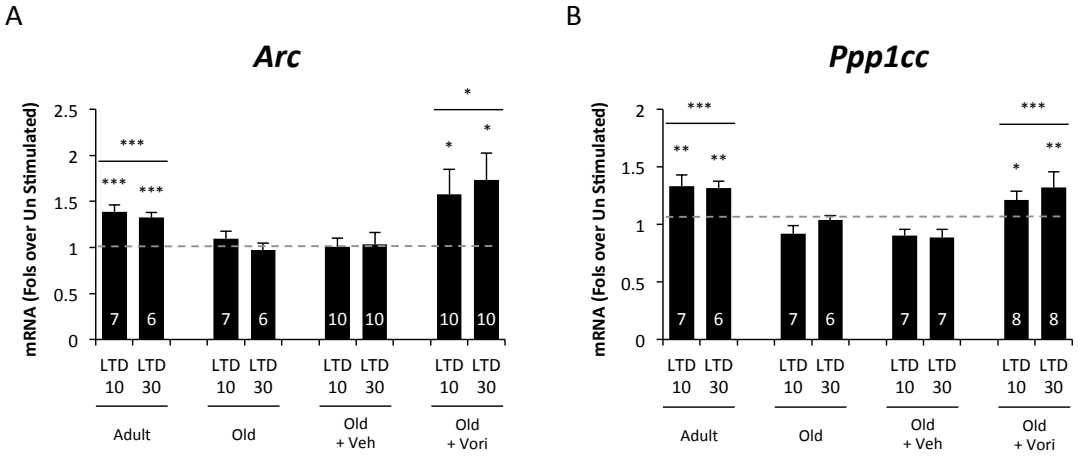

Figure R30: **Oral administration of Voriconazole reduces other IEGs transcription.**

RT-qPCR analysis of *Arc* (A) and *Ppp1cc* (B) mRNAs 10 and 30 minutes after NMDA induction in adult, old, Voriconazole- (Vori) and vehicle- (veh) treated mice. Data are represented as mean ± SEM (*p<0.05; **p<0.01; ***p<0.001). For statistical analysis see Supp. Table 30.

rescued the expression of *Arc* and *Ppp1cc* (Fig. R30A-B), two IEG whose transcriptional induction is also impaired in the hippocampus of old mice in response to LTD (Fig. R30A-B). Altogether, these results indicate that hippocampal cholesterol loss with age is, to a certain extent, responsible for the reduced transcription of IEG.

The results showing that IEG induction by LTD can be rescued in old animals by treatment with Voriconazole led us to hypothetize that cognition would be improved in old mice *in vivo*. To test this possibility, Voriconazole or vehicle treated mice were subjected to three different behavioural tests: novel object location, Morris water maze and contextual fear conditioning. In the novel location task, the exploration phase was similar in Voriconazole-treated and untreated animals; however, during the retention session, animals chronically treated with Voriconazole explored more the object that was placed in a novel position indicating a better spatial memory (Fig. R31A). In the hidden-platform version of the Morris water maze test, which evaluates hippocampal function, both groups showed improved performance during all successive trials throughout the 4 days of spatial

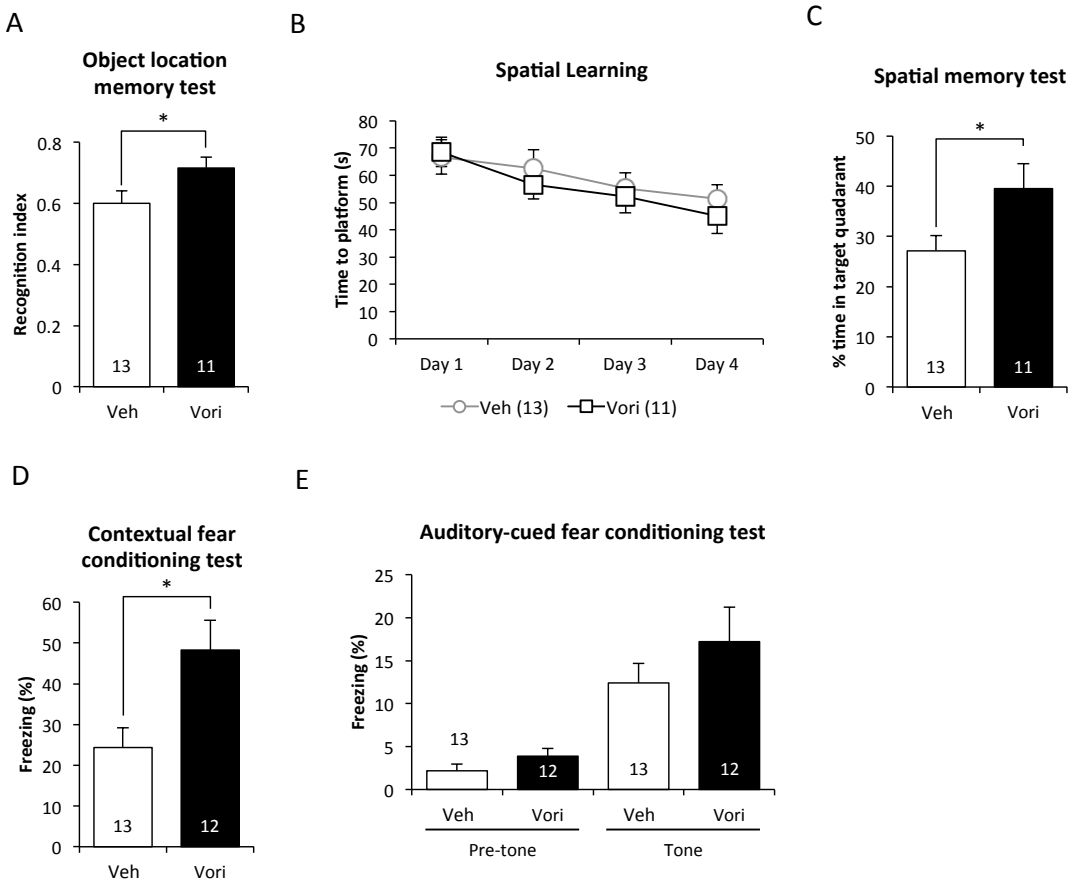

Fig. 31: **Oral administration of Voriconazole to old mice improves behaviour.**

A-E) behavioural tests of old mice treated for 45 days with Voriconazole (Vori) or Vehicle (Veh): (A) Object location memory test, (B) Spatial learning, (C) Spatial memory test, (D) Contextual fear conditioning test and (E) Auditory-cued fear conditioning test. Data are represented as mean ± SEM (*p<0.05). For statistical analysis see Supp. Table 31.

training. No group effect was found, indicating that controls and Voriconozole-treated animals learned the location of the platform at an equivalent rate (Fig.R31B), but in the memory probe test, Voriconazole-treated animals spent significantly more time in the target quadrant, compared with the control group, indicating that Voriconazole-treated showed a better spatial reference memory (Fig. R31C). In the contextual fear-conditioning test, which is primarily contingent on hippocampal function, Voriconazole-treated animals exhibited improved memory recall compared to controls (Fig. R31D). During the auditory-cued fear memory test, which depends on amygdala function but not hippocampus, both animal groups displayed similar levels of freezing behaviour (Fig. R31E) suggesting that Voriconazole increases contextual fear conditioning through an improvement of hippocampal function. Both groups presented similar sensitivity to the electric shock. All behavioural tests together indicate that the low cholesterol content associated to aged brain is in part responsible for the cognition decline observed in ageing, and that increasing the cholesterol content in brain is sufficient to enhance memory in the old.

The above series of experiment imply that the age associated cholesterol loss is deeply related to the cognitive decline in ageing, and that by restoring cholesterol levels in the old brain mnemonic processes at the behavioural level, but also at the molecular level, can be enhanced.

DISCUSSION

In this thesis we show that neuronal stimulation with low doses of NMDA, a protocol widely used to induce long term depression, triggers the fast transient activation of *Bdnf* promoters II and VI, whereas promoters I and IV present a slower response with a transcriptional activation that remains stable for a longer time, and that this differentiated pattern can be explained by H3K27 acetylation. Moreover, we show that the fine regulation of *Bdnf* promoters II and VI is disrupted in the aged brain because a low cholesterol environment impairs the signal transduction from the NMDA receptors to the nucleous, explaining at least in part, the age-associated cognitive deficits through IEGs transcription impairment.

1.- LTD induced *Bdnf* regulation in adult hippocampus:

The biological significance of this alternative promoter usage could be explained from the works developed by Baj et al (Baj et al., 2011). These authors have shown that the transcripts containing the 5´exons II and VI are transported to distal dendrites whereas the transcripts containing 5´exons I and IV are required in the soma or in proximal dendrites. By use of overexpression and silencing of specific *Bdnf* mRNA isoforms, the authors found that dendritic BDNF (from exons II and VI) plays a role in secondary dendrites' plasticity in response to external stimuli. Furthermore, the expression of individual *Bdnf* splice variants was shown to be relevant for the spatially restricted activation of TrkB receptors: *i.e.* overexpression of exon I or IV transcripts led to phosphorylation of 80–100% of TrkB receptors within the first 45 μm from the soma whereas overexpressing exon II or VI *Bdnf* variants led to 80% TrkB phosphorylation at 80 μm from the soma and beyond. Thus, the spatial segregation of *Bdnf* transcripts enables this neurotrophic factor to differentially shape distinct dendritic compartments.

At first sight it would seem that a fast induction of a promoter localized more than 50 kb 5´ away from the *Bdnf* coding exon (exon IX) is not, physiologically speaking, the optimal situation. However the fast induction of promoter II in our model would have an important biological significance. Because the ultimate destination of *Bdnf* mRNAs is dictated by the presence of different 5´UTR exons, it means that the fast induction of promoters II and VI at 10 min after LTD induction would be required to provide the stimulated cell with the adequate amounts of 5´exons II and VI-containing transcripts at the appropriate timing to be delivered to distal dendrites.

We have shown that, in adult non-stimulated neurons, *Bdnf* promoters are present in a bivalent state, partially repressed by EZH2. Application of NMDA at doses that produce chemical LTD leads to the remodelling of the transcriptional complexes, namely increased levels of activator H3K4Me3 and recruitment of H3K27Me3-demethylase JMJD3 and by the consequent decrease of the repressive mark H3K27Me3. We also found that LTD

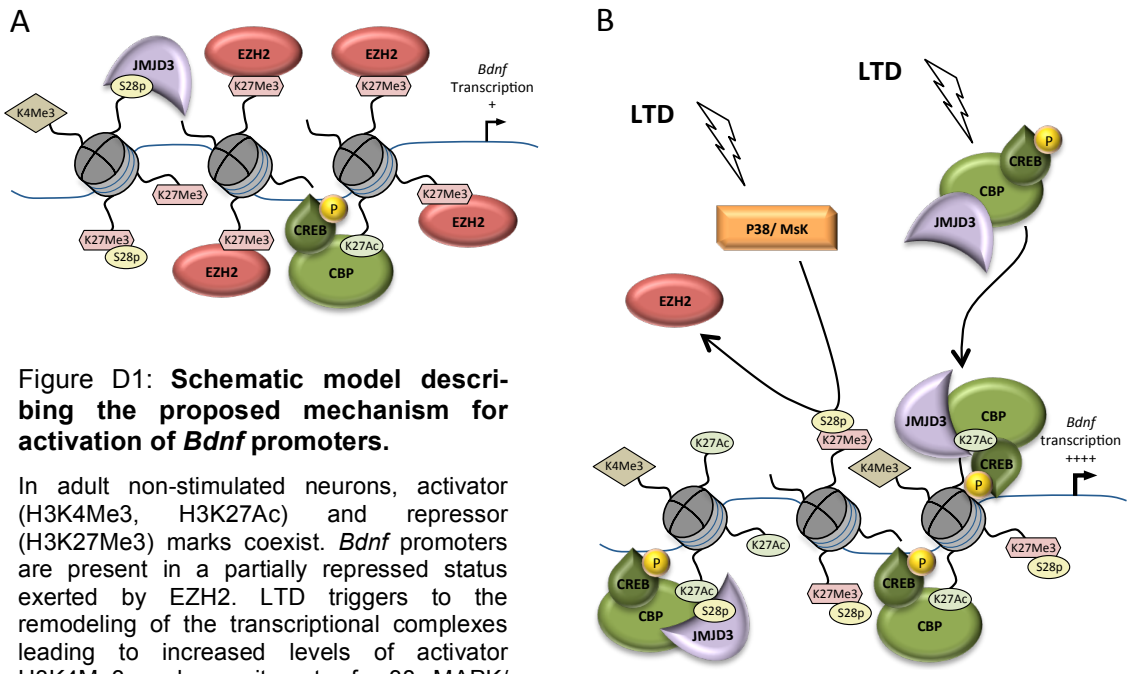

Figure D1: **Schematic model describing the proposed mechanism for activation of *Bdnf* promoters.**

In adult non-stimulated neurons, activator (H3K4Me3, H3K27Ac) and repressor (H3K27Me3) marks coexist. *Bdnf* promoters are present in a partially repressed status exerted by EZH2. LTD triggers to the remodeling of the transcriptional complexes leading to increased levels of activator H3K4Me3 and recruitment of p38 MAPK/ Msk1/2 that phosphorylate H3K27Me3 at its Ser 28 and displaces the repressor protein EZH2. LTD induction also leads to activation of CREB by phosphorylation at its Ser 133 and recruitment of the complex Ser133-CREB/CBP/JMJD3 to *Bdnf* promoters. The LTD stimulus triggers the increase of the activator mark H3K27Ac only at promoters II and VI, suggesting that H3K27 acetylation is an important factor in the high transient expression of these two promoters.

stimulus triggers the phosphorylation of the H3K27Me3 at its Ser 28 leading to the displacement of the repressor protein EZH2 (Fig. D1). In proof of functional association between these changes and activation of *Bdnf* expression, preventing H3K27Me3S28 phosphorylation blocks EZH2 release and the transcriptional stimulation of promoters II and VI.

In ES *in vitro*, PRC2 mediates di- and trimethylation of H3K27 to establish repression of specific genes. Stress, mitogenic signaling or retinoic acid induce differentiation *via* histone H3K27Me3S28 phosphorylation, displacement of polycomb proteins and gene expression (Gehani et al., 2010). Our data suggest that a similar mechanism may operate in fully mature neurons *in vitro*, in response to a memory-related stimulus. Although H3K27Me3S28 phosphorylation, EZH2 derepression and H3K27Me3 demethylation also occur after LTD at *Bdnf* promoters I and IV, blocking these processes with inhibitors does not impair the late occurring transcriptional induction of these two promoters, suggesting that the Polycomb derepression mechanism is mostly restricted to promoters II and VI.

The molecular mechanism by which a physiological mnemonic process like LTD affects *Bdnf* expression has not been studied previously. However, it has been shown that MeCP2 acts as a repressor mechanism on promoter IV through the association with the co-repressor molecule Sin3a and HDAC1 (Chen et al., 2003; Im et al., 2010; Klose and Bird, 2003; Martinowich et al., 2003). In these studies, it was shown that membrane depolarization by KCl correlated with DNA demethylation and the phosphorylation and

dissociation of MeCP2 from *Bdnf* promoter IV (Chen et al., 2003; Martinowich et al., 2003). It has also been shown that NMDA receptor activation de-represses transcription from *Bdnf* promoter I and IV in correlation with reduced occupancy by HDAC1 and MeCP2 in cultured hippocampal neurons (Tian et al., 2010a, 2010b). Since memory consolidation after fear conditioning involves LTD induction, it is possible that DNA demethylation and MeCP2 derepression would be involved in the activation of promoters I and IV after LTD.

It was recently shown that the chromodomain protein and transcription co-repressor chromodomain Y-like (CDYL) protein represses *Bdnf* promoter II in developing neurons by a polycomb-mediated mechanism and that derepression can be induced by electrical activity through the degradation of CDYL (Qi et al., 2014). We also analysed whether a CDYL-dependent mechanism would also contribute to the expression changes of any of the *Bdnf* transcripts triggered by NMDA. While CDYL was enriched at *Bdnf* promoter II, this was not the case for promoters I, IV and VI (Fig. D2A), the levels of CDYL bound to promoter II decreased significantly and remained low at 30 min after NMDA stimulation (Fig. D2B) in coincidence with protein degradation induced by the stimulus (Fig. D2C). However, as it has been shown in Figure R4, the basal levels of EZH2 are restored at promoter II, 30 min after induction. These data indicate first, that CDYL would not be involved in the de-repression of *Bdnf* promoter VI and second, that CDYL would not be involved in EZH2 recruitment to promoter II at 30 min after stimulation. However it cannot be excluded that CDYL degradation would be required also in mature neurons together with H3K27Me3S28 phosphorylation for EZH2 displacement from promoter II.

The regulation of neuronal differentiation by members of the Polycomb group of proteins has been widely described. In adult mice, a role for EZH2 in the regulation of adult neurogenesis has also been reported. In this work using *Ezh2* knockout mice, impaired learning and memory was attributed to the decreased proliferation of the

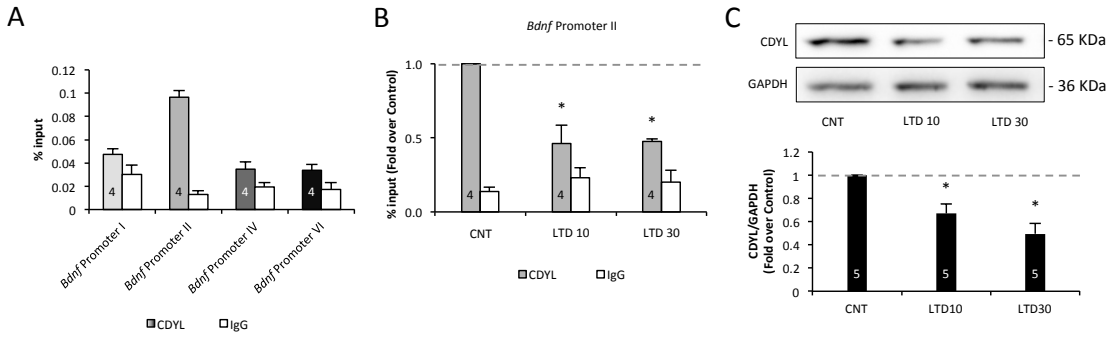

Figure D2: **NMDA stimulation modulates CDYL attachment at *Bdnf* promoter II in mature hippocampal neurons.**

A) ChIP analysis showing the presence of CDYL only at *Bdnf* promoter II. B) The ChIPs show that CDYL levels decrease at promoter II after NMDA stimulation, opening the possibility that CDYL-mediated de-repression of promoter II could be also playing a role in mature neurons. C) Western blot analysis and its cuantification show that NMDA stimulation induces CDYL degradation in mature neurons. Data are represented as mean ± SEM (*p<0.05; **p<0.01, ***p<0.001). For statistical analysis see Supp. Table 32.

progenitor cells (Zhang et al., 2014). We here show that EZH2 directly controls memory formation by regulating the expression of *Bdnf* gene in mature neurons.

After LTD induction, increases in the levels of the activator mark H3K27Ac were only observed at promoters II and VI, suggesting that H3K27 acetylation is an important factor in the high transient mRNA expression mediated by these two promoters (Fig. D1). A series of evidences are in support of the notion that transcripts II and VI rely on H3K27 acetylation. We have shown that H3K27 acetylation after NMDA stimulation at these promoters requires CREB phosphorylation. It is well known that neuronal stimulation by NMDA activates a signalling cascade resulting in CREB phosphorylation (Das et al., 1997; Nijholt et al., 2002). Phosphorylated CREB moves to the nucleus and interacts with the histone acetyl transferase CBP. Our results demonstrate that H3K27 acetylation is catalysed by the CREB-p/CBP complex, as inhibition of the CREB-p/CBP interaction impairs H3K27 acetylation and transcriptional activation of these two promoters. The presence of a CREB binding site has been observed at promoter IV and a possible role for CREB in the regulation of this promoter has been proposed but not directly demonstrated (Martinowich et al., 2003; West et al., 2001). In our work, we show that CREB-p/CBP complex is required for H3K27 acetylation and activation of promoters II and VI after LTD induction, but not for the activation of promoters I and IV.

Our results strengthen the notion that synaptic activity differentially controls the *Bdnf* promoters by use of epigenetic mechanisms that include H3K27 acetylation *via* CREB/CBP and Polycomb derepression in mature neurons. It is tempting to speculate that a similar epigenetic mechanism may regulate the expression of other early genes involved in learning and memory.

2.- The role of cholesterol in *Bdnf* regulation in old hippocampus:

Hippocampal cholesterol loss is a characteristic in the hippocampus of aged rodents and humans (Martin et al., 2008, 2014a; Söderberg et al., 1990; Sodero et al., 2011; Svennerholm et al., 1991, 1994, 1997). The data presented in the second chapter of this thesis suggest that age-associated cholesterol reduction contributes to cognitive decline in the aged brain by altering the epigenetic mechanisms involved in IEGs transcription. As a matter of fact, we have shown that hippocampal slices of the old mice fail to activate the signalling cascade in response to LTD, which is required for proper chromatin remodelling (HDAC4 detachment, CBP recruitment and H3K27 acetylation), resulting in impaired *Bdnf* transcriptional induction (Fig. D3). These results provide an additional mechanism to explain the reduced LTD and impaired memory in the brain of the old mouse, together with other biochemical deficits previously demonstrated by others (Billard and Rouaud, 2007; Lee et al., 2005; Martin et al., 2014a).

Early work indicated that LTD and NMDAR-dependent synaptic plasticity impairment in old animals are related to changes in the availability of the ligands required to activate the proper receptors in the post-synapse (Billard and Rouaud, 2007). Others showed that reduced LTD in ageing could be attributed to increased basal levels of phosphorylated AKT, probably due to increased levels of stress mediators, like interleukins, preventing GSK3ß activation and, as consequence, impairing glutamate receptor internalization and therefore reducing LTD (Martin et al., 2014a). Other groups attribute age-associated cognitive decline to changes in the composition of the NMDA receptors, and the interaction with membrane scaffolding proteins (Zamzow et al., 2013). One possible event that could conciliate all these results is the change in the lipidic environment of glutamate receptors during ageing; as this "simple" fact would be sufficient to alter not only receptors' ligand affinity but also their mobilization and internalization and the downstream signalling. In fact, enhanced learning and memory and improved electrophysiological response in the old was obtained by manipulating the ability of NMDAR to operate (Billard

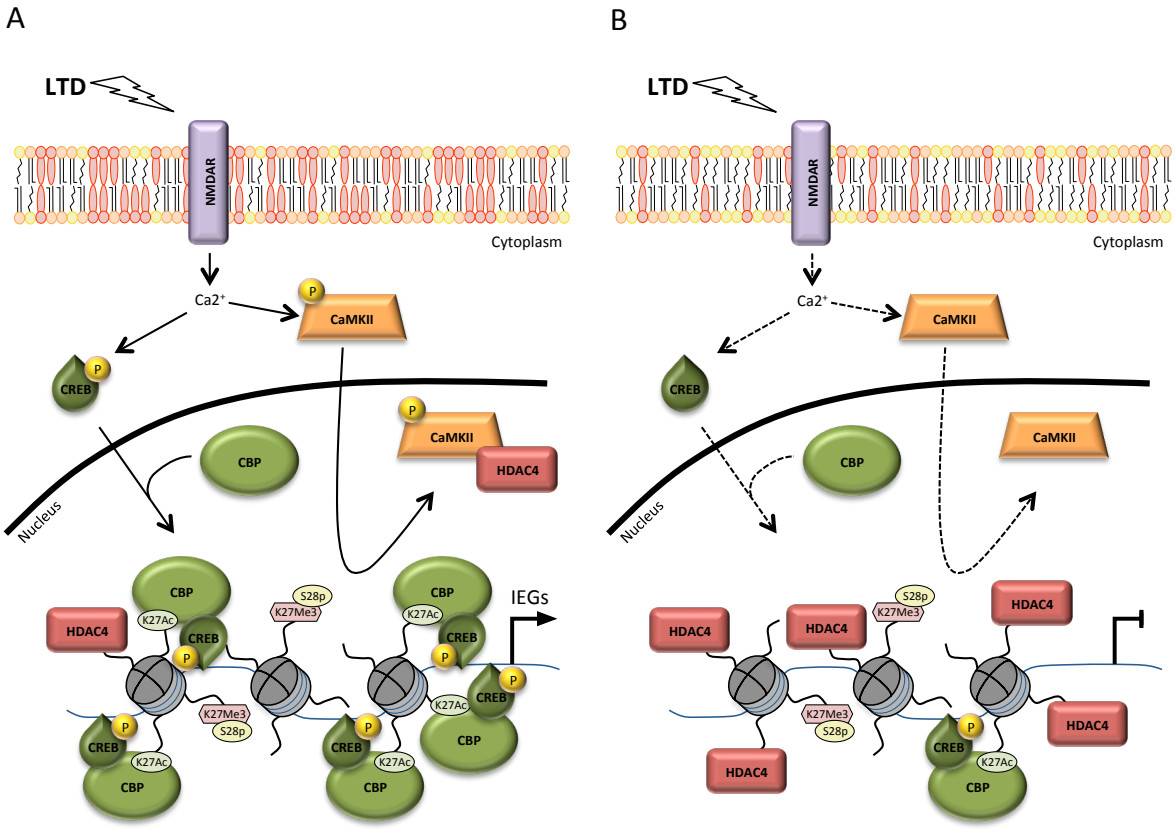

Figure D3: **Schematic model describing the impaired signaling transduction and epigenetic mechanism for IEG transcription in the old.**

A) In adult animals, LTD activates the phosphorylation cascade required for HDAC4 displacement from the chromatin and induction of H3K27 acetylation *via* CBP. B) In old mice, LTD poorly activates the transcription cascade, resulting in the preservation of HDAC4 and reduced CREB-mediated CBP binding, impairing immediate early memory gene transcription. C) Lipid legend.

and Rouaud, 2007; Kumar and Foster, 2013), and also by increasing membrane cholesterol levels (Martin et al., 2014). Moreover, numerous evidences support the view that changes in the lipidic composition of the plasma membrane and lipid rafts leads to NMDAR malfunction and neuronal excitability (Frank et al., 2004; Hering et al., 2003; Schrattenholz and Soskic, 2006).

Of the different lipid content changes occurring during aging, the loss of cholesterol is the one for which a functional association has been best characterized. Thus, Martín et al 2014 showed that adding cholesterol to old neurons is sufficient to rescue LTD *in vitro*, *in vivo* and in *ex vivo* paradigms (Martin et al., 2014a). These authors also showed that perfusion of cholesterol in the third ventricle of old mice reverts some of the cognitive deficits displayed. In concordance with these results, we present data in this thesis that point to the fact that cholesterol loss, as it takes place in the aged, impairs the glutamate receptor downstream signalling required to induce CREB and CaMKII phosphorylation and consequently the chromatin remodelling to facilitate *Bdnf* transcription (Fig. D3). That this failure is due to the low cholesterol typical of old neurons was demonstrated by increasing the cholesterol content in old hippocampal slices. This simple manipulation turned out to be sufficient to rescue CREB and CaMKII phosphorylation upon LTD, and HDAC4 detachment, CBP recruitment at *Bdnf* promoters. This manipulation was also sufficient for the increase in H3K27Ac, all in all leading to better *Bdnf* transcription by the old neurons. Another demonstration that the reduced expression of *Bdnf* in old neurons is due to the cholesterol loss comes from the opposite experiments, where removing cholesterol in hippocampal slices of young mice prevents the proper epigenetic regulatory pathway activation. Reduction of cholesterol by COase treatments led to impaired activation of the CREB and CaMKII kinases with the subsequent reduced chromatin remodelling and *Bdnf* transcription. Hence, these results reinforce the idea that a major and rather biochemical “upstream” problem in old neurons resides in the reduced levels of cholesterol in the plasma membrane. Intuitively, the paucity of this sterol would suffice to alter most neurotransmitter receptors downstream events required for the proper expression of learning and memory genes.

Supporting the view that disrupting the signalling cascade that leads to the epigenetic regulation for gene expression determines poor cognitive abilities, several reports have shown the number of genes expressed in young and old in response to cognitive stimuli are significantly different, and that modulating chromatin remodelling enzymes facilitates gene transcription in the old, in parallel with enhanced memory. Thus, Peleg and colleges (Peleg et al., 2010) showed that just 16 transcripts were altered in aged mice 1 hour after fear conditioning, while in young more than 2000 had changed. This reduced transcriptional plasticity was associated with impaired learning, and it was argued that

gene transcription differences were due to changes in H4K12 acetylation after fear conditioning. Consistently, plasticity induced gene transcription, H4H12Ac and memory in the old were all rescued by treating mice with the HDAC inhibitor SAHA 1 h before fear conditioning (Peleg et al., 2010). The association between learning and memory deficits in the old and epigenetic-mediated gene expression deficits was also shown by other means. Thus, it was shown that treating old rats 1 hour after novel object recognition with sodium butyrate, another HDAC inhibitor, improves memory retention 24 hours after training (Reolon et al., 2011). In addition to HDACs, deficits in DNA methylation can also underlie poor memory of the old. Thus, it was shown that brain ageing is accompanied by decreased DNA methylation, mainly due to reduced de novo methylation of the active chromatin, or euchromatin (Kang et al., 2001). Furthermore, Oliveira et al showed that the old hippocampus presents lower levels of DNMT3a2, which is associated to euchromatin (Chen et al., 2002). In this work, it was also shown that *Dnmt3a2* transcription depends on NMDAR activation, thus behaving like an IEGs. Consistently, increasing DNMT3a2 levels in the old hippocampus, by stereotaxically delivered recombinant adeno-associated virus, enhanced fear conditioning memories (Oliveira et al., 2012). While not directly demonstrated, it appears reasonable to argue that the membrane changes that characterize the old may be responsible for the HDAC and methylation deficits described above. The lipidic changes may certainly impair neurotransmitter receptor activation strength, being not sufficient to reach the threshold needed to activate chromatin remodelling and IEGs transcription.

There are numerous evidences that modulation of plasma membrane lipid composition, in ageing and in disease, can enhance memory and learning. Thus, in Niemann Pick type A mice, that mimic this rare and severe neurological disease characterized by the abnormal accumulation of sphingomyelin, Arroyo et al showed that the administration of dexamethasone orally increases the levels and activity of the enzyme neutral sphyngomyelinase, resulting in a reduction in sphingomyelin levels and enhancing spatial memories (Arroyo et al., 2014). Cholesterol modulation was also shown to play a role in the cognitive deficits of old mice and in certain pathological situation of the old. In regard to the latter, a recent study demonstrated that systemic administration of cholesterol-filled nanoparticles can cross the blood-brain barrier and increases cholesterol content in striatal neurons, rescuing Huntington disease deficits in a mouse model (Valenza et al., 2015). Concerning the normal cognitive deficits of the old, previous work from this laboratory has shown that intraventricular perfusion of cholesterol in old rats improved cognition and cognition-related electrophysiological parameters (Martin et al., 2014a). While these last results show the importance of cholesterol loss in the cognitive deficits of the old, direct brain cholesterol manipulation through replenishment, whether

direct brain perfusion or *via* systemically administered nanoparticles, does not appear a most convenient strategy for therapeutic use. A more practical solution would be interfering with the mechanism involved in cholesterol loss during aging.

As commented earlier, brain cholesterol reduction in the aged can be the consequence of increased catabolism, reduced synthesis or/and reduced transference from astrocytes (Martin et al., 2014b). The degree of participation of any of these mechanisms varies in different brain regions. Thus, reduced synthesis and transference appears to be the main mechanism operating in the striatum, whereas increased catabolism is the main factor in the hippocampus (Martin et al., 2008; Valenza et al., 2005). In the hippocampus, higher catabolism with age appears to be due to increased expression of the brain specific cholesterol hydroxylase Cyp46A1 (Martin et al., 2008). In turn, increased expression of Cyp46A1 is due to oxidative stress accumulation (Ohyama et al., 2006). In agreement with this possibility, enzyme levels and activity increase in models of cortical injury, autoimmune encephalomyelitis and Alzheimer's disease (Bogdanovic et al., 2001; Cartagena et al., 2008; Teunissen et al., 2007). It then appeared reasonable to us that the inhibition of Cyp46A1 activity could be a suitable strategy, at least in part, to prevent the cholesterol loss that normally occurs with age. In fact, our *in vivo* experiments confirmed this hypothesis; orally administrated Voriconazole, the Cyp46A1 inhibitor, rescued chromatin remodelling and *Bdnf* transcription upon LTD and enhanced memory in the old treated mice. Moreover, we showed that the rescued transcription by Voriconazole treatment is not restricted to *Bdnf*, but also to others IEGs such as *Arc* and *Ppp1cc*, suggesting that increased cholesterol levels would facilitate the normal transcription after neuronal stimulation, and therefore enhance learning and memory.

From all the data presented in the second chapter of this thesis, it appears reasonable to propose that, apart from non pathological age-associated cognitive decline, also pathological conditions such as Alzheimer's and Huntington's disease, all characterized by significant changes in cholesterol content (Leoni and Caccia, 2014; Molander-Melin et al., 2005; Papassotiropoulos et al.; Roher et al., 2002; Valenza et al., 2005, 2010), may obtain benefits by strategies that prevent the loss of this sterol: this would in turn facilitate the restoration of numerous membrane signalling pathways, among them, those required for proper learning and memory gene activation.

All in all, the work in this thesis has contributed to unveil some of the epigenetic mechanisms involved in the expression of a synaptic plasticity gene, *Bdnf*, in response to a chemical paradigm of learning and memory and highlights the importance of brain cholesterol homeostasis in gene expression regulation and learning and memory processes.

CONCLUSIONS

1.- *Bdnf* promoters are found in a bivalent epigenetic state in the adult, with the coexistence on the same promoters of activating marks such as H3K4Me3 and H3K27Ac with the repressive mark H3K27Me3.

2.- NMDA-LTD triggers two different types of transcriptional responses of *Bdnf* promoters: a fast transient induction of promoters II and VI and a slower, more stable response of promoters I and IV.

3.- NMDA uses the p38/Msk1/2 pathway for H3K27Me3S28 phosphorylation, which is required for EZH2 displacement from *Bdnf* promoters II and VI after stimulus.

4.- NMDA-LTD leads to CREB activation *via* CamKII-PKC/MSK1 kinases. Activated CREB recruits the histone acetyl transferase CBP to *Bdnf* promoters.

5. CBP recruits the histone demethylase JMJD3, contributing to de-repress and fully activate *Bdnf* expression by decreasing H3K27Me3 and by acetylating H3K27 at Bdnf promoters II and VI upon LTD.

6.- The old hippocampus presents lower *Bdnf* transcripts II and VI levels, correlating with increased H3K27Me3 and H3K27Me3S28p, and decreased H3K27Ac and CBP comared to the adult, suggesting impaired activation on the corresponding promoters.

7.- NMDA-LTD in the old fails to induce the normal downstream activation cascade that leads to chromatin remodelling at *Bdnf* promoters, resulting in impaired *Bdnf* transcription after stimulation.

8.- Cholesterol at the plasma membrane is necessary for LTD signal transduction to the nucleus, achieving *Bdnf* chromatin remodelling and transcription.

9.- Cyp46A1 inhibition by orally administrated Voriconazole rescues the age-associated cholesterol loss in the old, enhancing learning and memory.

10.- Voriconazole treatment rescues the nuclear signalling transduction upon LTD, facilitating H3K27Ac at *Bdnf* promoters and its transcription. Moreover, this transcriptional rescue it is not restricted to *Bdnf*, but also to other IEGs such as *Ppp1c*c and *Arc*.

CONCLUSIONES

1.- En el adulto, los promotores de *Bdnf* se encuentran es un estado epigenético bivalente, coexistiendo en el mismo promotor marcas activadoras como H3K4Me3 y H3K27Ac con la marca represora H3K27Me3.

2.- La NMDA-LTD desencadena dos tipos de respuestas transcripcionales de los promotores de *Bdnf*: una respuesta rápida y transitoria de los promotores II y VI, y una respuesta lenta, y más sostenida, de los promotores I y IV.

3.- El NMDA se sirve de la *via* de p38/Msk1-2 para la fosforilación de H3K27Me3S28, la que se requiere para el desplazamiento de EZH2 en los promotores II y VI en respuesta a estímulo.

4.- La NMDA-LTD conduce a la activación de CREB mediante las quinasas CaMKII-PKC/MSK1. Una vez activo, CREB recluta la histona acetyltransferasa CBP a los promotores de *Bdnf*.

5.- CBP recluta a la desmetilasa de histonas JMJD3, contribuyendo a la desrepresión y la completa activación de la expresión de *Bdnf*, reduciendo la metilación de H3K27 e incrementando la acetilación de H3K27 en los promotores II y VI de *Bdnf* tras la LTD.

6.- El hipocampo de ratones viejos presenta niveles bajos de los transcritos II y VI de *Bdnf*, acompañado de un incremento en H3K27Me3 y H3K27Me3S28p, y una reducción de H3K27Ac y CBP, sugiriendo déficits en la activación de los correspondientes promotores.

7.- La NMDA-LTD en el ratón viejo no es capaz de inducir la cascada de activación que lleva al remodelado de la cromatina en los promotores de *Bdnf*, resultando en una incapacidad de transcribir *Bdnf* después del estímulo.

8.- El colesterol en la membrana plasmática es necesario para la eficiente transducción al núcleo de la señal de LTD, facilitando el remodelado de la cromatina y transcripción de *Bdnf*.

9.- La inhibición de Cyp46A1 por la administración oral de Voriconazole, rescata la perdida de colesterol asociada al envejecimiento, mejorando el aprendizaje y la memoria.

10.- El tratamiento con Voriconazole rescata la transducción de la señal nuclear en respuesta a LTD, facilitando la H3K27Ac en los promotores de *Bdnf*, así como su transcripción. Además, este recate de la transcripción no está restringido solamente a *Bdnf*, sino que también otros IEGs como *Ppp1cc* y *Arc*.

REFERENCES

Ahn, S., Ginty, D.D., and Linden, D.J. (1999). A late phase of cerebellar long-term depression requires activation of CaMKIV and CREB. Neuron *23*, 559–568.

Aid, T., Kazantseva, A., Piirsoo, M., Palm, K., and Timmusk, T. (2007). Mouse and rat BDNF gene structure and expression revisited. J. Neurosci. Res. *85*, 525–535.

Alarcón, J.M., Malleret, G., Touzani, K., Vronskaya, S., Ishii, S., Kandel, E.R., and Barco, A. (2004). Chromatin acetylation, memory, and LTP are impaired in CBP+/- mice: a model for the cognitive deficit in Rubinstein-Taybi syndrome and its amelioration. Neuron *42*, 947–959.

An, J.J., Gharami, K., Liao, G.-Y., Woo, N.H., Lau, A.G., Vanevski, F., Torre, E.R., Jones, K.R., Feng, Y., Lu, B., et al. (2008). Distinct role of long 3' UTR BDNF mRNA in spine morphology and synaptic plasticity in hippocampal neurons. Cell *134*, 175–187.

Arroyo, A.I., Camoletto, P.G., Morando, L., Sassoe-Pognetto, M., Giustetto, M., Van Veldhoven, P.P., Schuchman, E.H., and Ledesma, M.D. (2014). Pharmacological reversion of sphingomyelin-induced dendritic spine anomalies in a Niemann Pick disease type A mouse model. EMBO Mol. Med. *6*, 398–413.

Azuara, V., Perry, P., Sauer, S., Spivakov, M., Jørgensen, H.F., John, R.M., Gouti, M., Casanova, M., Warnes, G., Merkenschlager, M., et al. (2006). Chromatin signatures of pluripotent cell lines. Nat. Cell Biol. *8*, 532–538.

Bach, M.E., Barad, M., Son, H., Zhuo, M., Lu, Y.F., Shih, R., Mansuy, I., Hawkins, R.D., and Kandel, E.R. (1999). Age-related defects in spatial memory are correlated with defects in the late phase of hippocampal long-term potentiation in vitro and are attenuated by drugs that enhance the cAMP signaling pathway. Proc. Natl. Acad. Sci. U. S. A. *96*, 5280–5285.

Backs, J., Song, K., Bezprozvannaya, S., Chang, S., and Olson, E.N. (2006). CaM kinase II selectively signals to histone deacetylase 4 during cardiomyocyte hypertrophy. J. Clin. Invest. *116*, 1853–1864.

Baj, G., Leone, E., Chao, M. V, and Tongiorgi, E. (2011). Spatial segregation of BDNF transcripts enables BDNF to differentially shape distinct dendritic compartments. Proc. Natl. Acad. Sci. U. S. A. *108*, 16813–16818.

Ball, M.J. (1977). Neuronal loss, neurofibrillary tangles and granulovacuolar degeneration in the hippocampus with ageing and dementia. A quantitative study. Acta Neuropathol. *37*, 111–118.

Baltan, S. (2012). Histone deacetylase inhibitors preserve function in aging axons. J. Neurochem. *123 Suppl* , 108–115.

Bannister, A.J., and Kouzarides, T. (2011). Regulation of chromatin by histone modifications. Cell Res. *21*, 381–395.

Barde, Y.A., Edgar, D., and Thoenen, H. (1982). Purification of a new neurotrophic factor from mammalian brain. EMBO J. *1*, 549–553.

Barnes, C.A. (1994). Normal aging: regionally specific changes in hippocampal synaptic transmission. Trends Neurosci. *17*, 13–18.

Bartke, T., Vermeulen, M., Xhemalce, B., Robson, S.C., Mann, M., and Kouzarides, T. (2010). Nucleosome-interacting proteins regulated by DNA and histone methylation. Cell *143*, 470–484.

Bernstein, B.E., Mikkelsen, T.S., Xie, X., Kamal, M., Huebert, D.J., Cuff, J., Fry, B., Meissner, A., Wernig, M., Plath, K., et al. (2006). A bivalent chromatin structure marks key developmental genes in embryonic stem cells. Cell *125*, 315–326.

Best, J.L., Amezcua, C.A., Mayr, B., Flechner, L., Murawsky, C.M., Emerson, B., Zor, T., Gardner, K.H., and Montminy, M. (2004). Identification of small-molecule antagonists that inhibit an activator: coactivator interaction. Proc. Natl. Acad. Sci. U. S. A. *101*, 17622–17627.

Bestor, T.H., Gundersen, G., Kolstø, A.B., and Prydz, H. (1992). CpG islands in mammalian gene promoters are inherently resistant to de novo methylation. Genet. Anal. Tech. Appl. *9*, 48–53.

Billard, J.-M., and Rouaud, E. (2007). Deficit of NMDA receptor activation in CA1 hippocampal area of aged rats is rescued by D-cycloserine. Eur. J. Neurosci. *25*, 2260–2268.

Bird, A. (2002). DNA methylation patterns and epigenetic memory. Genes Dev. *16*, 6–21.

Blalock, E.M., Chen, K.-C., Sharrow, K., Herman, J.P., Porter, N.M., Foster, T.C., and Landfield, P.W. (2003). Gene microarrays in hippocampal aging: statistical profiling identifies novel processes correlated with cognitive impairment. J. Neurosci. *23*, 3807–3819.

Bogdanovic, N., Bretillon, L., Lund, E.G., Diczfalusy, U., Lannfelt, L., Winblad, B., Russell, D.W., and Björkhem, I. (2001). On the turnover of brain cholesterol in patients with Alzheimer's disease. Abnormal induction of the cholesterol-catabolic enzyme CYP46 in glial cells. Neurosci. Lett. *314*, 45–48.

Borun, T.W., Pearson, D., and Paik, W.K. (1972). Studies of histone methylation during the HeLa S-3 cell cycle. J. Biol. Chem. *247*, 4288–4298.

Boulle, F., van den Hove, D.L. a, Jakob, S.B., Rutten, B.P., Hamon, M., van Os, J., Lesch,

K.-P., Lanfumey, L., Steinbusch, H.W., and Kenis, G. (2012). Epigenetic regulation of the BDNF gene: implications for psychiatric disorders. Mol. Psychiatry *17*, 584–596.

Boyer, L.A., Plath, K., Zeitlinger, J., Brambrink, T., Medeiros, L.A., Lee, T.I., Levine, S.S., Wernig, M., Tajonar, A., Ray, M.K., et al. (2006). Polycomb complexes repress developmental regulators in murine embryonic stem cells. Nature *441*, 349–353.

Brachet, A., Norwood, S., Brouwers, J.F., Palomer, E., Helms, J.B., Dotti, C.G., and Esteban, J.A. (2015). LTP-triggered cholesterol redistribution activates Cdc42 and drives AMPA receptor synaptic delivery. J. Cell Biol. *208*, 791–806.

Bramham, C.R., and Wells, D.G. (2007). Dendritic mRNA: transport, translation and function. Nat. Rev. Neurosci. *8*, 776–789.

Brandon, E.P., Zhuo, M., Huang, Y.Y., Qi, M., Gerhold, K.A., Burton, K.A., Kandel, E.R., McKnight, G.S., and Idzerda, R.L. (1995). Hippocampal long-term depression and depotentiation are defective in mice carrying a targeted disruption of the gene encoding the RI beta subunit of cAMP-dependent protein kinase. Proc. Natl. Acad. Sci. U. S. A. *92*, 8851–8855.

Bredy, T.W., and Barad, M. (2008). The histone deacetylase inhibitor valproic acid enhances acquisition, extinction, and reconsolidation of conditioned fear. Learn. Mem. *15*, 39–45.

Bredy, T.W., Wu, H., Crego, C., Zellhoefer, J., Sun, Y.E., and Barad, M. (2007). Histone modifications around individual BDNF gene promoters in prefrontal cortex are associated with extinction of conditioned fear. Learn. Mem. *14*, 268–276.

Brody, H. (1955). Organization of the cerebral cortex. III. A study of aging in the human cerebral cortex. J. Comp. Neurol. *102*, 511–516.

Burke, S.N., and Barnes, C.A. (2006). Neural plasticity in the ageing brain. Nat. Rev. Neurosci. *7*, 30–40.

Byvoet, P., Shepherd, G.R., Hardin, J.M., and Noland, B.J. (1972). The distribution and turnover of labeled methyl groups in histone fractions of cultured mammalian cells. Arch. Biochem. Biophys. *148*, 558–567.

Cartagena, C.M., Ahmed, F., Burns, M.P., Pajoohesh-Ganji, A., Pak, D.T., Faden, A.I., and Rebeck, G.W. (2008). Cortical injury increases cholesterol 24S hydroxylase (Cyp46) levels in the rat brain. J. Neurotrauma *25*, 1087–1098.

Chahrour, M., Jung, S.Y., Shaw, C., Zhou, X., Wong, S.T.C., Qin, J., and Zoghbi, H.Y. (2008). MeCP2, a key contributor to neurological disease, activates and represses transcription. Science *320*, 1224–1229.

Chen, T., Ueda, Y., Xie, S., and Li, E. (2002). A novel Dnmt3a isoform produced from an alternative promoter localizes to euchromatin and its expression correlates with active de novo methylation. J. Biol. Chem. *277*, 38746–38754.

Chen, W.G., Chang, Q., Lin, Y., Meissner, A., West, A.E., Griffith, E.C., Jaenisch, R., and Greenberg, M.E. (2003). Derepression of BDNF transcription involves calcium-dependent phosphorylation of MeCP2. Science *302*, 885–889.

Chiaruttini, C., Sonego, M., Baj, G., Simonato, M., and Tongiorgi, E. (2008). BDNF mRNA splice variants display activity-dependent targeting to distinct hippocampal laminae. Mol. Cell. Neurosci. *37*, 11–19.

Chiaruttini, C., Vicario, A., Li, Z., Baj, G., Braiuca, P., Wu, Y., Lee, F.S., Gardossi, L., Baraban, J.M., and Tongiorgi, E. (2009). Dendritic trafficking of BDNF mRNA is mediated by translin and blocked by the G196A (Val66Met) mutation. Proc. Natl. Acad. Sci. U. S. A. *106*, 16481–16486.

Choi, H.S., Choi, B.Y., Cho, Y.-Y., Zhu, F., Bode, A.M., and Dong, Z. (2005). Phosphorylation of Ser28 in histone H3 mediated by mixed lineage kinase-like mitogen-activated protein triple kinase alpha. J. Biol. Chem. *280*, 13545–13553.

Chouliaras, L., van den Hove, D.L.A., Kenis, G., Draanen, M. van, Hof, P.R., van Os, J., Steinbusch, H.W.M., Schmitz, C., and Rutten, B.P.F. (2013). Histone deacetylase 2 in the mouse hippocampus: attenuation of age-related increase by caloric restriction. Curr. Alzheimer Res. *10*, 868–876.

Chwang, W.B., Arthur, J.S., Schumacher, A., and Sweatt, J.D. (2007). The nuclear kinase mitogen- and stress-activated protein kinase 1 regulates hippocampal chromatin remodeling in memory formation. J. Neurosci. *27*, 12732–12742.

Clayton, A.L., Rose, S., Barratt, M.J., and Mahadevan, L.C. (2000). Phosphoacetylation of histone H3 on c-fos- and c-jun-associated nucleosomes upon gene activation. EMBO J. *19*, 3714–3726.

Clouaire, T., and Stancheva, I. (2008). Methyl-CpG binding proteins: specialized transcriptional repressors or structural components of chromatin? Cell. Mol. Life Sci. *65*, 1509–1522.

Coleman, P.D., Flood, D.G., and West, M.J. (1987). Volumes of the components of the hippocampus in the aging F344 rat. J. Comp. Neurol. *266*, 300–306.

Collingridge, G.L., Isaac, J.T.R., and Wang, Y.T. (2004). Receptor trafficking and synaptic plasticity. Nat. Rev. Neurosci. *5*, 952–962.

Collingridge, G.L., Olsen, R.W., Peters, J., and Spedding, M. (2009). A nomenclature for

ligand-gated ion channels. Neuropharmacology *56*, 2–5.

Collingridge, G.L., Peineau, S., Howland, J.G., and Wang, Y.T. (2010). Long-term depression in the CNS. Nat. Rev. Neurosci. *11*, 459–473.

Cook, P.J., Ju, B.G., Telese, F., Wang, X., Glass, C.K., and Rosenfeld, M.G. (2009). Tyrosine dephosphorylation of H2AX modulates apoptosis and survival decisions. Nature *458*, 591–596.

Curcio, C.A., and Hinds, J.W. (1983). Stability of synaptic density and spine volume in dentate gyrus of aged rats. Neurobiol. Aging *4*, 77–87.

Curran, T., Bravo, R., and Müller, R. (1985). Transient induction of c-fos and c-myc in an immediate consequence of growth factor stimulation. Cancer Surv. *4*, 655–681.

Das, S., Grunert, M., Williams, L., and Vincent, S.R. (1997). NMDA and D1 receptors regulate the phosphorylation of CREB and the induction of c-fos in striatal neurons in primary culture. Synapse *25*, 227–233.

Deinhardt, K., and Chao, M. V (2014). Shaping neurons: Long and short range effects of mature and proBDNF signalling upon neuronal structure. Neuropharmacology *76 Pt C*, 603–609.

Dincheva, I., Glatt, C.E., and Lee, F.S. (2012). Impact of the BDNF Val66Met Polymorphism on Cognition: Implications for Behavioral Genetics. Neurosci. *18*, 439–451.

Ding, Q., Vaynman, S., Akhavan, M., Ying, Z., and Gomez-Pinilla, F. (2006). Insulin-like growth factor I interfaces with brain-derived neurotrophic factor-mediated synaptic plasticity to modulate aspects of exercise-induced cognitive function. Neuroscience *140*, 823–833.

Dolton, M.J., and McLachlan, A.J. (2014). Voriconazole pharmacokinetics and exposure-response relationships: assessing the links between exposure, efficacy and toxicity. Int. J. Antimicrob. Agents *44*, 183–193.

Ehlers, M.D. (2000). Reinsertion or degradation of AMPA receptors determined by activity-dependent endocytic sorting. Neuron *28*, 511–525.

Feng, J., Zhou, Y., Campbell, S.L., Le, T., Li, E., Sweatt, J.D., Silva, A.J., and Fan, G. (2010). Dnmt1 and Dnmt3a maintain DNA methylation and regulate synaptic function in adult forebrain neurons. Nat. Neurosci. *13*, 423–430.

Fernández-Monreal, M., Brown, T.C., Royo, M., and Esteban, J.A. (2012). The balance between receptor recycling and trafficking toward lysosomes determines synaptic strength during long-term depression. J. Neurosci. *32*, 13200–13205.

Ferreiro, I., Joaquin, M., Islam, A., Gomez-Lopez, G., Barragan, M., Lombardía, L., Domínguez, O., Pisano, D.G., Lopez-Bigas, N., Nebreda, A.R., et al. (2010). Whole genome analysis of p38 SAPK-mediated gene expression upon stress. BMC Genomics *11*, 144.

Fischle, W. (2008). Talk is cheap--cross-talk in establishment, maintenance, and readout of chromatin modifications. Genes Dev. *22*, 3375–3382.

Flood, D.G., Guarnaccia, M., and Coleman, P.D. (1987). Dendritic extent in human CA2-3 hippocampal pyramidal neurons in normal aging and senile dementia. Brain Res. *409*, 88–96.

Foster, T.C., and Norris, C.M. (1997). Age-associated changes in Ca(2+)-dependent processes: relation to hippocampal synaptic plasticity. Hippocampus *7*, 602–612.

Fraga, M.F., Ballestar, E., Paz, M.F., Ropero, S., Setien, F., Ballestar, M.L., Heine-Suñer, D., Cigudosa, J.C., Urioste, M., Benitez, J., et al. (2005). Epigenetic differences arise during the lifetime of monozygotic twins. Proc. Natl. Acad. Sci. U. S. A. *102*, 10604–10609.

Frank, C., Giammarioli, A.M., Pepponi, R., Fiorentini, C., and Rufini, S. (2004). Cholesterol perturbing agents inhibit NMDA-dependent calcium influx in rat hippocampal primary culture. FEBS Lett. *566*, 25–29.

Fritsch, C., Brown, J.L., Kassis, J.A., and Müller, J. (1999). The DNA-binding polycomb group protein pleiohomeotic mediates silencing of a Drosophila homeotic gene. Development *126*, 3905–3913.

Fujii, S., Saito, K., Miyakawa, H., Ito, K., and Kato, H. (1991). Reversal of long-term potentiation (depotentiation) induced by tetanus stimulation of the input to CA1 neurons of guinea pig hippocampal slices. Brain Res. *555*, 112–122.

Galani, R., Weiss, I., Cassel, J.C., and Kelche, C. (1998). Spatial memory, habituation, and reactions to spatial and nonspatial changes in rats with selective lesions of the hippocampus, the entorhinal cortex or the subiculum. Behav. Brain Res. *96*, 1–12.

Gardoni, F., Schrama, L.H., van Dalen, J.J., Gispen, W.H., Cattabeni, F., and Di Luca, M. (1999). AlphaCaMKII binding to the C-terminal tail of NMDA receptor subunit NR2A and its modulation by autophosphorylation. FEBS Lett. *456*, 394–398.

Gean, P.-W., Chang, F.-C., Yi, P.-L., Lin, J.-H., and Tsai, J.-J. (1995). Activation of Metabotropic Glutamate Receptors in Conjunction with Postsynaptic Depolarization Triggers a Long-Term Depression of the N-Methyl-D-Aspartate Receptor-Mediated Synaptic Potential in the Rat Hippocampus. J. Biomed. Sci. *2*, 166–173.

Gehani, S.S., Agrawal-Singh, S., Dietrich, N., Christophersen, N.S., Helin, K., and Hansen, K. (2010). Polycomb group protein displacement and gene activation through MSK-dependent H3K27me3S28 phosphorylation. Mol. Cell *39*, 886–900.

Gershey, E.L., Haslett, G.W., Vidali, G., and Allfrey, V.G. (1969). Chemical studies of histone methylation. Evidence for the occurrence of 3-methylhistidine in avian erythrocyte histone fractions. J. Biol. Chem. *244*, 4871–4877.

Ghosh, A., Carnahan, J., and Greenberg, M.E. (1994). Requirement for BDNF in activity-dependent survival of cortical neurons. Science *263*, 1618–1623.

Gibson, C.L., and Murphy, S.P. (2010). Benefits of histone deacetylase inhibitors for acute brain injury: a systematic review of animal studies. J. Neurochem. *115*, 806–813.

Goelet, P., Castellucci, V.F., Schacher, S., and Kandel, E.R. (1986). The long and the short of long-term memory--a molecular framework. Nature *322*, 419–422.

Gonzalez, G.A., and Montminy, M.R. (1989). Cyclic AMP stimulates somatostatin gene transcription by phosphorylation of CREB at serine 133. Cell *59*, 675–680.

Goritz, C., Mauch, D.H., and Pfrieger, F.W. (2005). Multiple mechanisms mediate cholesterol-induced synaptogenesis in a CNS neuron. Mol. Cell. Neurosci. *29*, 190–201.

Greer, E.L., and Shi, Y. (2012). Histone methylation: a dynamic mark in health, disease and inheritance. Nat. Rev. Genet. *13*, 343–357.

Grill, J.D., and Riddle, D.R. (2002). Age-related and laminar-specific dendritic changes in the medial frontal cortex of the rat. Brain Res. *937*, 8–21.

Grozinger, C.M., Chao, E.D., Blackwell, H.E., Moazed, D., and Schreiber, S.L. (2001). Identification of a Class of Small Molecule Inhibitors of the Sirtuin Family of NAD-dependent Deacetylases by Phenotypic Screening. J. Biol. Chem. *276*, 38837–38843.

Guan, J.-S., Haggarty, S.J., Giacometti, E., Dannenberg, J.-H., Joseph, N., Gao, J., Nieland, T.J.F., Zhou, Y., Wang, X., Mazitschek, R., et al. (2009). HDAC2 negatively regulates memory formation and synaptic plasticity. Nature *459*, 55–60.

Gupta, R.A., Shah, N., Wang, K.C., Kim, J., Horlings, H.M., Wong, D.J., Tsai, M.-C., Hung, T., Argani, P., Rinn, J.L., et al. (2010a). Long non-coding RNA HOTAIR reprograms chromatin state to promote cancer metastasis. Nature *464*, 1071–1076.

Gupta, S., Kim, S.Y., Artis, S., Molfese, D.L., Schumacher, A., Sweatt, J.D., Paylor, R.E., and Lubin, F.D. (2010b). Histone methylation regulates memory formation. J. Neurosci. *30*, 3589–3599.

Guzowski, J.F. (2002). Insights into immediate-early gene function in hippocampal

memory consolidation using antisense oligonucleotide and fluorescent imaging approaches. Hippocampus *12*, 86–104.

Hanks, S.D., and Flood, D.G. (1991). Region-specific stability of dendritic extent in normal human aging and regression in Alzheimer's disease. I. CA1 of hippocampus. Brain Res. *540*, 63–82.

Hattiangady, B., Rao, M.S., Shetty, G.A., and Shetty, A.K. (2005). Brain-derived neurotrophic factor, phosphorylated cyclic AMP response element binding protein and neuropeptide Y decline as early as middle age in the dentate gyrus and CA1 and CA3 subfields of the hippocampus. Exp. Neurol. *195*, 353–371.

Head, E., Mehta, R., Hartley, J., Kameka, M., Cummings, B.J., Cotman, C.W., Ruehl, W.W., and Milgram, N.W. (1995). Spatial learning and memory as a function of age in the dog. Behav. Neurosci. *109*, 851–858.

Hebb, D.O. (1949). The organization of behavior; a neuropsychological theory.

Heinemann, B., Nielsen, J.M., Hudlebusch, H.R., Lees, M.J., Larsen, D.V., Boesen, T., Labelle, M., Gerlach, L.-O., Birk, P., and Helin, K. (2014). Inhibition of demethylases by GSK-J1/J4. Nature *514*, E1–E2.

Hering, H., Lin, C.-C., and Sheng, M. (2003). Lipid rafts in the maintenance of synapses, dendritic spines, and surface AMPA receptor stability. J. Neurosci. *23*, 3262–3271.

Hong, L., Schroth, G.P., Matthews, H.R., Yau, P., and Bradbury, E.M. (1993). Studies of the DNA binding properties of histone H4 amino terminus. Thermal denaturation studies reveal that acetylation markedly reduces the binding constant of the H4 "tail" to DNA. J. Biol. Chem. *268*, 305–314.

Hong, S., Cho, Y.-W., Yu, L.-R., Yu, H., Veenstra, T.D., and Ge, K. (2007). Identification of JmjC domain-containing UTX and JMJD3 as histone H3 lysine 27 demethylases. Proc. Natl. Acad. Sci. U. S. A. *104*, 18439–18444.

Hsieh, C.L. (1999). In vivo activity of murine de novo methyltransferases, Dnmt3a and Dnmt3b. Mol. Cell. Biol. *19*, 8211–8218.

Hu, S.-C., Chrivia, J., and Ghosh, A. (1999). Regulation of CBP-Mediated Transcription by Neuronal Calcium Signaling. Neuron *22*, 799–808.

Huang, E.J., and Reichardt, L.F. (2003). Trk receptors: roles in neuronal signal transduction. Annu. Rev. Biochem. *72*, 609–642.

Im, H.-I., Hollander, J.A., Bali, P., and Kenny, P.J. (2010). MeCP2 controls BDNF expression and cocaine intake through homeostatic interactions with microRNA-212. Nat. Neurosci. *13*, 1120–1127.

Ishimaru, N., Fukuchi, M., Hirai, A., Chiba, Y., Tamura, T., Takahashi, N., Tabuchi, A., Tsuda, M., and Shiraishi, M. (2010). Differential epigenetic regulation of BDNF and NT-3 genes by trichostatin A and 5-aza-2′-deoxycytidine in Neuro-2a cells. Biochem. Biophys. Res. Commun. *394*, 173–177.

Jayaraman, R. (1972). Transcription of bacteriophage T4 DNA by Escherichia coli RNA polymerase in vitro: identification of some immediate-early and delayed-early genes. J. Mol. Biol. *70*, 253–263.

Jenuwein, T., and Allis, C.D. (2001). Translating the histone code. Science *293*, 1074–1080.

Kaech, S., and Banker, G. (2006). Culturing hippocampal neurons. Nat. Protoc. *1*, 2406–2415.

Kameyama, K., Lee, H.K., Bear, M.F., and Huganir, R.L. (1998). Involvement of a postsynaptic protein kinase A substrate in the expression of homosynaptic long-term depression. Neuron *21*, 1163–1175.

Kang, Y.K., Koo, D.B., Park, J.S., Choi, Y.H., Lee, K.K., and Han, Y.M. (2001). Differential inheritance modes of DNA methylation between euchromatic and heterochromatic DNA sequences in ageing fetal bovine fibroblasts. FEBS Lett. *498*, 1–5.

Karpova, N.N., Rantamäki, T., Di Lieto, A., Lindemann, L., Hoener, M.C., and Castrén, E. (2010). Darkness reduces BDNF expression in the visual cortex and induces repressive chromatin remodeling at the BDNF gene in both hippocampus and visual cortex. Cell. Mol. Neurobiol. *30*, 1117–1123.

Kenchappa, R.S., Tep, C., Korade, Z., Urra, S., Bronfman, F.C., Yoon, S.O., and Carter, B.D. (2010). p75 neurotrophin receptor-mediated apoptosis in sympathetic neurons involves a biphasic activation of JNK and up-regulation of tumor necrosis factor-alpha-converting enzyme/ADAM17. J. Biol. Chem. *285*, 20358–20368.

Kimura, K., Wakamatsu, A., Suzuki, Y., Ota, T., Nishikawa, T., Yamashita, R., Yamamoto, J., Sekine, M., Tsuritani, K., Wakaguri, H., et al. (2006). Diversification of transcriptional modulation: large-scale identification and characterization of putative alternative promoters of human genes. Genome Res. *16*, 55–65.

Klose, R., and Bird, A. (2003). Molecular biology. MeCP2 repression goes nonglobal. Science *302*, 793–795.

Koppel, I., and Timmusk, T. (2013). Differential regulation of Bdnf expression in cortical neurons by class-selective histone deacetylase inhibitors. Neuropharmacology *75*, 106–115.

Koshibu, K., Graff, J., Beullens, M., Heitz, F.D., Berchtold, D., Russig, H., Farinelli, M., Bollen, M., and Mansuy, I.M. (2009). Protein Phosphatase 1 Regulates the Histone Code for Long-Term Memory. J. Neurosci. *29*, 13079–13089.

Koshimizu, H., Hazama, S., Hara, T., Ogura, A., and Kojima, M. (2010). Distinct signaling pathways of precursor BDNF and mature BDNF in cultured cerebellar granule neurons. Neurosci. Lett. *473*, 229–232.

Kramer, R.M., Roberts, E.F., Um, S.L., Börsch-Haubold, A.G., Watson, S.P., Fisher, M.J., and Jakubowski, J.A. (1996). p38 mitogen-activated protein kinase phosphorylates cytosolic phospholipase A2 (cPLA2) in thrombin-stimulated platelets. Evidence that proline-directed phosphorylation is not required for mobilization of arachidonic acid by cPLA2. J. Biol. Chem. *271*, 27723–27729.

Kruidenier, L., Chung, C., Cheng, Z., Liddle, J., Che, K., Joberty, G., Bantscheff, M., Bountra, C., Bridges, A., Diallo, H., et al. (2012). A selective jumonji H3K27 demethylase inhibitor modulates the proinflammatory macrophage response. Nature *488*, 404–408.

Kumar, A., and Foster, T.C. (2013). Linking redox regulation of NMDAR synaptic function to cognitive decline during aging. J. Neurosci. *33*, 15710–15715.

Kuzumaki, N., Ikegami, D., Tamura, R., Hareyama, N., Imai, S., Narita, M., Torigoe, K., Niikura, K., Takeshima, H., Ando, T., et al. (2011). Hippocampal epigenetic modification at the brain-derived neurotrophic factor gene induced by an enriched environment. Hippocampus *21*, 127–132.

de la Barre, A.E., Angelov, D., Molla, A., and Dimitrov, S. (2001). The N-terminus of histone H2B, but not that of histone H3 or its phosphorylation, is essential for chromosome condensation. EMBO J. *20*, 6383–6393.

Lanahan, A., and Worley, P. (1998). Immediate-early genes and synaptic function. Neurobiol. Learn. Mem. *70*, 37–43.

Lau, P.N.I., and Cheung, P. (2011). Histone code pathway involving H3 S28 phosphorylation and K27 acetylation activates transcription and antagonizes polycomb silencing. Proc. Natl. Acad. Sci. U. S. A. *108*, 2801–2806.

Lau, A.G., Irier, H.A., Gu, J., Tian, D., Ku, L., Liu, G., Xia, M., Fritsch, B., Zheng, J.Q., Dingledine, R., et al. (2010). Distinct 3'UTRs differentially regulate activity-dependent translation of brain-derived neurotrophic factor (BDNF). Proc. Natl. Acad. Sci. U. S. A. *107*, 15945–15950.

Lee, K.K., and Workman, J.L. (2007). Histone acetyltransferase complexes: one size doesn't fit all. Nat. Rev. Mol. Cell Biol. *8*, 284–295.

Lee, H.-K., Kameyama, K., Huganir, R.L., and Bear, M.F. (1998). NMDA Induces Long-Term Synaptic Depression and Dephosphorylation of the GluR1 Subunit of AMPA Receptors in Hippocampus. Neuron *21*, 1151–1162.

Lee, H.-K., Min, S.S., Gallagher, M., and Kirkwood, A. (2005). NMDA receptor-independent long-term depression correlates with successful aging in rats. Nat. Neurosci. *8*, 1657–1659.

Lee, T.I., Jenner, R.G., Boyer, L.A., Guenther, M.G., Levine, S.S., Kumar, R.M., Chevalier, B., Johnstone, S.E., Cole, M.F., Isono, K., et al. (2006). Control of developmental regulators by Polycomb in human embryonic stem cells. Cell *125*, 301–313.

Leoni, V., and Caccia, C. (2014). Study of cholesterol metabolism in Huntington′s disease. Biochem. Biophys. Res. Commun. *446*, 697–701.

Levenson, J.M., and Sweatt, J.D. (2006). Epigenetic mechanisms: a common theme in vertebrate and invertebrate memory formation. Cell. Mol. Life Sci. *63*, 1009–1016.

Levenson, J.M., O'Riordan, K.J., Brown, K.D., Trinh, M. a, Molfese, D.L., and Sweatt, J.D. (2004). Regulation of histone acetylation during memory formation in the hippocampus. J. Biol. Chem. *279*, 40545–40559.

Li, B.X., and Xiao, X. (2009). Discovery of a small-molecule inhibitor of the KIX-KID interaction. Chembiochem *10*, 2721–2724.

Li, H., Zhong, X., Chau, K.F., Williams, E.C., and Chang, Q. (2011). Loss of activity-induced phosphorylation of MeCP2 enhances synaptogenesis, LTP and spatial memory. Nat. Neurosci. *14*, 1001–1008.

Lin, J.W., Ju, W., Foster, K., Lee, S.H., Ahmadian, G., Wyszynski, M., Wang, Y.T., and Sheng, M. (2000). Distinct molecular mechanisms and divergent endocytotic pathways of AMPA receptor internalization. Nat. Neurosci. *3*, 1282–1290.

Lipsky, R.H., Xu, K., Zhu, D., Kelly, C., Terhakopian, A., Novelli, A., and Marini, A.M. (2001). Nuclear factor kappaB is a critical determinant in N-methyl-D-aspartate receptor-mediated neuroprotection. J. Neurochem. *78*, 254–264.

Lo, W.S., Trievel, R.C., Rojas, J.R., Duggan, L., Hsu, J.Y., Allis, C.D., Marmorstein, R., and Berger, S.L. (2000). Phosphorylation of serine 10 in histone H3 is functionally linked in vitro and in vivo to Gcn5-mediated acetylation at lysine 14. Mol. Cell *5*, 917–926.

Lochner, A., and Moolman, J.A. (2006). The Many Faces of H89: A Review. Cardiovasc. Drug Rev. *24*, 261–274.

Lu, B., Pang, P.T., and Woo, N.H. (2005). The yin and yang of neurotrophin action. Nat.

Rev. Neurosci. *6*, 603–614.

Lu, B., Nagappan, G., and Lu, Y. (2014). BDNF and synaptic plasticity, cognitive function, and dysfunction. Handb. Exp. Pharmacol. *220*, 223–250.

Lubin, F.D., and Sweatt, J.D. (2007). The IkappaB kinase regulates chromatin structure during reconsolidation of conditioned fear memories. Neuron *55*, 942–957.

Lubin, F.D., Roth, T.L., and Sweatt, J.D. (2008). Epigenetic regulation of BDNF gene transcription in the consolidation of fear memory. J. Neurosci. *28*, 10576–10586.

Luger, K., Rechsteiner, T.J., Flaus, A.J., Waye, M.M., and Richmond, T.J. (1997). Characterization of nucleosome core particles containing histone proteins made in bacteria. J. Mol. Biol. *272*, 301–311.

Lüscher, C., Xia, H., Beattie, E.C., Carroll, R.C., von Zastrow, M., Malenka, R.C., and Nicoll, R.A. (1999). Role of AMPA receptor cycling in synaptic transmission and plasticity. Neuron *24*, 649–658.

Manahan-Vaughan, D., Kulla, A., and Frey, J.U. (2000). Requirement of translation but not transcription for the maintenance of long-term depression in the CA1 region of freely moving rats. J. Neurosci. *20*, 8572–8576.

Mao, Z., Bonni, A., Xia, F., Nadal-Vicens, M., and Greenberg, M.E. (1999). Neuronal activity-dependent cell survival mediated by transcription factor MEF2. Science *286*, 785–790.

Marmigère, F., Rage, F., and Tapia-Arancibia, L. (2001). Regulation of brain-derived neurotrophic factor transcripts by neuronal activation in rat hypothalamic neurons. J. Neurosci. Res. *66*, 377–389.

Martin, M.G., Perga, S., Trovò, L., Rasola, A., Holm, P., Rantamäki, T., Harkany, T., Castrén, E., Chiara, F., and Dotti, C.G. (2008). Cholesterol loss enhances TrkB signaling in hippocampal neurons aging in vitro. Mol. Biol. Cell *19*, 2101–2112.

Martin, M.G., Ahmed, T., Korovaichuk, A., Venero, C., Menchon, S.A., Salas, I., Munck, S., Herreras, O., Balschun, D., and Dotti, C.G. (2014a). Constitutive hippocampal cholesterol loss underlies poor cognition in old rodents. EMBO Mol. Med. *6*, 902–917.

Martin, M.G., Pfrieger, F., and Dotti, C.G. (2014b). Cholesterol in brain disease: sometimes determinant and frequently implicated. EMBO Rep. *15*, 1036–1052.

Martinowich, K., Hattori, D., Wu, H., Fouse, S., He, F., Hu, Y., Fan, G., and Sun, Y.E. (2003). DNA methylation-related chromatin remodeling in activity-dependent BDNF gene regulation. Science *302*, 890–893.

Massey, P. V, and Bashir, Z.I. (2007). Long-term depression: multiple forms and implications for brain function. Trends Neurosci. *30*, 176–184.

Mauch, D.H., Nägler, K., Schumacher, S., Göritz, C., Müller, E.C., Otto, A., and Pfrieger, F.W. (2001). CNS synaptogenesis promoted by glia-derived cholesterol. Science *294*, 1354–1357.

Maya Vetencourt, J.F., Tiraboschi, E., Spolidoro, M., Castrén, E., and Maffei, L. (2011). Serotonin triggers a transient epigenetic mechanism that reinstates adult visual cortex plasticity in rats. Eur. J. Neurosci. *33*, 49–57.

Mayford, M., Wang, J., Kandel, E.R., and O'Dell, T.J. (1995). CaMKII regulates the frequency-response function of hippocampal synapses for the production of both LTD and LTP. Cell *81*, 891–904.

McKinsey, T. a, Zhang, C.L., Lu, J., and Olson, E.N. (2000). Signal-dependent nuclear export of a histone deacetylase regulates muscle differentiation. Nature *408*, 106–111.

Metzger, E., Imhof, A., Patel, D., Kahl, P., Hoffmeyer, K., Friedrichs, N., Müller, J.M., Greschik, H., Kirfel, J., Ji, S., et al. (2010). Phosphorylation of histone H3T6 by PKCbeta(I) controls demethylation at histone H3K4. Nature *464*, 792–796.

Millanes-Romero, A., Herranz, N., Perrera, V., Iturbide, A., Loubat-Casanovas, J., Gil, J., Jenuwein, T., García de Herreros, A., and Peiró, S. (2013). Regulation of heterochromatin transcription by Snail1/LOXL2 during epithelial-to-mesenchymal transition. Mol. Cell *52*, 746–757.

Miller, C. a, and Sweatt, J.D. (2007). Covalent modification of DNA regulates memory formation. Neuron *53*, 857–869.

Miller, C. a, Gavin, C.F., White, J. a, Parrish, R.R., Honasoge, A., Yancey, C.R., Rivera, I.M., Rubio, M.D., Rumbaugh, G., and Sweatt, J.D. (2010). Cortical DNA methylation maintains remote memory. Nat. Neurosci. *13*, 664–666.

Miller, C.A., Campbell, S.L., and Sweatt, J.D. (2008). DNA methylation and histone acetylation work in concert to regulate memory formation and synaptic plasticity. Neurobiol. Learn. Mem. *89*, 599–603.

Miranda, T.B., and Jones, P.A. (2007). DNA methylation: the nuts and bolts of repression. J. Cell. Physiol. *213*, 384–390.

Modarresi, F., Faghihi, M.A., Lopez-Toledano, M.A., Fatemi, R.P., Magistri, M., Brothers, S.P., van der Brug, M.P., and Wahlestedt, C. (2012). Inhibition of natural antisense transcripts in vivo results in gene-specific transcriptional upregulation. Nat. Biotechnol. *30*, 453–459.

Molander-Melin, M., Blennow, K., Bogdanovic, N., Dellheden, B., Mansson, J.-E., and Fredman, P. (2005). Structural membrane alterations in Alzheimer brains found to be associated with regional disease development; increased density of gangliosides GM1 and GM2 and loss of cholesterol in detergent-resistant membrane domains. J. Neurochem. *92*, 171–182.

Morishita, W., Connor, J.H., Xia, H., Quinlan, E.M., Shenolikar, S., and Malenka, R.C. (2001). Regulation of synaptic strength by protein phosphatase 1. Neuron *32*, 1133–1148.

Morse, S., Butler, A., Davis, R., Soller, I., and Lubin, F. (2015). Environmental Enrichment Reverses Histone Methylation Changes in the Aged Hippocampus and Restores Age-Related Memory Deficits. Biology (Basel). *4*, 298–313.

Mousavi, K., Zare, H., Wang, A.H., and Sartorelli, V. (2012). Polycomb Protein Ezh1 Promotes RNA Polymerase II Elongation. Mol. Cell *45*, 255–262.

Murray, K. (1964). THE OCCURRENCE OF EPSILON-N-METHYL LYSINE IN HISTONES. Biochemistry *3*, 10–15.

Nedivi, E., Hevroni, D., Naot, D., Israeli, D., and Citri, Y. (1993). Numerous candidate plasticity-related genes revealed by differential cDNA cloning. Nature *363*, 718–722.

Newman, M.C., and Kaszniak, A.W. (2000). Spatial Memory and Aging: Performance on a Human Analog of the Morris Water Maze. Aging, Neuropsychol. Cogn. (Neuropsychology, Dev. Cogn. Sect. B) *7*, 86–93.

Nguyen, P. V, Abel, T., and Kandel, E.R. (1994). Requirement of a critical period of transcription for induction of a late phase of LTP. Science *265*, 1104–1107.

Nijholt, I., Blank, T., Ahi, J., and Spiess, J. (2002). In vivo CREB phosphorylation mediated by dopamine and NMDA receptor activation in mouse hippocampus and caudate nucleus. Brain Res. Gene Expr. Patterns *1*, 101–106.

Nishimune, A., Isaac, J.T., Molnar, E., Noel, J., Nash, S.R., Tagaya, M., Collingridge, G.L., Nakanishi, S., and Henley, J.M. (1998). NSF binding to GluR2 regulates synaptic transmission. Neuron *21*, 87–97.

Norris, C.M., Korol, D.L., and Foster, T.C. (1996). Increased susceptibility to induction of long-term depression and long-term potentiation reversal during aging. J. Neurosci. *16*, 5382–5392.

Nowak, S.J., Pai, C.-Y., and Corces, V.G. (2003). Protein phosphatase 2A activity affects histone H3 phosphorylation and transcription in Drosophila melanogaster. Mol. Cell. Biol. *23*, 6129–6138.

Oe, S., and Yoneda, Y. (2010). Cytoplasmic polyadenylation element-like sequences are

involved in dendritic targeting of BDNF mRNA in hippocampal neurons. FEBS Lett. *584*, 3424–3430.

Ogawa, Y., Sun, B.K., and Lee, J.T. (2008). Intersection of the RNA interference and X-inactivation pathways. Science *320*, 1336–1341.

Ohshima, T., Ogura, H., Tomizawa, K., Hayashi, K., Suzuki, H., Saito, T., Kamei, H., Nishi, A., Bibb, J.A., Hisanaga, S.-I., et al. (2005). Impairment of hippocampal long-term depression and defective spatial learning and memory in p35 mice. J. Neurochem. *94*, 917–925.

Ohyama, Y., Meaney, S., Heverin, M., Ekström, L., Brafman, A., Shafir, M., Andersson, U., Olin, M., Eggertsen, G., Diczfalusy, U., et al. (2006). Studies on the transcriptional regulation of cholesterol 24-hydroxylase (CYP46A1): marked insensitivity toward different regulatory axes. J. Biol. Chem. *281*, 3810–3820.

Okano, M., Bell, D.W., Haber, D.A., and Li, E. (1999). DNA methyltransferases Dnmt3a and Dnmt3b are essential for de novo methylation and mammalian development. Cell *99*, 247–257.

Oliveira, A.M.M., Hemstedt, T.J., and Bading, H. (2012). Rescue of aging-associated decline in Dnmt3a2 expression restores cognitive abilities. Nat. Neurosci. *15*, 1111–1113.

Onishchenko, N., Karpova, N., Sabri, F., Castrén, E., and Ceccatelli, S. (2008). Long-lasting depression-like behavior and epigenetic changes of BDNF gene expression induced by perinatal exposure to methylmercury. J. Neurochem. *106*, 1378–1387.

Paik, W.K., and Kim, S. (1969). Enzymatic methylation of histones. Arch. Biochem. Biophys. *134*, 632–637.

Pakkenberg, B., and Gundersen, H.J. (1997). Neocortical neuron number in humans: effect of sex and age. J. Comp. Neurol. *384*, 312–320.

Papassotiropoulos, A., Lütjohann, D., Bagli, M., Locatelli, S., Jessen, F., Buschfort, R., Ptok, U., Björkhem, I., von Bergmann, K., and Heun, R. 24S-hydroxycholesterol in cerebrospinal fluid is elevated in early stages of dementia. J. Psychiatr. Res. *36*, 27–32.

Pattabiraman, P.P., Tropea, D., Chiaruttini, C., Tongiorgi, E., Cattaneo, A., and Domenici, L. (2005). Neuronal activity regulates the developmental expression and subcellular localization of cortical BDNF mRNA isoforms in vivo. Mol. Cell. Neurosci. *28*, 556–570.

Peineau, S., Taghibiglou, C., Bradley, C., Wong, T.P., Liu, L., Lu, J., Lo, E., Wu, D., Saule, E., Bouschet, T., et al. (2007). LTP inhibits LTD in the hippocampus via regulation of GSK3beta. Neuron *53*, 703–717.

Peleg, S., Sananbenesi, F., Zovoilis, A., Burkhardt, S., Bahari-Javan, S., Agis-Balboa,

R.C., Cota, P., Wittnam, J.L., Gogol-Doering, A., Opitz, L., et al. (2010). Altered histone acetylation is associated with age-dependent memory impairment in mice. Science *328*, 753–756.

Penner, M.R., Roth, T.L., Barnes, C.A., and Sweatt, J.D. (2010). An epigenetic hypothesis of aging-related cognitive dysfunction. Front. Aging Neurosci. *2*, 9.

Penner, M.R., Roth, T.L., Chawla, M.K., Hoang, L.T., Roth, E.D., Lubin, F.D., Sweatt, J.D., Worley, P.F., and Barnes, C. a (2011). Age-related changes in Arc transcription and DNA methylation within the hippocampus. Neurobiol. Aging *32*, 2198–2210.

Perovic, M., Tesic, V., Mladenovic Djordjevic, A., Smiljanic, K., Loncarevic-Vasiljkovic, N., Ruzdijic, S., and Kanazir, S. (2013). BDNF transcripts, proBDNF and proNGF, in the cortex and hippocampus throughout the life span of the rat. Age (Dordr). *35*, 2057–2070.

Pi, H.J., Otmakhov, N., Lemelin, D., De Koninck, P., and Lisman, J. (2010). Autonomous CaMKII can promote either long-term potentiation or long-term depression, depending on the state of T305/T306 phosphorylation. J. Neurosci. *30*, 8704–8709.

Porras, A., Zuluaga, S., Black, E., Valladares, A., Alvarez, A.M., Ambrosino, C., Benito, M., and Nebreda, A.R. (2004). P38 alpha mitogen-activated protein kinase sensitizes cells to apoptosis induced by different stimuli. Mol. Biol. Cell *15*, 922–933.

Powell, D.J., Hajduch, E., Kular, G., and Hundal, H.S. (2003). Ceramide Disables 3-Phosphoinositide Binding to the Pleckstrin Homology Domain of Protein Kinase B (PKB)/Akt by a PKC -Dependent Mechanism. Mol. Cell. Biol. *23*, 7794–7808.

Pruunsild, P., Kazantseva, A., Aid, T., Palm, K., and Timmusk, T. (2007). Dissecting the human BDNF locus: bidirectional transcription, complex splicing, and multiple promoters. Genomics *90*, 397–406.

Pruunsild, P., Sepp, M., Orav, E., Koppel, I., and Timmusk, T. (2011). Identification of cis-elements and transcription factors regulating neuronal activity-dependent transcription of human BDNF gene. J. Neurosci. *31*, 3295–3308.

Qi, C., Liu, S., Qin, R., Zhang, Y., Wang, G., Shang, Y., Wang, Y., and Liang, J. (2014). Coordinated regulation of dendrite arborization by epigenetic factors CDYL and EZH2. J. Neurosci. *34*, 4494–4508.

Ramón y Cajal, S. (1909). Histologie du système nerveux de l'homme & des vertébrés.

Rapp, P.R., Kansky, M.T., and Roberts, J.A. (1997). Impaired spatial information processing in aged monkeys with preserved recognition memory. Neuroreport *8*, 1923–1928.

Rasmussen, T., Schliemann, T., Sørensen, J.C., Zimmer, J., and West, M.J. (1996).

Memory impaired aged rats: no loss of principal hippocampal and subicular neurons. Neurobiol. Aging *17*, 143–147.

Reichardt, L.F. (2006). Neurotrophin-regulated signalling pathways. Philos. Trans. R. Soc. Lond. B. Biol. Sci. *361*, 1545–1564.

Reolon, G.K., Maurmann, N., Werenicz, A., Garcia, V.A., Schröder, N., Wood, M.A., and Roesler, R. (2011). Posttraining systemic administration of the histone deacetylase inhibitor sodium butyrate ameliorates aging-related memory decline in rats. Behav. Brain Res. *221*, 329–332.

Roher, A.E., Weiss, N., Kokjohn, T.A., Kuo, Y.-M., Kalback, W., Anthony, J., Watson, D., Luehrs, D.C., Sue, L., Walker, D., et al. (2002). Increased A beta peptides and reduced cholesterol and myelin proteins characterize white matter degeneration in Alzheimer's disease. Biochemistry *41*, 11080–11090.

Rosenzweig, E.S., and Barnes, C.A. (2003). Impact of aging on hippocampal function: plasticity, network dynamics, and cognition. Prog. Neurobiol. *69*, 143–179.

Rossetto, D., Avvakumov, N., and Côté, J. (2012). Histone phosphorylation: a chromatin modification involved in diverse nuclear events. Epigenetics *7*, 1098–1108.

Roth, T.L., Lubin, F.D., Funk, A.J., and Sweatt, J.D. (2009). Lasting epigenetic influence of early-life adversity on the BDNF gene. Biol. Psychiatry *65*, 760–769.

Rothbart, S.B., Dickson, B.M., Raab, J.R., Grzybowski, A.T., Krajewski, K., Guo, A.H., Shanle, E.K., Josefowicz, S.Z., Fuchs, S.M., Allis, C.D., et al. (2015). An Interactive Database for the Assessment of Histone Antibody Specificity. Mol. Cell *59*, 502–511.

Rowe, W.B., Blalock, E.M., Chen, K.-C., Kadish, I., Wang, D., Barrett, J.E., Thibault, O., Porter, N.M., Rose, G.M., and Landfield, P.W. (2007). Hippocampal expression analyses reveal selective association of immediate-early, neuroenergetic, and myelinogenic pathways with cognitive impairment in aged rats. J. Neurosci. *27*, 3098–3110.

Russell, D.W., Halford, R.W., Ramirez, D.M.O., Shah, R., and Kotti, T. (2009). Cholesterol 24-hydroxylase: an enzyme of cholesterol turnover in the brain. Annu. Rev. Biochem. *78*, 1017–1040.

Saha, R.N., Wissink, E.M., Bailey, E.R., Zhao, M., Fargo, D.C., Hwang, J.-Y., Daigle, K.R., Fenn, J.D., Adelman, K., and Dudek, S.M. (2011). Rapid activity-induced transcription of Arc and other IEGs relies on poised RNA polymerase II. Nat. Neurosci. *14*, 848–856.

Saklatvala, J., Rawlinson, L., Waller, R.J., Sarsfield, S., Lee, J.C., Morton, L.F., Barnes, M.J., and Farndale, R.W. (1996). Role for p38 mitogen-activated protein kinase in platelet

aggregation caused by collagen or a thromboxane analogue. J. Biol. Chem. *271*, 6586–6589.

Santos-Rosa, H., Schneider, R., Bannister, A.J., Sherriff, J., Bernstein, B.E., Emre, N.C.T., Schreiber, S.L., Mellor, J., and Kouzarides, T. (2002). Active genes are tri-methylated at K4 of histone H3. Nature *419*, 407–411.

Schmidt, H.D., Sangrey, G.R., Darnell, S.B., Schassburger, R.L., Cha, J.-H.J., Pierce, R.C., and Sadri-Vakili, G. (2012). Increased brain-derived neurotrophic factor (BDNF) expression in the ventral tegmental area during cocaine abstinence is associated with increased histone acetylation at BDNF exon I-containing promoters. J. Neurochem. *120*, 202–209.

Schrattenholz, A., and Soskic, V. (2006). NMDA receptors are not alone: dynamic regulation of NMDA receptor structure and function by neuregulins and transient cholesterol-rich membrane domains leads to disease-specific nuances of glutamate-signalling. Curr. Top. Med. Chem. *6*, 663–686.

Scoville, W.B., and Milner, B. (1957). Loss of recent memory after bilateral hippocampal lesions. J. Neurol. Neurosurg. Psychiatry *20*, 11–21.

Shafaati, M., Mast, N., Beck, O., Nayef, R., Heo, G.Y., Bjorkhem-Bergman, L., Lutjohann, D., Bjorkhem, I., and Pikuleva, I.A. (2009). The antifungal drug voriconazole is an efficient inhibitor of brain cholesterol 24S-hydroxylase in vitro and in vivo. J. Lipid Res. *51*, 318–323.

Sheng, M., McFadden, G., and Greenberg, M.E. (1990). Membrane depolarization and calcium induce c-fos transcription via phosphorylation of transcription factor CREB. Neuron *4*, 571–582.

Sheng, M., Thompson, M.A., and Greenberg, M.E. (1991). CREB: a Ca(2+)-regulated transcription factor phosphorylated by calmodulin-dependent kinases. Science *252*, 1427–1430.

Shi, X., Hong, T., Walter, K.L., Ewalt, M., Michishita, E., Hung, T., Carney, D., Peña, P., Lan, F., Kaadige, M.R., et al. (2006). ING2 PHD domain links histone H3 lysine 4 methylation to active gene repression. Nature *442*, 96–99.

Simon, J.A., and Lange, C.A. (2008). Roles of the EZH2 histone methyltransferase in cancer epigenetics. Mutat. Res. *647*, 21–29.

Söderberg, M., Edlund, C., Kristensson, K., and Dallner, G. (1990). Lipid compositions of different regions of the human brain during aging. J. Neurochem. *54*, 415–423.

Sodero, A.O., Weissmann, C., Ledesma, M.D., and Dotti, C.G. (2011). Cellular stress

from excitatory neurotransmission contributes to cholesterol loss in hippocampal neurons aging in vitro. Neurobiol. Aging *32*, 1043–1053.

Sodero, A.O., Vriens, J., Ghosh, D., Stegner, D., Brachet, A., Pallotto, M., Sassoè-Pognetto, M., Brouwers, J.F., Helms, J.B., Nieswandt, B., et al. (2012). Cholesterol loss during glutamate-mediated excitotoxicity. EMBO J. *31*, 1764–1773.

Sossin, W.S., and Barker, P.A. (2007). Something old, something new: BDNF-induced neuron survival requires TRPC channel function. Nat. Neurosci. *10*, 537–538.

Squire, L.R. (1992). Declarative and Nondeclarative Memory: Multiple Brain Systems Supporting Learning and Memory. J. Cogn. Neurosci. *4*, 232–243.

Strack, S., and Colbran, R.J. (1998). Autophosphorylation-dependent targeting of calcium/ calmodulin-dependent protein kinase II by the NR2B subunit of the N-methyl- D-aspartate receptor. J. Biol. Chem. *273*, 20689–20692.

Strahl, B.D., and Allis, C.D. (2000). The language of covalent histone modifications. Nature *403*, 41–45.

Sun, Y., Lim, Y., Li, F., Liu, S., Lu, J.-J., Haberberger, R., Zhong, J.-H., and Zhou, X.-F. (2012). ProBDNF collapses neurite outgrowth of primary neurons by activating RhoA. PLoS One *7*, e35883.

Svennerholm, L., Boström, K., Helander, C.G., and Jungbjer, B. (1991). Membrane lipids in the aging human brain. J. Neurochem. *56*, 2051–2059.

Svennerholm, L., Boström, K., Jungbjer, B., and Olsson, L. (1994). Membrane lipids of adult human brain: lipid composition of frontal and temporal lobe in subjects of age 20 to 100 years. J. Neurochem. *63*, 1802–1811.

Svennerholm, L., Boström, K., and Jungbjer, B. (1997). Changes in weight and compositions of major membrane components of human brain during the span of adult human life of Swedes. Acta Neuropathol. *94*, 345–352.

Takei, S., Morinobu, S., Yamamoto, S., Fuchikami, M., Matsumoto, T., and Yamawaki, S. (2011). Enhanced hippocampal BDNF/TrkB signaling in response to fear conditioning in an animal model of posttraumatic stress disorder. J. Psychiatr. Res. *45*, 460–468.

Tan, M., Luo, H., Lee, S., Jin, F., Yang, J.S., Montellier, E., Buchou, T., Cheng, Z., Rousseaux, S., Rajagopal, N., et al. (2011). Identification of 67 histone marks and histone lysine crotonylation as a new type of histone modification. Cell *146*, 1016–1028.

Tang, B., Dean, B., and Thomas, E.A. (2011). Disease- and age-related changes in histone acetylation at gene promoters in psychiatric disorders. Transl. Psychiatry *1*, e64.

Teunissen, C.E., Floris, S., Sonke, M., Dijkstra, C.D., De Vries, H.E., and Lütjohann, D. (2007). 24S-hydroxycholesterol in relation to disease manifestations of acute experimental autoimmune encephalomyelitis. J. Neurosci. Res. *85*, 1499–1505.

Thelen, K.M., Falkai, P., Bayer, T.A., and Lütjohann, D. (2006). Cholesterol synthesis rate in human hippocampus declines with aging. Neurosci. Lett. *403*, 15–19.

Thibault, O., and Landfield, P.W. (1996). Increase in single L-type calcium channels in hippocampal neurons during aging. Science *272*, 1017–1020.

Tian, F., Marini, A.M., and Lipsky, R.H. (2010a). NMDA receptor activation induces differential epigenetic modification of Bdnf promoters in hippocampal neurons. Amino Acids *38*, 1067–1074.

Tian, F., Marini, A.M., and Lipsky, R.H. (2010b). Effects of histone deacetylase inhibitor Trichostatin A on epigenetic changes and transcriptional activation of Bdnf promoter 1 by rat hippocampal neurons. Ann. N. Y. Acad. Sci. *1199*, 186–193.

Tie, F., Banerjee, R., Conrad, P.A., Scacheri, P.C., and Harte, P.J. (2012). Histone demethylase UTX and chromatin remodeler BRM bind directly to CBP and modulate acetylation of histone H3 lysine 27. Mol. Cell. Biol. *32*, 2323–2334.

Timmusk, T., Palm, K., Metsis, M., Reintam, T., Paalme, V., Saarma, M., and Persson, H. (1993). Multiple promoters direct tissue-specific expression of the rat BDNF gene. Neuron *10*, 475–489.

Tollefsbol, T.O. (2011). Handbook of Epigenetics.

Tongiorgi, E., Righi, M., and Cattaneo, A. (1997). Activity-dependent dendritic targeting of BDNF and TrkB mRNAs in hippocampal neurons. J. Neurosci. *17*, 9492–9505.

Tsankova, N.M., Berton, O., Renthal, W., Kumar, A., Neve, R.L., and Nestler, E.J. (2006). Sustained hippocampal chromatin regulation in a mouse model of depression and antidepressant action. Nat. Neurosci. *9*, 519–525.

Uemura, E. (1985). Age-related changes in the subiculum of Macaca mulatta: synaptic density. Exp. Neurol. *87*, 403–411.

Valenza, M., Rigamonti, D., Goffredo, D., Zuccato, C., Fenu, S., Jamot, L., Strand, A., Tarditi, A., Woodman, B., Racchi, M., et al. (2005). Dysfunction of the cholesterol biosynthetic pathway in Huntington's disease. J. Neurosci. *25*, 9932–9939.

Valenza, M., Leoni, V., Karasinska, J.M., Petricca, L., Fan, J., Carroll, J., Pouladi, M.A., Fossale, E., Nguyen, H.P., Riess, O., et al. (2010). Cholesterol defect is marked across multiple rodent models of Huntington's disease and is manifest in astrocytes. J. Neurosci. *30*, 10844–10850.

Valenza, M., Chen, J.Y., Di Paolo, E., Ruozi, B., Belletti, D., Ferrari Bardile, C., Leoni, V., Caccia, C., Brilli, E., Di Donato, S., et al. (2015). Cholesterol-loaded nanoparticles ameliorate synaptic and cognitive function in Huntington's disease mice. EMBO Mol. Med.

Valor, L.M., Pulopulos, M.M., Jimenez-Minchan, M., Olivares, R., Lutz, B., and Barco, A. (2011). Ablation of CBP in forebrain principal neurons causes modest memory and transcriptional defects and a dramatic reduction of histone acetylation but does not affect cell viability. J. Neurosci. *31*, 1652–1663.

Vo, N., and Goodman, R.H. (2001). CREB-binding protein and p300 in transcriptional regulation. J. Biol. Chem. *276*, 13505–13508.

Waddington, C. (1957). The strategy of the genes a discussion of some aspects of theoretical biology. (London: Allen & Unwin).

Walker, M.P., LaFerla, F.M., Oddo, S.S., and Brewer, G.J. (2013). Reversible epigenetic histone modifications and Bdnf expression in neurons with aging and from a mouse model of Alzheimer's disease. Age (Dordr). *35*, 519–531.

Wang, C.M., Tsai, S.N., Yew, T.W., Kwan, Y.W., and Ngai, S.M. (2010). Identification of histone methylation multiplicities patterns in the brain of senescence-accelerated prone mouse 8. Biogerontology *11*, 87–102.

Wang, W.-S., Kang, S., Liu, W.-T., Li, M., Liu, Y., Yu, C., Chen, J., Chi, Z.-Q., He, L., and Liu, J.-G. (2012). Extinction of aversive memories associated with morphine withdrawal requires ERK-mediated epigenetic regulation of brain-derived neurotrophic factor transcription in the rat ventromedial prefrontal cortex. J. Neurosci. *32*, 13763–13775.

Waterland, R.A., and Jirtle, R.L. (2003). Transposable elements: targets for early nutritional effects on epigenetic gene regulation. Mol. Cell. Biol. *23*, 5293–5300.

Weaver, I.C.G., Cervoni, N., Champagne, F.A., D'Alessio, A.C., Sharma, S., Seckl, J.R., Dymov, S., Szyf, M., and Meaney, M.J. (2004). Epigenetic programming by maternal behavior. Nat. Neurosci. *7*, 847–854.

West, A.E., Chen, W.G., Dalva, M.B., Dolmetsch, R.E., Kornhauser, J.M., Shaywitz, A.J., Takasu, M.A., Tao, X., and Greenberg, M.E. (2001). Calcium regulation of neuronal gene expression. Proc. Natl. Acad. Sci. U. S. A. *98*, 11024–11031.

West, M.J., Coleman, P.D., Flood, D.G., and Troncoso, J.C. (1994). Differences in the pattern of hippocampal neuronal loss in normal ageing and Alzheimer's disease. Lancet (London, England) *344*, 769–772.

Woo, C.J., Kharchenko, P. V, Daheron, L., Park, P.J., and Kingston, R.E. (2010). A region of the human HOXD cluster that confers polycomb-group responsiveness. Cell *140*, 99–

110.

Woo, N.H., Teng, H.K., Siao, C.-J., Chiaruttini, C., Pang, P.T., Milner, T.A., Hempstead, B.L., and Lu, B. (2005). Activation of p75NTR by proBDNF facilitates hippocampal long-term depression. Nat. Neurosci. *8*, 1069–1077.

Yan, J.-Z., Xu, Z., Ren, S.-Q., Hu, B., Yao, W., Wang, S.-H., Liu, S.-Y., and Lu, W. (2011). Protein kinase C promotes N-methyl-D-aspartate (NMDA) receptor trafficking by indirectly triggering calcium/calmodulin-dependent protein kinase II (CaMKII) autophosphorylation. J. Biol. Chem. *286*, 25187–25200.

Yang, S., Megill, A., Ardiles, A.O., Ransom, S., Tran, T., Koh, M.T., Lee, H.-K., Gallagher, M., and Kirkwood, A. (2013). Integrity of mGluR-LTD in the associative/commissural inputs to CA3 correlates with successful aging in rats. J. Neurosci. *33*, 12670–12678.

Zamzow, D.R., Elias, V., Shumaker, M., Larson, C., and Magnusson, K.R. (2013). An increase in the association of GluN2B containing NMDA receptors with membrane scaffolding proteins was related to memory declines during aging. J. Neurosci. *33*, 12300–12305.

Zhang, J., Ji, F., Liu, Y., Lei, X., Li, H., Ji, G., Yuan, Z., and Jiao, J. (2014). Ezh2 regulates adult hippocampal neurogenesis and memory. J. Neurosci. *34*, 5184–5199.

Zheng, B., Ohkawa, S., Li, H., Roberts-Wilson, T.K., and Price, S.R. (2010). FOXO3a mediates signaling crosstalk that coordinates ubiquitin and atrogin-1/MAFbx expression during glucocorticoid-induced skeletal muscle atrophy. FASEB J. *24*, 2660–2669.

Zhong, H., Voll, R.E., and Ghosh, S. (1998). Phosphorylation of NF-kappa B p65 by PKA stimulates transcriptional activity by promoting a novel bivalent interaction with the coactivator CBP/p300. Mol. Cell *1*, 661–671.

Zhong, S.P., Ma, W.Y., and Dong, Z. (2000). ERKs and p38 kinases mediate ultraviolet B-induced phosphorylation of histone H3 at serine 10. J. Biol. Chem. *275*, 20980–20984.

Zhou, Z., Hong, E.J., Cohen, S., Zhao, W.-N., Ho, H.-Y.H., Schmidt, L., Chen, W.G., Lin, Y., Savner, E., Griffith, E.C., et al. (2006). Brain-specific phosphorylation of MeCP2 regulates activity-dependent Bdnf transcription, dendritic growth, and spine maturation. Neuron *52*, 255–269.

Zhu, J.J., Qin, Y., Zhao, M., Van Aelst, L., and Malinow, R. (2002). Ras and Rap Control AMPA Receptor Trafficking during Synaptic Plasticity. Cell *110*, 443–455.

Zilberman, D., Cao, X., and Jacobsen, S.E. (2003). ARGONAUTE4 control of locus-specific siRNA accumulation and DNA and histone methylation. Science *299*, 716–719.

SUPPLEMENTARY TABLES

Supp. Table 1: Primer List

Rat

EXPRESSION PRIMERS	Forward	Reverse
Bdnf Exon I	5'- TTTCAACATCGATGCCAGT -3'	5'- ATCCACCTTGGCGATTACAG -3'
Bdnf Exon II	5'- AGTCCATTCAGCACCTTGGA -3'	5'- CTACCACCTCGGACAAATCC -3'
Bdnf Exon IV	5'- AAATGGAGCTTCTCACTGAAGG -3'	5'- ATTGCATGGCGGAGGTAATA -3'
Bdnf Exon VI	5'- CAACAATGTGACTCCACTGC -3'	5'- CAACAATGTGACTCCACTGC -3'
Jmjd3	5'- CTGAAACTGCCTGCCTTCAT -3'	5'- CTAAGCATGTTGCCTGTGGA -3'
Gapdh	5'- ATGACTCTACCCACGGCAAG -3'	5'- GATCTCGCTCCTGGAAGATG -3'
GusB	5'- GCCAATGAGCCTGTCTCTTC -3'	5'- TCCAGTTCTTGGGGAATCTG -3'
Pgk1	5'- AATGATGCTTTTGGGACTGC -3'	5'- TCAAAAATCCACCAGCCTTC -3'

CHIP PRIMERS	Forward	Reverse
Bdnf Promoter I	5'- GCCTCTCGCCTAGTCATCAG -3'	5'- CCCCACAACTTTCCCTTTTC -3'
Bdnf Promoter II	5'- GGACTGGAGGGGGTTGTTAT -3'	5'- TCAGACAAGCATCAGCTTTGA -3'
Bdnf Promoter IV	5'- GTGAGTTCGCTAGGACTGGAA -3'	5'- GGCATTGCATGCTTTGTAGA -3'
Bdnf Promoter VI	5'- CTCCCACAGAACTTGGGTGT -3'	5'- TTTGCAACTCTCCCCATCTT -3'
βActin	5'- CATCGCCAAACTCTTCATCC -3'	5'- GAGCGAGAGAGAAAGCGAGA -3'
hoxA1	5'- TCTTGCGCACTGTACATTCA -3'	5'- CCTCCATAGGACCAGAGAAGAA -3'

Mouse

EXPRESSION PRIMERS	Forward	Reverse
Bdnf Transcript I	5'- TTTCAACATCGATGCCAGTT -3'	5'- ATCCACCTTGGCGACTACAG -3'
Bdnf Transcript II	5'- CCATCCACACGTGACAAAAC -3'	5'- TGCTCTAGACGGTTTCTTCCA -3'
Bdnf Transcript IV	5'- AAATGGAGCTTCTCGCTGAA -3'	5'- ATTGCATGGCGGAGGTAATA -3'
Bdnf Transcript VI	5'- GAGACCCGGTTCCTTCAACT -3'	5'- CTTTCTCGTCTGCCCCAAG -3'
Arc	5'- AGCCAGGAGAATGACACCAG -3'	5'- GTGATGCCCTTTCCAGACAT -3'
Ppp1cc	5'- GGCTTGGACCCTCTCACTTC -3'	5'- AACATCGACAGCATCATCCA -3'
Gapdh	5'- CTCCCACTCTTCCACCTTCG -3'	5'- CATACCAGGAAATGAGCTTGACAA -3'
GusB	5'- AGCCGCTACGGGCGTCG -3'	5'- GCTGCTTCTTGGGTGATGTCA -3'
Pgk1	5'- TACCTGCTGGCTGGATGG -3'	5'- CACAGCCTCGGCATATTTCT -3'

CHIP PRIMERS	Forward	Reverse
Bdnf Promoter I	5'- GCCTCTCGCCTAGTCACAG -3'	5'- CCCCACAACTTTCCCTTTTC -3'
Bdnf Promoter II	5'- CTGGCTGTTCAAAGCTGATG -3'	5'- GGATGGAATACAAGACGGTTG -3'
Bdnf Promoter IV	5'- AAAAACGGTCCAAAGACCAC -3'	5'- TCACTAAGCCCCCTTCCTCT -3'
Bdnf Promoter VI	5'- AAACCAGGGGAGAAAGATTTG -3'	5'- GGAGGAAGCGAGTGTGAGTC -3'
βActin	5'- CCTGTACATCTGGGCCTACG -3'	5'- ATGAAGAGTTTTGGCGATGG -3'
hoxA1	5'- GCCACAAGAGAGCCAGGA -3'	5'- TGAACTGGCAAGAGGTGAGA -3'
Cox1	5'- GAGAGGGGGAAAAGTTGGTG -3'	5'- TGTCTTTCCGCTTAGGCTTT -3'

Supp. Table 2: Antibodies List

Antibody against	Raised in (Isotype)	ChIP	WB	IP	DB	Origin & Ref.
Hitone H3	Rabbit (IgG)	0.1 µg	1:1000	-	-	Cell Signaling ref. 4499
Trimethyl-Histone H3 (Lys4)	Rabbit (Serum)	4 µL	-	-	-	Active Motif ref. 39159
Acetyl-Histone H3 (Lys9)	Rabbit (IgG)	-	1:1000	-	-	Cell Signaling ref. 9649
Trimethyl-Histone H3 (Lys9)	Rabbit (IgG)	4 µg	-	-	-	Abcam ref. ab8898
Acetyl-Histone H3 (Lys14)	Rabbit (IgG)	-	1:1000	-	-	Cell Signaling ref. 4318
Acetyl-Histone H3 (Lys18)	Rabbit (IgG)	-	1:1000	-	-	Cell Signaling ref. 9675
Acetyl-Histone H3 (Lys27)	Rabbit (IgG)	0.1 µg	1:1000	-	-	Cell Signaling ref. 4353
Trimethyl-Histone H3 (Lys27)	Rabbit (IgG)	4 µg	-	-	1:1000	Millipore ref. 07-449
Trimethyl-Phsopho-Histone H3 (Lys27Ser28)	Rabbit (Serum)	5 µL	-	-	1:1000	Diagenode ref. CS-091-100 (Lot 1)
JMJD3	Rabbit (IgG)	10 µg	1:250	-	-	Abcam ref. ab38113
EZH2	Rabbit (IgG)	10 µg	-	-	-	Abcam ref. ab3748
HDAC4	Rabbit (IgG)	10 µg	-	-	-	Active motif ref. 40969
Phospho-CREB (Ser133)	Rabbit (IgG)	-	1:1000	-	-	Cell Signaling ref. 9191
CREB	Rabbit (IgG)	10 µg	1:1000	-	-	Abcam ref. ab31387
CBP	Rabbit (IgG)	5 µg	-	-	-	Santa Cruz ref. sc-583
CBP	Mouse (IgG)	-	1:500	-	-	Abcam ref. ab79270
Phospho-αCaMKII (Thr268)	Rabbit (IgG)	-	1:2000	-	-	Abcam ref. ab2724
αCaMKII	Rabbit (IgG)	-	1:1000	-	-	Abcam ref. ab183670
p-38	Rabbit (IgG)	2 µg	1:1000	-	-	Abcam ref. ab170099
Phospho-p38 (Thr180/Tyr182)	Rabbit (IgG)	-	1:1000	-	-	Cell Signaling ref.4511
CDYL	Rabbit (IgG)	5 µg	1:500	-	-	Abcam ref. ab5188
FLAG-M2	Mouse (IgG1)	-	-	25µL	-	Sigma ref. F3165
normal rabbit IgG	Rabbit (IgG)		assay dependet			Santa Cruz ref. sc-2027
normal mouse IgG	Mouse (IgG)		assay dependet			Santa Cruz ref. sc-2025

Supp. Table 3: Figure R1

A)

Bdnf Transctipt I

min	Mean	N	SEM
0	1.00	13	0.00
10	0.95	12	0.08
30	1.34	13	0.12
60	1.25	8	0.09
90	1.27	9	0.10
180	1.37	9	0.09

Bdnf Transctipt II

min	Mean	N	SEM
0	1.00	13	0.00
10	1.27	13	0.07
30	2.07	12	0.23
60	1.29	9	0.12
90	1.22	9	0.13
180	1.10	9	0.14

Bdnf Transctipt IV

min	Mean	N	SEM
0	1.00	13	0.00
10	1.01	12	0.08
30	1.31	13	0.07
60	1.36	9	0.06
90	1.38	8	0.07
180	1.14	9	0.06

Bdnf Transctipt VI

min	Mean	N	SEM
0	1.00	14	0.00
10	1.46	14	0.15
30	2.13	14	0.13
60	1.07	9	0.10
90	1.00	9	0.07
180	0.89	9	0.14

B)

Bonferroni adjustment

95% confidence interval	99% confidence interval	99.9% confidence interval
(*) p < 1.67E-02	(**) p < 3.33E-03	(***) p < 3.33E-04

	min	Mean	N	SEM	Kruskal-Wallis Test	Mann-Whitney U Test		
						Control / LTD 10	Control / LTD 30	LTD10 / LTD 30
Bdnf Transctipt I	0	1.00	13	0.00	2.31E-02	1.00E+00	1.04E-02	3.50E-02
	10	0.95	12	0.08				
	30	1.34	13	0.12				

	min	Mean	N	SEM	Kruskal-Wallis Test	Mann-Whitney U Test		
						Control / LTD 10	Control / LTD 30	LTD10 / LTD 30
Bdnf Transctipt II	0	1.00	13	0.00	1.95E-07	3.64E-06	4.76E-06	1.10E-03
	10	1.27	13	0.07				
	30	2.07	12	0.23				

	min	Mean	N	SEM	Kruskal-Wallis Test	Mann-Whitney U Test		
						Control / LTD 10	Control / LTD 30	LTD10 / LTD 30
Bdnf Transctipt VI	0	1.00	13	0.00	9.22E-05	1.27E-01	3.64E-06	4.68E-03
	10	1.01	12	0.08				
	30	1.31	13	0.07				

	min	Mean	N	SEM	Kruskal-Wallis Test	Mann-Whitney U Test		
						Control / LTD 10	Control / LTD 30	LTD10 / LTD 30
Bdnf Transctipt VI	0	1.00	14	0.00	4.08E-06	5.96E-03	1.49E-06	2.82E-03
	10	1.46	14	0.15				
	30	2.13	14	0.13				

Supp. Table 4: Figure R2

A)

		Mean	N	SEM
H3K27Ac	*Bdnf* Promoter I	0.30	5	0.08
	Bdnf Promoter II	0.15	5	0.05
	Bdnf Promoter IV	0.36	5	0.07
	Bdnf Promoter VI	0.33	5	0.08
	ßActin	0.61	4	0.12
	hoxA1	0.02	4	0.01

		Mean	N	SEM
IgG	*Bdnf* Promoter I	0.045	5	0.018
	Bdnf Promoter II	0.025	5	0.016
	Bdnf Promoter IV	0.041	5	0.019
	Bdnf Promoter VI	0.008	5	0.003
	ßActin	0.006	4	0.003
	hoxA1	0.004	4	0.002

B)

		Mean	N	SEM
H3K4Me3	*Bdnf* Promoter I	1.78	5	0.27
	Bdnf Promoter II	0.66	5	0.22
	Bdnf Promoter IV	0.86	5	0.21
	Bdnf Promoter VI	1.16	5	0.38
	ßActin	1.80	4	0.10
	hoxA1	0.62	4	0.03

		Mean	N	SEM
IgG	*Bdnf* Promoter I	0.045	5	0.018
	Bdnf Promoter II	0.025	5	0.016
	Bdnf Promoter IV	0.041	5	0.019
	Bdnf Promoter VI	0.008	5	0.003
	ßActin	0.006	4	0.003
	hoxA1	0.004	4	0.002

C)

		Mean	N	SEM
H3K27Me3	*Bdnf* Promoter I	1.69	5	0.63
	Bdnf Promoter II	2.61	5	0.89
	Bdnf Promoter IV	1.61	5	0.36
	Bdnf Promoter VI	2.53	5	0.81
	ßActin	0.21	4	0.19
	hoxA1	4.39	4	1.05

		Mean	N	SEM
IgG	*Bdnf* Promoter I	0.045	5	0.018
	Bdnf Promoter II	0.025	5	0.016
	Bdnf Promoter IV	0.041	5	0.019
	Bdnf Promoter VI	0.008	5	0.003
	ßActin	0.006	4	0.003
	hoxA1	0.004	4	0.002

D)

		Mean	N	SEM
EZH2	*Bdnf* Promoter I	2.05	4	0.30
	Bdnf Promoter II	2.47	4	0.44
	Bdnf Promoter IV	1.78	4	0.25
	Bdnf Promoter VI	2.01	4	0.27
	ßActin	0.25	4	0.08
	hoxA1	2.08	4	0.26

		Mean	N	SEM
IgG	*Bdnf* Promoter I	0.008	4	0.001
	Bdnf Promoter II	0.013	4	0.003
	Bdnf Promoter IV	0.008	4	0.002
	Bdnf Promoter VI	0.012	4	0.003
	ßActin	0.014	4	0.005
	hoxA1	0.010	4	0.002

E)

		Mean	N	SEM
JMJD3	*Bdnf* Promoter I	0.41	4	0.11
	Bdnf Promoter II	0.54	4	0.14
	Bdnf Promoter IV	0.41	4	0.14
	Bdnf Promoter VI	0.40	4	0.12
	ßActin	0.52	4	0.12
	hoxA1	0.05	4	0.02

		Mean	N	SEM
IgG	*Bdnf* Promoter I	0.026	4	0.015
	Bdnf Promoter II	0.031	4	0.024
	Bdnf Promoter IV	0.040	4	0.001
	Bdnf Promoter VI	0.040	4	0.032
	ßActin	0.038	4	0.028
	hoxA1	0.022	4	0.013

Supp. Table 5: Figure R3

A)

		Mean	N	SEM	Mann-Whitney U Test
Bdnf Promoter I	EZH2	0.91	5	0.13	5.77E-01
	JMJD3	1.23	4	0.26	2.19E-01
	H3K4Me3	1.02	7	0.13	1.52E-01
	H3K27Ac	0.91	7	0.14	6.33E-01
	H3K27Me3	1.00	7	0.14	1.52E-01
	H3K27Me3S28p	1.34	7	0.30	1.52E-01

			Mean	N	SEM
Bdnf Promoter I	EZH2	IgG	0.126	5	0.053
	JMJD3	IgG	0.083	4	0.012
	H3K4Me3	IgG	0.003	7	0.001
	H3K27Ac	IgG	0.030	7	0.010
	H3K27Me3	IgG	0.007	7	0.003
	H3K27Me3S28p	IgG	0.165	7	0.058

		Mean	N	SEM	Mann-Whitney U Test
Bdnf Promoter II	EZH2	0.54	6	0.12	3.35E-03
	JMJD3	1.47	4	0.06	1.19E-02
	H3K4Me3	1.41	6	0.11	2.09E-03
	H3K27Ac	1.36	6	0.06	1.53E-03
	H3K27Me3	1.15	7	0.16	6.33E-01
	H3K27Me3S28p	2.10	6	0.53	1.11E-03

			Mean	N	SEM
Bdnf Promoter II	EZH2	IgG	0.123	6	0.050
	JMJD3	IgG	0.091	4	0.023
	H3K4Me3	IgG	0.005	6	0.003
	H3K27Ac	IgG	0.070	6	0.033
	H3K27Me3	IgG	0.014	7	0.010
	H3K27Me3S28p	IgG	0.206	6	0.070

		Mean	N	SEM	Mann-Whitney U Test
Bdnf Promoter IV	EZH2	0.57	6	0.03	2.09E-03
	JMJD3	1.80	4	0.24	1.19E-02
	H3K4Me3	0.95	7	0.20	1.52E-01
	H3K27Ac	0.86	7	0.07	1.19E-02
	H3K27Me3	0.87	6	0.05	6.01E-04
	H3K27Me3S28p	1.11	7	0.26	6.33E-01

			Mean	N	SEM
Bdnf Promoter IV	EZH2	IgG	0.091	6	0.032
	JMJD3	IgG	0.107	4	0.023
	H3K4Me3	IgG	0.005	7	0.002
	H3K27Ac	IgG	0.040	7	0.014
	H3K27Me3	IgG	0.008	6	0.004
	H3K27Me3S28p	IgG	0.229	7	0.076

		Mean	N	SEM	Mann-Whitney U Test
Bdnf Promoter VI	EZH2	0.54	6	0.12	3.35E-03
	JMJD3	1.55	4	0.10	1.19E-02
	H3K4Me3	1.38	6	0.03	2.82E-03
	H3K27Ac	1.50	6	0.18	2.09E-03
	H3K27Me3	0.59	6	0.04	1.11E-03
	H3K27Me3S28p	1.77	6	0.26	1.11E-03

			Mean	N	SEM
Bdnf Promoter VI	EZH2	IgG	0.066	6	0.017
	JMJD3	IgG	0.083	4	0.011
	H3K4Me3	IgG	0.003	6	0.001
	H3K27Ac	IgG	0.036	6	0.010
	H3K27Me3	IgG	0.006	6	0.004
	H3K27Me3S28p	IgG	0.254	6	0.054

B)

		Mean	N	SEM	Mann-Whitney U Test
ßActin	EZH2	1.10	5	0.17	9.47E-02
	JMJD3	1.34	4	0.20	2.19E-01
	H3K4Me3	1.10	7	0.17	6.33E-01
	H3K27Ac	0.96	7	0.08	6.33E-01
	H3K27Me3	1.07	7	0.24	6.33E-01
	H3K27Me3S28p	1.14	6	0.13	2.77E-01

			Mean	N	SEM
ßActin	EZH2	IgG	0.269	5	0.104
	JMJD3	IgG	0.070	4	0.007
	H3K4me3	IgG	0.006	7	0.002
	H3K27Ac	IgG	0.016	7	0.006
	H3K27me3	IgG	0.052	7	0.012
	H3K27me3S28p	IgG	0.397	6	0.072

		Mean	N	SEM	Mann-Whitney U Test
hoxA1	EZH2	1.14	5	0.36	5.50E-01
	JMJD3	1.12	4	0.21	2.19E-01
	H3K4Me3	0.83	6	0.08	1.00E+00
	H3K27Ac	0.69	7	0.10	6.33E-01
	H3K27Me3	0.87	7	0.17	6.33E-01
	H3K27Me3S28p	0.92	7	0.10	6.33E-01

			Mean	N	SEM
hoxA1	EZH2	IgG	0.071	5	0.018
	JMJD3	IgG	0.061	4	0.023
	H3K4me3	IgG	0.002	6	0.001
	H3K27Ac	IgG	0.131	7	0.050
	H3K27me3	IgG	0.003	7	0.002
	H3K27me3S28p	IgG	0.097	7	0.029

Supp. Table 6: Figure R4

A)

		Mean	N	SEM	Mann-Whitney U Test
Bdnf Promoter I	EZH2	1.20	5	0.21	5.77E-01
	JMJD3	1.27	4	0.31	2.19E-01
	H3K4Me3	0.92	6	0.16	2.77E-01
	H3K27Ac	0.61	5	0.17	5.72E-02
	H3K27Me3	0.96	5	0.22	5.26E-01
	H3K27Me3S28p	1.13	6	0.21	1.00E+00

			Mean	N	SEM
Bdnf Promoter I	EZH2	IgG	0.101	5	0.023
	JMJD3	IgG	0.069	4	0.029
	H3K4Me3	IgG	0.007	6	0.003
	H3K27Ac	IgG	0.031	5	0.008
	H3K27Me3	IgG	0.005	5	0.002
	H3K27Me3S28p	IgG	0.285	6	0.108

		Mean	N	SEM	Mann-Whitney U Test
Bdnf Promoter II	EZH2	1.06	5	0.14	9.26E-02
	JMJD3	0.95	4	0.13	1.00E+00
	H3K4Me3	0.67	6	0.14	4.03E-02
	H3K27Ac	0.54	5	0.12	1.53E-03
	H3K27Me3	1.01	5	0.20	5.26E-01
	H3K27Me3S28p	0.71	6	0.17	2.77E-01

			Mean	N	SEM
Bdnf Promoter II	EZH2	IgG	0.110	5	0.026
	JMJD3	IgG	0.068	4	0.025
	H3K4Me3	IgG	0.008	6	0.003
	H3K27Ac	IgG	0.031	5	0.008
	H3K27Me3	IgG	0.002	5	0.001
	H3K27Me3S28p	IgG	0.175	6	0.123

		Mean	N	SEM	Mann-Whitney U Test
Bdnf Promoter IV	EZH2	1.41	5	0.22	5.50E-01
	JMJD3	1.09	4	0.23	1.00E+00
	H3K4Me3	0.86	6	0.17	2.77E-01
	H3K27Ac	0.49	5	0.16	1.53E-03
	H3K27Me3	0.77	5	0.11	4.52E-02
	H3K27Me3S28p	1.02	5	0.37	1.25E-01

			Mean	N	SEM
Bdnf Promoter IV	EZH2	IgG	0.108	5	0.035
	JMJD3	IgG	0.161	4	0.075
	H3K4Me3	IgG	0.008	6	0.003
	H3K27Ac	IgG	0.024	5	0.010
	H3K27Me3	IgG	0.004	5	0.001
	H3K27Me3S28p	IgG	0.179	5	0.056

		Mean	N	SEM	Mann-Whitney U Test
Bdnf Promoter VI	EZH2	1.06	5	0.14	9.26E-02
	JMJD3	0.99	4	0.17	1.00E+00
	H3K4Me3	0.92	6	0.17	1.00E+00
	H3K27Ac	0.54	5	0.10	2.82E-03
	H3K27Me3	1.00	6	0.20	5.26E-01
	H3K27Me3S28p	1.06	6	0.21	2.77E-01

			Mean	N	SEM
Bdnf Promoter VI	EZH2	IgG	0.119	5	0.026
	JMJD3	IgG	0.235	4	0.063
	H3K4Me3	IgG	0.006	6	0.003
	H3K27Ac	IgG	0.018	5	0.004
	H3K27Me3	IgG	0.003	6	0.002
	H3K27Me3S28p	IgG	0.351	6	0.106

B)

		Mean	N	SEM	Mann-Whitney U Test
βActin	EZH2	1.45	5	0.30	9.47E-02
	JMJD3	1.27	4	0.08	1.39E-02
	H3K4Me3	1.10	6	0.13	2.77E-01
	H3K27Ac	0.68	5	0.07	1.53E-03
	H3K27Me3	0.86	5	0.15	5.26E-01
	H3K27Me3S28p	1.27	5	0.37	5.26E-01

			Mean	N	SEM
βActin	EZH2	IgG	0.210	5	0.047
	JMJD3	IgG	0.115	4	0.035
	H3K4Me3	IgG	0.013	6	0.007
	H3K27Ac	IgG	0.014	5	0.004
	H3K27Me3	IgG	0.044	5	0.009
	H3K27Me3S28p	IgG	0.310	5	0.120

		Mean	N	SEM	Mann-Whitney U Test
hoxA1	EZH2	1.14	5	0.36	5.50E-01
	JMJD3	1.12	4	0.21	1.00E+00
	H3K4Me3	0.83	6	0.08	5.72E-02
	H3K27Ac	0.69	5	0.10	1.53E-03
	H3K27Me3	0.87	5	0.17	5.26E-01
	H3K27Me3S28p	0.92	6	0.10	2.77E-01

			Mean	N	SEM
hoxA1	EZH2	IgG	0.087	5	0.035
	JMJD3	IgG	0.107	4	0.019
	H3K4Me3	IgG	0.003	6	0.001
	H3K27Ac	IgG	0.153	5	0.054
	H3K27Me3	IgG	0.002	5	0.001
	H3K27Me3S28p	IgG	0.235	6	0.055

Supp. Table 7: Figure R6

A)

						Bonferroni adjustment	95% confidence interval		99% confidence interval		99,9% confidence interval	
						Kruskal-Wallis Test	(*) p < 1.25E-02		(**) p < 2.50E-03		(***) p < 2.50E-04	
							Mann-Whitney U Test					
		SB-203580	Mean	N	SEM		Control/LTD30	Control/Control +	Control/LTD30+	LTD30/Control+	LTD30/LTD30+	Control+/LTD30+
Bdnf Transcript I	Control	-	1.00	13	0.00	5.04E-02	1.04E-02	2.72E-01	3.14E-03	1.44E-01	6.22E-01	2.59E-01
	LTD 30	-	1.34	13	0.13							
	Control	+	1.11	12	0.08							
	LTD 30	+	1.32	12	0.12							
Bdnf Transcript II	Control	-	1.00	13	0.00	1.01E-05	4.76E-06	8.21E-04	1.00E+00	2.47E-05	6.02E-05	2.51E-01
	LTD 30	-	2.07	12	0.15							
	Control	+	0.71	14	0.08							
	LTD 30	+	0.89	14	0.11							
Bdnf Transcript IV	Control	-	1.00	13	0.00	1.42E-03	3.64E-06	1.81E-01	5.95E-05	7.26E-02	6.98E-01	8.08E-02
	LTD 30	-	1.31	13	0.06							
	Control	+	1.19	14	0.08							
	LTD 30	+	1.53	14	0.14							
Bdnf Transcript VI	Control	-	1.00	14	0.00	4.52E-02	1.49E-06	3.49E-02	6.73E-01	2.49E-05	1.27E-04	4.91E-01
	LTD 30	-	2.13	14	0.13							
	Control	+	1.14	14	0.09							
	LTD 30	+	1.04	14	0.16							

B)

H3K27Me3S28p

						Bonferroni adjustment	95% confidence interval		99% confidence interval		99,9% confidence interval	
						Kruskal-Wallis Test	(*) p < 1.25E-02		(**) p < 2.50E-03		(***) p < 2.50E-04	
							Mann-Whitney U Test					
		SB-203580	Mean	N	SEM		Control/LTD10	Control/Control +	Control/LTD10+	LTD10/Control+	LTD10/LTD10+	Control+/LTD10+
Bdnf Promoter I	Control	-	1.00	7	0.00	5.06E-01	1.52E-01	3.26E-01	3.26E-01	4.25E-01	4.25E-01	8.27E-01
	LTD 10	-	1.34	7	0.30							
	Control	+	0.95	3	0.27							
	LTD 10	+	0.94	3	0.22							
Bdnf Promoter II	Control	-	1.00	6	0.00	1.93E-03	1.11E-03	3.26E-01	3.24E-03	2.01E-02	2.01E-02	5.13E-01
	LTD 10	-	2.10	6	0.53							
	Control	+	0.94	3	0.10							
	LTD 10	+	0.80	3	0.10							
Bdnf Promoter IV	Control	-	1.00	7	0.00	6.03E-01	6.33E-01	3.26E-01	3.70E-02	5.69E-01	9.09E-01	5.13E-01
	LTD 10	-	1.11	7	0.26							
	Control	+	1.25	3	0.39							
	LTD 10	+	1.29	3	0.09							
Bdnf Promoter VI	Control	-	1.00	6	0.00	2.63E-03	1.11E-03	3.24E-03	3.26E-01	7.07E-02	2.01E-02	5.13E-01
	LTD 10	-	1.77	6	0.26							
	Control	+	1.14	3	0.10							
	LTD 10	+	0.97	3	0.08							

IgG

		SB-203580	Mean	N	SEM
Bdnf Promoter I	Control	-	0.212	7	0.049
	LTD 10	-	0.165	7	0.058
	Control	+	0.238	3	0.086
	LTD 10	+	0.364	3	0.046
Bdnf Promoter II	Control	-	0.289	6	0.071
	LTD 10	-	0.206	6	0.070
	Control	+	0.278	3	0.071
	LTD 10	+	0.239	3	0.111
Bdnf Promoter IV	Control	-	0.284	7	0.040
	LTD 10	-	0.229	7	0.076
	Control	+	0.173	3	0.069
	LTD 10	+	0.166	3	0.095
Bdnf Promoter VI	Control	-	0.336	6	0.035
	LTD 10	-	0.254	6	0.054
	Control	+	0.122	3	0.014
	LTD 10	+	0.146	3	0.034

C)

EZH2

						Bonferroni adjustment	95% confidence interval		99% confidence interval		99,9% confidence interval	
						Kruskal-Wallis Test	(*) p < 1.25E-02		(**) p < 2.50E-03		(***) p < 2.50E-04	
							Mann-Whitney U Test					
		SB-203580	Mean	N	SEM		Control/LTD10	Control/Control +	Control/LTD10+	LTD10/Control+	LTD10/LTD10+	Control+/LTD10+
Bdnf Promoter I	Control	-	1.00	5	0.00	2.66E-01	5.77E-01	1.80E-01	1.80E-01	4.62E-01	8.64E-02	2.48E-01
	LTD 10	-	0.91	5	0.13							
	Control	+	1.12	4	0.15							
	LTD 10	+	1.50	4	0.26							
Bdnf Promoter II	Control	-	1.00	6	0.00	1.68E-03	3.35E-03	1.87E-01	8.30E-03	1.05E-02	1.05E-02	5.64E-01
	LTD 10	-	0.54	6	0.12							
	Control	+	1.09	4	0.06							
	LTD 10	+	1.18	4	0.07							
Bdnf Promoter IV	Control	-	1.00	6	0.00	5.69E-03	2.09E-03	1.00E+00	1.00E+00	1.05E-02	1.05E-02	2.48E-01
	LTD 10	-	0.57	6	0.03							
	Control	+	1.05	4	0.12							
	LTD 10	+	1.37	4	0.27							
Bdnf Promoter VI	Control	-	1.00	6	0.00	1.68E-03	3.35E-03	1.87E-01	8.30E-03	1.05E-02	1.05E-02	5.64E-01
	LTD 10	-	0.54	6	0.12							
	Control	+	1.09	4	0.06							
	LTD 10	+	1.18	4	0.07							

IgG

		SB-203580	Mean	N	SEM
Bdnf Promoter I	Control	-	0.122	5	0.032
	LTD 10	-	0.126	5	0.053
	Control	+	0.048	4	0.007
	LTD 10	+	0.069	4	0.016
Bdnf Promoter II	Control	-	0.166	6	0.026
	LTD 10	-	0.123	6	0.050
	Control	+	0.063	4	0.021
	LTD 10	+	0.094	4	0.041
Bdnf Promoter IV	Control	-	0.157	6	0.033
	LTD 10	-	0.091	6	0.032
	Control	+	0.053	4	0.013
	LTD 10	+	0.103	4	0.047
Bdnf Promoter VI	Control	-	0.152	6	0.041
	LTD 10	-	0.066	6	0.017
	Control	+	0.069	4	0.010
	LTD 10	+	0.132	4	0.049

Supp. Table 8: Figure R7

A)

		Mean	N	SEM
Cox2	MFEs p38 WT	0.042	3	0.001
	MFEs p38 KO	0.020	3	0.003

		Mean	N	SEM
IgG	MFEs p38 WT	0.020	3	0.006
	MFEs p38 KO	0.023	3	0.001

B)

		Mean	N	SEM	Mann-Whitney U Test
p38	*Bdnf* Promoter I	0.96	4	0.08	1.00E+00
	Bdnf Promoter II	2.04	4	0.22	1.39E-02
	Bdnf Promoter IV	0.93	4	0.13	1.00E+00
	Bdnf Promoter VI	1.91	4	0.16	1.39E-02

		Mean	N	SEM
IgG	*Bdnf* Promoter I	0.59	4	0.10
	Bdnf Promoter II	0.79	4	0.20
	Bdnf Promoter IV	0.99	4	0.29
	Bdnf Promoter VI	0.54	4	0.08

C)

		Mean	N	SEM	Mann-Whitney U Test
p38	*ßActin*	1.00	4	0.24	1.00E+00
	hoxA1	0.92	4	0.11	1.00E+00

		Mean	N	SEM
IgG	*ßActin*	1.11	4	0.21
	hoxA1	0.93	4	0.19

Supp. Table 9: Figure R8

A)

						Bonferroni adjustment	95% confidence interval (*) p < 1.25E-02		99% confidence interval (**) p < 2.50E-03		99,9% confidence interval (***) p < 2.50E-04	
							Mann-Whitney U Test					
		GSK-J4	Mean	N	SEM	Kruskal-Wallis Test	Control/LTD30	Control/Control +	Control/LTD30+	LTD30/Control+	LTD30/LTD30+	Control+/LTD30+
	Control	-	1.00	13	0.00							
Bdnf	LTD 30	-	1.34	13	0.13	3.75E-03	1.04E-02	1.87E-03	4.55E-04	2.51E-01	6.16E-01	2.66E-01
Transcript I	Control	+	1.15	9	0.09							
	LTD 30	+	1.57	9	0.21							
	Control	-	1.00	13	0.00							
Bdnf	LTD 30	-	2.07	12	0.15	9.55E-05	4.76E-06	5.46E-01	3.12E-02	9.80E-04	3.87E-04	4.18E-01
Transcript II	Control	+	0.89	8	0.17							
	LTD 30	+	0.77	8	0.12							
	Control	-	1.00	13	0.00							
Bdnf	LTD 30	-	1.31	13	0.06	1.29E-02	3.64E-06	1.67E-01	6.52E-04	6.55E-02	4.43E-01	1.26E-01
Transcript IV	Control	+	1.12	9	0.10							
	LTD 30	+	1.52	9	0.18							
	Control	-	1.00	14	0.00							
Bdnf	LTD 30	-	2.13	14	0.13	3.37E-02	1.49E-06	5.34E-01	2.68E-01	3.62E-03	1.74E-04	3.55E-01
Transcript VI	Control	+	1.04	8	0.22							
	LTD 30	+	1.11	8	0.12							

B)

							Bonferroni adjustment	95% confidence interval (*) p < 1.25E-02		99% confidence interval (**) p < 2.50E-03		99,9% confidence interval (***) p < 2.50E-04	
								Mann-Whitney U Test					
			GSK-J4	Mean	N	SEM	Kruskal-Wallis Test	Control/LTD10	Control/Control +	Control/LTD10+	LTD10/Control+	LTD10/LTD10+	Control+/LTD10+
		Control	-	1.00	7	0.00							
	Bdnf	LTD 10	-	1.00	7	0.14	6.16E-01	1.52E-01	3.26E-01	3.26E-01	5.69E-01	5.69E-01	8.27E-01
	Promoter I	Control	+	1.14	3	0.27							
		LTD 10	+	1.16	3	0.20							
		Control	-	1.00	7	0.00							
	Bdnf	LTD 10	-	1.15	7	0.16	9.60E-01	6.33E-01	3.26E-01	3.26E-01	9.09E-01	9.09E-01	5.13E-01
	Promoter II	Control	+	1.21	3	0.27							
H3K27Me3		LTD 10	+	1.05	3	0.18							
		Control	-	1.00	6	0.00							
	Bdnf	LTD 10	-	0.87	6	0.05	2.11E-02	6.01E-04	2.99E-01	2.99E-01	1.97E-01	7.07E-02	5.13E-01
	Promoter IV	Control	+	1.06	3	0.15							
		LTD 10	+	1.18	3	0.14							
		Control	-	1.00	6	0.00							
	Bdnf	LTD 10	-	0.59	6	0.04	5.06E-03	1.11E-03	3.26E-01	3.26E-01	2.01E-02	2.01E-02	8.27E-01
	Promoter VI	Control	+	0.99	3	0.12							
		LTD 10	+	1.01	3	0.03							

			GSK-J4	Mean	N	SEM
		Control	-	0.003	7	0.001
	Bdnf	LTD 10	-	0.007	7	0.003
	Promoter I	Control	+	0.009	3	0.005
		LTD 10	+	0.009	3	0.005
		Control	-	0.006	7	0.002
	Bdnf	LTD 10	-	0.014	7	0.010
	Promoter II	Control	+	0.008	3	0.006
IgG		LTD 10	+	0.008	3	0.006
		Control	-	0.007	6	0.002
	Bdnf	LTD 10	-	0.008	6	0.004
	Promoter IV	Control	+	0.009	3	0.003
		LTD 10	+	0.009	3	0.003
		Control	-	0.005	6	0.002
	Bdnf	LTD 10	-	0.006	6	0.004
	Promoter VI	Control	+	0.007	3	0.003
		LTD 10	+	0.007	3	0.003

C)

							Bonferroni adjustment	95% confidence interval (*) p < 1.25E-02		99% confidence interval (**) p < 2.50E-03		99,9% confidence interval (***) p < 2.50E-04	
								Mann-Whitney U Test					
			GSK-J4	Mean	N	SEM	Kruskal-Wallis Test	Control/LTD30	Control/Control +	Control/LTD30+	LTD30/Control+	LTD30/LTD30+	Control+/LTD30+
		Control	-	1.00	4	0.00							
	Bdnf	LTD 10	-	1.00	4	0.05	9.84E-01	1.00E+00	1.00E+00	1.00E+00	5.64E-01	7.73E-01	7.73E-01
	Promoter I	Control	+	0.93	4	0.09							
		LTD 10	+	0.93	4	0.11							
		Control	-	1.00	4	0.00							
	Bdnf	LTD 10	-	1.09	4	0.07	4.62E-01	2.19E-01	2.19E-01	2.19E-01	5.64E-01	7.73E-01	3.86E-01
	Promoter II	Control	+	1.17	4	0.13							
H3K9Me3		LTD 10	+	1.08	4	0.11							
		Control	-	1.00	4	0.00							
	Bdnf	LTD 10	-	0.87	4	0.11	4.13E-01	2.19E-01	1.00E+00	2.19E-01	1.49E-01	7.73E-01	3.86E-01
	Promoter IV	Control	+	1.11	4	0.15							
		LTD 10	+	0.97	4	0.27							
		Control	-	1.00	4	0.00							
	Bdnf	LTD 10	-	1.25	4	0.18	5.38E-01	2.19E-01	2.19E-01	2.19E-01	1.00E+00	7.73E-01	1.00E+00
	Promoter VI	Control	+	1.24	4	0.23							
		LTD 10	+	1.22	4	0.14							

			GSK-J4	Mean	N	SEM
		Control	-	0.028	4	0.021
	Bdnf	LTD 10	-	0.060	4	0.048
	Promoter I	Control	+	0.028	4	0.016
		LTD 10	+	0.032	4	0.019
		Control	-	0.018	4	0.009
	Bdnf	LTD 10	-	0.050	4	0.043
	Promoter II	Control	+	0.026	4	0.014
IgG		LTD 10	+	0.047	4	0.019
		Control	-	0.022	4	0.012
	Bdnf	LTD 10	-	0.045	4	0.031
	Promoter IV	Control	+	0.032	4	0.018
		LTD 10	+	0.056	4	0.029
		Control	-	0.020	4	0.011
	Bdnf	LTD 10	-	0.046	4	0.035
	Promoter VI	Control	+	0.039	4	0.020
		LTD 10	+	0.079	4	0.041

Supp. Table 10: Figure R9

A)

	Mean	N	SEM	Mann-Whitney U Test
Jmjd3	1.00	5	0.00	5.35E-03
	0.51	5	0.08	

B)

	Mean	N	SEM	Mann-Whitney U Test
JMJD3	0.00	4	0.00	2.09E-02
	0.12	4	0.06	

C)

		Lentivirus	Mean	N	SEM
JMJD3	*Bdnf* Promoter I	Scr	0.48	3	0.03
		Sh	0.06	3	0.04
	Bdnf Promoter II	Scr	0.75	3	0.05
		Sh	0.14	3	0.03
	Bdnf Promoter IV	Scr	0.81	3	0.05
		Sh	0.09	3	0.09
	Bdnf Promoter VI	Scr	0.85	3	0.19
		Sh	0.09	3	0.04

		Lentivirus	Mean	N	SEM
IgG	*Bdnf* Promoter I	Scr	0.04	3	0.03
		Sh	0.06	3	0.02
	Bdnf Promoter II	Scr	0.07	3	0.03
		Sh	0.09	3	0.01
	Bdnf Promoter IV	Scr	0.06	3	0.05
		Sh	0.01	3	0.01
	Bdnf Promoter VI	Scr	0.04	3	0.04
		Sh	0.05	3	0.01

D)

	Lentivirus		Mean	N	SEM	Mann-Whitney U Test Control/LTD10
Bdnf Promoter I	Sc	Control	1.00	3	0.00	3.69E-02
		LTD 30	1.41	3	0.09	
	Sh	Control	1.00	3	0.00	3.69E-02
		LTD 30	1.50	3	0.12	
Bdnf Promoter II	Sc	Control	1.00	3	0.00	3.69E-02
		LTD 30	1.57	3	0.18	
	Sh	Control	1.00	3	0.00	4.87E-01
		LTD 30	1.04	3	0.08	
Bdnf Promoter IV	Sc	Control	1.00	3	0.00	3.69E-02
		LTD 30	1.51	3	0.05	
	Sh	Control	1.00	3	0.00	3.69E-02
		LTD 30	1.29	3	0.01	
Bdnf Promoter VI	Sc	Control	1.00	3	0.00	3.69E-02
		LTD 30	1.35	3	0.02	
	Sh	Control	1.00	3	0.00	4.87E-01
		LTD 30	0.99	3	0.04	

E)

	Lentivirus		Mean	N	SEM	Mann-Whitney U Test Control/LTD10
Bdnf Promoter I	Sc	Control	1.00	5	0.00	5.77E-01
		LTD 10	0.99	5	0.18	
	Sh	Control	1.00	5	0.00	5.77E-01
		LTD 10	0.97	5	0.12	
Bdnf Promoter II	Sc	Control	1.00	5	0.00	5.77E-01
		LTD 10	0.89	5	0.12	
	Sh	Control	1.00	5	0.00	5.77E-01
		LTD 10	0.95	5	0.10	
Bdnf Promoter IV	Sc	Control	1.00	5	0.00	5.35E-03
		LTD 10	0.59	5	0.08	
	Sh	Control	1.00	5	0.00	1.89E-01
		LTD 10	0.87	5	0.10	
Bdnf Promoter VI	Sc	Control	1.00	5	0.00	5.35E-03
		LTD 10	0.53	5	0.07	
	Sh	Control	1.00	5	0.00	5.77E-01
		LTD 10	0.99	5	0.07	

		Lentivirus	Mean	N	SEM
IgG	*Bdnf* Promoter I	Sc	Control	0.03	5	0.01
			LTD 10	0.02	5	0.01
		Sh	Control	0.03	5	0.01
			LTD 10	0.01	5	0.00
	Bdnf Promoter II	Sc	Control	0.01	5	0.00
			LTD 10	0.01	5	0.01
		Sh	Control	0.03	5	0.02
			LTD 10	0.02	5	0.01
	Bdnf Promoter IV	Sc	Control	0.01	5	0.00
			LTD 10	0.01	5	0.01
		Sh	Control	0.01	5	0.01
			LTD 10	0.06	5	0.03
	Bdnf Promoter VI	Sc	Control	0.04	5	0.03
			LTD 10	0.00	5	0.00
		Sh	Control	0.06	5	0.02
			LTD 10	0.03	5	0.01

Supp. Table 11: Figure R10

B)

			AP	Mean	N	SEM
H3K27Me3S28p	*Bdnf* Promoter I	Control	-	0.23	4	0.01
			+	0.08	4	0.02
		LTD 10	-	0.26	4	0.03
			+	0.07	4	0.03
	Bdnf Promoter II	Control	-	0.22	4	0.02
			+	0.07	4	0.01
		LTD 10	-	0.35	4	0.05
			+	0.06	4	0.03
	Bdnf Promoter IV	Control	-	0.14	4	0.01
			+	0.04	4	0.01
		LTD 10	-	0.18	4	0.04
			+	0.04	4	0.02
	Bdnf Promoter VI	Control	-	0.21	4	0.02
			+	0.06	4	0.02
		LTD 10	-	0.28	4	0.01
			+	0.05	4	0.02

			AP	Mean	N	SEM
IgG	*Bdnf* Promoter I	Control	-	0.070	4	0.006
			+	0.049	4	0.022
		LTD 10	-	0.042	4	0.008
			+	0.079	4	0.018
	Bdnf Promoter II	Control	-	0.076	4	0.011
			+	0.051	4	0.018
		LTD 10	-	0.053	4	0.014
			+	0.069	4	0.019
	Bdnf Promoter IV	Control	-	0.067	4	0.007
			+	0.034	4	0.007
		LTD 10	-	0.064	4	0.013
			+	0.047	4	0.017
	Bdnf Promoter VI	Control	-	0.078	4	0.017
			+	0.050	4	0.021
		LTD 10	-	0.071	4	0.006
			+	0.052	4	0.003

C)

			AP	Mean	N	SEM	Mann-Whitney U Test
H3K27Me3	*Bdnf* Promoter I	Control	+	1.00	4	0.00	2.19E-01
		LTD 10		0.90	4	0.09	
	Bdnf Promoter II	Control	+	1.00	4	0.00	2.19E-01
		LTD 10		0.83	4	0.17	
	Bdnf Promoter IV	Control	+	1.00	4	0.00	1.39E-02
		LTD 10		0.66	4	0.07	
	Bdnf Promoter VI	Control	+	1.00	4	0.00	1.39E-02
		LTD 10		0.50	4	0.08	

			AP	Mean	N	SEM
IgG	*Bdnf* Promoter I	Control	+	0.006	4	0.002
		LTD 10		0.011	4	0.004
	Bdnf Promoter II	Control	+	0.006	4	0.002
		LTD 10		0.008	4	0.003
	Bdnf Promoter IV	Control	+	0.005	4	0.001
		LTD 10		0.014	4	0.007
	Bdnf Promoter VI	Control	+	0.004	4	0.001
		LTD 10		0.005	4	0.000

Supp. Table 12: Figure R11

C)

	JMJD3 (pmols)	Mean	N	SEM	Mann-Whitney U Test
% of demethylated H3K27Me3S28p peptide	0	0.00	4	0.00	
	3.5	23.44	4	2.39	
	7	32.28	4	0.95	
	14	45.31	4	4.76	
% of demethylated H3K27Me3 peptide	14	39.44	4	6.24	1.00E+00

Supp. Table 13: Figure R12

A)

Bonferroni adjustment	95% confidence interval	99% confidence interval	99.9% confidence interval
	(*) p < 1.67E-02	(**) p < 3.33E-03	(***) p < 3.33E-04

		Mean	N	SEM	Kruskal-Wallis Test	Mann-Whitney U Test		
						Control / LTD 10	Control / LTD 30	LTD10 / LTD 30
pS133-CREB	CNT	1.00	4	0.00	1.06E-02	1.39E-02	1.39E-02	8.33E-02
	LTD 10	1.88	4	0.28				
	LTD 30	1.35	4	0.09				

B)

Bonferroni adjustment	95% confidence interval	99% confidence interval	99,9% confidence interval
	(*) p < 1.25E-02	(**) p < 2.50E-03	(***) p < 2.50E-04

		KN93	Mean	N	SEM	Kruskal-Wallis Test	Mann-Whitney U Test					
							Control/LTD10	Control/Control +	Control/LTD10+	LTD10/Control+	LTD10/LTD10+	Control+/LTD10+
pS133-CREB	CNT	-	1.00	7	0.00	7.32E-03	8.29E-04	6.33E-01	1.52E-01	1.81E-02	2.53E-02	4.06E-01
	LTD10	-	1.79	7	0.16							
	CNT	+	1.09	7	0.14							
	LTD10	+	1.29	7	0.17							

C)

Bonferroni adjustment	95% confidence interval	99% confidence interval	99,9% confidence interval
	(*) p < 1.25E-02	(**) p < 2.50E-03	(***) p < 2.50E-04

		Cheleritryne	Mean	N	SEM	Kruskal-Wallis Test	Mann-Whitney U Test					
							Control/LTD10	Control/Control +	Control/LTD10+	LTD10/Control+	LTD10/LTD10+	Control+/LTD10+
pS133-CREB	CNT	-	1.00	7	0.00	3.41E-03	8.29E-04	6.33E-01	6.33E-01	2.68E-03	8.81E-03	8.48E-01
	LTD10	-	1.79	7	0.16							
	CNT	+	1.08	7	0.13							
	LTD10	+	1.05	7	0.16							

D)

Bonferroni adjustment	95% confidence interval	99% confidence interval	99,9% confidence interval
	(*) p < 1.25E-02	(**) p < 2.50E-03	(***) p < 2.50E-04

		H89	Mean	N	SEM	Kruskal-Wallis Test	Mann-Whitney U Test					
							Control/LTD10	Control/Control +	Control/LTD10+	LTD10/Control+	LTD10/LTD10+	Control+/LTD10+
pS133-CREB	CNT	-	1.00	7	0.00	3.31E-03	8.29E-04	6.33E-01	6.33E-01	8.81E-03	2.68E-03	7.49E-01
	LTD10	-	1.79	7	0.16							
	CNT	+	1.02	7	0.17							
	LTD10	+	0.93	7	0.17							

Supp. Table 14: Figure R13

A)

					Bonferroni adjustment	95% confidence interval	99% confidence interval	99.9% confidence interval
						(*) p < 1.67E-02	(**) p < 3.33E-03	(***) p < 3.33E-04
					Kruskal-Wallis Test	Mann-Whitney U Test		
		Mean	N	SEM		Control / LTD 10	Control / LTD 30	LTD10 / LTD 30
	CNT	1.00	6	0.00				
H3K27Ac	LTD 10	1.33	6	0.11	5.89E-04	2.82E-03	2.09E-03	6.17E-03
	LTD 30	0.60	6	0.06				

B)

					Bonferroni adjustment	95% confidence interval	99% confidence interval	99.9% confidence interval
						(*) p < 1.67E-02	(**) p < 3.33E-03	(***) p < 3.33E-04
					Kruskal-Wallis Test	Mann-Whitney U Test		
		Mean	N	SEM		Control / LTD 10	Control / LTD 30	LTD10 / LTD 30
	CNT	1.00	6	0.00				
H3K9Ac	LTD 10	1.06	6	0.17	7.25E-01	5.77E-01	5.77E-01	4.65E-01
	LTD 30	0.88	6	0.20				

C)

					Bonferroni adjustment	95% confidence interval	99% confidence interval	99.9% confidence interval
						(*) p < 1.67E-02	(**) p < 3.33E-03	(***) p < 3.33E-04
					Kruskal-Wallis Test	Mann-Whitney U Test		
		Mean	N	SEM		Control / LTD 10	Control / LTD 30	LTD10 / LTD 30
	CNT	1.00	6	0.00				
H3K14Ac	LTD 10	1.15	6	0.17	1.63E-01	5.77E-01	9.47E-02	1.17E-01
	LTD 30	0.74	6	0.24				

D)

					Bonferroni adjustment	95% confidence interval	99% confidence interval	99.9% confidence interval
						(*) p < 1.67E-02	(**) p < 3.33E-03	(***) p < 3.33E-04
					Kruskal-Wallis Test	Mann-Whitney U Test		
		Mean	N	SEM		Control / LTD 10	Control / LTD 30	LTD10 / LTD 30
	CNT	1.00	6	0.00				
H3K18Ac	LTD 10	0.82	6	0.07	1.88E-01	1.39E-02	1.00E+00	5.64E-01
	LTD 30	0.87	6	0.16				

Supp. Table 15: Figure R14

A)

		CCIIh	Mean	N	SEM	Kruskal-Wallis Test	Bonferroni adjustment	95% confidence interval (*) p < 1.25E-02	99% confidence interval (**) p < 2.50E-03	99,9% confidence interval (***) p < 2.50E-04		
							Mann-Whitney U Test					
							Control/LTD30	Control/Control +	Control/LTD30+	LTD30/Control+	LTD30/LTD30+	Control+/LTD30+
Bdnf Transcript I	Control	-	1.00	13	0.00	4.64E-04	1.04E-02	5.34E-01	9.25E-06	1.91E-01	8.22E-02	7.77E-03
	LTD 30	-	1.34	13	0.13							
	Control	+	1.13	8	0.10							
	LTD 30	+	1.69	8	0.13							
Bdnf Transcript II	Control	-	1.00	13	0.00	4.08E-04	4.76E-06	5.46E-01	1.00E+00	3.86E-04	2.62E-03	8.17E-01
	LTD 30	-	2.07	12	0.15							
	Control	+	0.92	8	0.07							
	LTD 30	+	1.01	8	0.20							
Bdnf Transcript IV	Control	-	1.00	13	0.00	8.58E-05	3.64E-06	3.39E-05	1.64E-05	1.14E-01	5.97E-02	9.82E-03
	LTD 30	-	1.31	13	0.06							
	Control	+	1.18	8	0.08							
	LTD 30	+	1.57	8	0.08							
Bdnf Transcript VI	Control	-	1.00	14	0.00	1.87E-03	1.49E-06	5.34E-01	1.95E-05	2.57E-04	1.30E-03	6.64E-03
	LTD 30	-	2.13	14	0.13							
	Control	+	1.07	7	0.11							
	LTD 30	+	1.49	7	0.04							

B)

H3K27Ac

		CCIIh	Mean	N	SEM	Kruskal-Wallis Test	Bonferroni adjustment	95% confidence interval (*) p < 1.25E-02	99% confidence interval (**) p < 2.50E-03	99,9% confidence interval (***) p < 2.50E-04		
							Mann-Whitney U Test					
							Control/LTD10	Control/Control +	Control/LTD10+	LTD10/Control+	LTD10/LTD10+	Control+/LTD10+
Bdnf Promoter I	Control	-	1.00	7	0.00	9.92E-01	6.33E-01	5.26E-01	5.26E-01	8.08E-01	9.35E-01	9.17E-01
	LTD 10	-	0.91	7	0.14							
	Control	+	0.89	5	0.20							
	LTD 10	+	0.86	5	0.21							
Bdnf Promoter II	Control	-	1.00	6	0.00	3.83E-03	1.53E-03	5.26E-01	5.72E-02	9.02E-03	9.02E-03	2.51E-01
	LTD 10	-	1.36	6	0.06							
	Control	+	0.88	5	0.14							
	LTD 10	+	0.70	5	0.13							
Bdnf Promoter IV	Control	-	1.00	7	0.00	3.99E-01	1.19E-02	5.26E-01	5.26E-01	9.35E-01	6.85E-01	9.17E-01
	LTD 10	-	0.86	7	0.07							
	Control	+	0.98	5	0.35							
	LTD 10	+	0.98	5	0.24							
Bdnf Promoter VI	Control	-	1.00	6	0.00	8.90E-04	2.09E-03	7.32E-02	2.82E-03	6.17E-03	6.17E-03	7.54E-01
	LTD 10	-	1.50	6	0.18							
	Control	+	0.72	5	0.13							
	LTD 10	+	0.79	5	0.09							

IgG

		CCIIh	Mean	N	SEM
Bdnf Promoter I	Control	-	0.031	7	0.006
	LTD 10	-	0.030	7	0.010
	Control	+	0.091	5	0.012
	LTD 10	+	0.082	5	0.036
Bdnf Promoter II	Control	-	0.065	6	0.015
	LTD 10	-	0.070	6	0.033
	Control	+	0.072	5	0.016
	LTD 10	+	0.137	5	0.047
Bdnf Promoter IV	Control	-	0.050	7	0.011
	LTD 10	-	0.040	7	0.014
	Control	+	0.106	5	0.024
	LTD 10	+	0.068	5	0.033
Bdnf Promoter VI	Control	-	0.027	6	0.005
	LTD 10	-	0.036	6	0.010
	Control	+	0.056	5	0.015
	LTD 10	+	0.145	5	0.078

C)

CREB

		CCIIh	Mean	N	SEM	Kruskal-Wallis Test	Bonferroni adjustment	95% confidence interval (*) p < 1.25E-02	99% confidence interval (**) p < 2.50E-03	99,9% confidence interval (***) p < 2.50E-04		
							Mann-Whitney U Test					
							Control/LTD10	Control/Control +	Control/LTD10+	LTD10/Control+	LTD10/LTD10+	Control+/LTD10+
Bdnf Promoter I	Control	-	1.00	5	0.00	3.42E-03	5.35E-03	1.04E-02	5.35E-03	2.53E-02	6.02E-01	5.26E-02
	LTD 10	-	2.50	5	0.44							
	Control	+	1.19	5	0.09							
	LTD 10	+	2.12	5	0.29							
Bdnf Promoter II	Control	-	1.00	5	0.00	2.22E-03	5.35E-03	1.04E-02	5.35E-03	2.53E-02	1.75E-01	2.53E-02
	LTD 10	-	2.23	5	0.40							
	Control	+	0.84	5	0.11							
	LTD 10	+	2.45	5	0.10							
Bdnf Promoter IV	Control	-	1.00	5	0.00	6.34E-03	5.35E-03	3.93E-01	5.35E-03	2.53E-02	9.17E-01	5.26E-02
	LTD 10	-	2.74	5	0.84							
	Control	+	1.04	5	0.12							
	LTD 10	+	2.94	5	0.83							
Bdnf Promoter VI	Control	-	1.00	5	0.00	4.59E-03	5.35E-03	3.93E-01	5.35E-03	2.53E-02	9.17E-01	2.53E-02
	LTD 10	-	2.42	5	0.30							
	Control	+	0.98	5	0.10							
	LTD 10	+	2.93	5	0.80							

IgG

		CCIIh	Mean	N	SEM
Bdnf Promoter I	Control	-	0.346	5	0.020
	LTD 10	-	0.302	5	0.015
	Control	+	0.300	5	0.122
	LTD 10	+	0.401	5	0.071
Bdnf Promoter II	Control	-	0.506	5	0.113
	LTD 10	-	0.500	5	0.057
	Control	+	0.448	5	0.106
	LTD 10	+	0.668	5	0.089
Bdnf Promoter IV	Control	-	0.545	5	0.085
	LTD 10	-	0.479	5	0.133
	Control	+	0.430	5	0.067
	LTD 10	+	0.506	5	0.067
Bdnf Promoter VI	Control	-	0.593	5	0.115
	LTD 10	-	0.646	5	0.073
	Control	+	0.430	5	0.150
	LTD 10	+	0.654	5	0.041

D)

Bonferroni adjustment — 95% confidence interval (*) p < 1.25E-02 — 99% confidence interval (**) p < 2.50E-03 — 99,9% confidence interval (***) p < 2.50E-04

CBP

		CCIIh	Mean	N	SEM	Kruskal-Wallis Test	Mann-Whitney U Test					
							Control/LTD10	Control/Control +	Control/LTD10+	LTD10/Control+	LTD10/LTD10+	Control+/LTD10+
	Control	-	1.00	5	0.00							
Bdnf	LTD 10	-	1.77	5	0.10							
Promoter I	Control	+	1.16	5	0.16	8.04E-03	5.35E-03	3.93E-01	9.47E-02	5.26E-02	9.02E-03	1.80E-01
	LTD 10	+	0.77	5	0.14							
	Control	-	1.00	5	0.00							
Bdnf	LTD 10	-	1.87	5	0.27							
Promoter II	Control	+	0.92	5	0.19	1.03E-02	5.35E-03	3.93E-01	9.47E-02	5.26E-02	9.02E-03	4.56E-01
	LTD 10	+	0.78	5	0.12							
	Control	-	1.00	5	0.00							
Bdnf	LTD 10	-	2.07	5	0.17							
Promoter IV	Control	+	0.81	5	0.16	8.48E-03	5.35E-03	3.93E-01	5.77E-01	2.53E-02	9.02E-03	1.01E-01
	LTD 10	+	1.12	5	0.15							
	Control	-	1.00	5	0.00							
Bdnf	LTD 10	-	2.81	5	0.28							
Promoter VI	Control	+	0.98	5	0.07	1.29E-02	5.35E-03	3.93E-01	5.77E-01	2.53E-02	9.02E-03	6.55E-01
	LTD 10	+	1.08	5	0.16							

IgG

		CCIIh	Mean	N	SEM
	Control	-	0.105	5	0.026
Bdnf	LTD 10	-	0.125	5	0.045
Promoter I	Control	+	0.037	5	0.017
	LTD 10	+	0.207	5	0.059
	Control	-	0.116	5	0.034
Bdnf	LTD 10	-	0.118	5	0.037
Promoter II	Control	+	0.074	5	0.057
	LTD 10	+	0.160	5	0.053
	Control	-	0.181	5	0.061
Bdnf	LTD 10	-	0.073	5	0.003
Promoter IV	Control	+	0.058	5	0.022
	LTD 10	+	0.180	5	0.121
	Control	-	0.122	5	0.047
Bdnf	LTD 10	-	0.127	5	0.049
Promoter VI	Control	+	0.047	5	0.019
	LTD 10	+	0.133	5	0.070

E)

Bonferroni adjustment — 95% confidence interval (*) p < 1.25E-02 — 99% confidence interval (**) p < 2.50E-03 — 99,9% confidence interval (***) p < 2.50E-04

JMJD3

		CCIIh	Mean	N	SEM	Kruskal-Wallis Test	Mann-Whitney U Test					
							Control/LTD10	Control/Control +	Control/LTD10+	LTD10/Control+	LTD10/LTD10+	Control+/LTD10+
	Control	-	1.00	4	0.00							
Bdnf	LTD 10	-	1.23	4	0.26							
Promoter I	Control	+	1.11	3	0.38	8.29E-01	2.19E-01	4.35E-01	4.35E-01	1.00E+00	4.80E-01	5.13E-01
	LTD 10	+	1.00	3	0.09							
	Control	-	1.00	4	0.00							
Bdnf	LTD 10	-	1.47	4	0.06							
Promoter II	Control	+	0.75	3	0.09	8.50E-03	1.19E-02	1.93E-02	1.93E-02	3.39E-02	3.39E-02	8.27E-01
	LTD 10	+	0.78	3	0.11							
	Control	-	1.00	4	0.00							
Bdnf	LTD 10	-	1.80	4	0.24							
Promoter IV	Control	+	1.02	3	0.35	2.22E-02	1.19E-02	4.35E-01	1.93E-02	7.71E-02	3.39E-02	2.75E-01
	LTD 10	+	0.59	3	0.17							
	Control	-	1.00	4	0.00							
Bdnf	LTD 10	-	1.55	4	0.10							
Promoter VI	Control	+	0.76	3	0.20	2.77E-02	1.19E-02	4.35E-01	2.19E-01	3.39E-02	2.09E-02	7.24E-01
	LTD 10	+	0.84	4	0.14							

IgG

		CCIIh	Mean	N	SEM
	Control	-	0.084	4	0.013
Bdnf	LTD 10	-	0.083	4	0.012
Promoter I	Control	+	0.069	3	0.029
	LTD 10	+	0.056	3	0.028
	Control	-	0.073	4	0.011
Bdnf	LTD 10	-	0.091	4	0.023
Promoter II	Control	+	0.019	3	0.015
	LTD 10	+	0.139	3	0.084
	Control	-	0.138	4	0.039
Bdnf	LTD 10	-	0.107	4	0.023
Promoter IV	Control	+	0.224	3	0.109
	LTD 10	+	0.082	3	0.053
	Control	-	0.102	4	0.027
Bdnf	LTD 10	-	0.083	4	0.011
Promoter VI	Control	+	0.089	3	0.027
	LTD 10	+	0.053	4	0.025

F)

Bonferroni adjustment — 95% confidence interval (*) p < 1.25E-02 — 99% confidence interval (**) p < 2.50E-03 — 99,9% confidence interval (***) p < 2.50E-04

H3K27Me3

		CCIIh	Mean	N	SEM	Kruskal-Wallis Test	Mann-Whitney U Test					
							Control/LTD10	Control/Control +	Control/LTD10+	LTD10/Control+	LTD10/LTD10+	Control+/LTD10+
	Control	-	1.00	7	0.00							
Bdnf	LTD 10	-	1.00	7	0.14							
Promoter I	Control	+	1.01	3	0.07	5.32E-01	1.52E-01	3.26E-01	3.26E-01	2.10E-01	7.32E-01	5.13E-01
	LTD 10	+	1.23	3	0.31							
	Control	-	1.00	7	0.00							
Bdnf	LTD 10	-	1.15	7	0.16							
Promoter II	Control	+	1.18	3	0.17	2.33E-01	6.33E-01	3.26E-01	3.24E-03	5.69E-01	2.10E-01	5.13E-01
	LTD 10	+	1.51	3	0.28							
	Control	-	1.00	6	0.00							
Bdnf	LTD 10	-	0.87	6	0.05							
Promoter IV	Control	+	1.44	3	0.32	5.14E-03	6.01E-04	1.84E-03	2.99E-01	2.01E-02	3.02E-01	5.13E-01
	LTD 10	+	1.24	3	0.33							
	Control	-	1.00	6	0.00							
Bdnf	LTD 10	-	0.59	6	0.04							
Promoter VI	Control	+	0.94	3	0.03	5.04E-03	1.11E-03	3.57E-01	3.57E-01	2.01E-02	2.01E-02	1.27E-01
	LTD 10	+	1.35	3	0.18							

IgG

		CCIIh	Mean	N	SEM
	Control	-	0.003	7	0.001
Bdnf	LTD 10	-	0.007	7	0.003
Promoter I	Control	+	0.006	3	0.001
	LTD 10	+	0.006	3	0.001
	Control	-	0.006	7	0.002
Bdnf	LTD 10	-	0.014	7	0.010
Promoter II	Control	+	0.005	3	0.002
	LTD 10	+	0.005	3	0.002
	Control	-	0.007	6	0.002
Bdnf	LTD 10	-	0.008	6	0.004
Promoter IV	Control	+	0.007	3	0.001
	LTD 10	+	0.007	3	0.001
	Control	-	0.005	6	0.002
Bdnf	LTD 10	-	0.006	6	0.004
Promoter VI	Control	+	0.006	3	0.001
	LTD 10	+	0.006	3	0.001

Supp. Table 16: Figure R15

		Mean	N	SEM	Mann-Whitney U Test
pS276-p65	Control	1.00	6	0.00	3.05E-01
	LTD 10	1.10	6	0.11	

Supp. Table 17: Figure R17

					Bonferroni adjustment	95% confidence interval	99% confidence interval	99.9% confidence interval
						(*) p < 1.67E-02	(**) p < 3.33E-03	(***) p < 3.33E-04
							Mann-Whitney U Test	
		Mean	N	SEM	Kruskal-Wallis Test	Control / LTD 10	Control / LTD 30	LTD10 / LTD 30
Bdnf Transctipt I	Control	1.00	8	0.00	6.73E-03	1.67E-02	7.10E-03	3.89E-02
	LTD 10	0.98	6	0.08				
	LTD 30	1.24	8	0.09				
							Mann-Whitney U Test	
		Mean	N	SEM	Kruskal-Wallis Test	Control / LTD 10	Control / LTD 30	LTD10 / LTD 30
Bdnf Transctipt II	Control	1.00	8	0.00	1.09E-04	3.31E-04	2.55E-04	9.90E-02
	LTD 10	1.30	6	0.11				
	LTD 30	1.52	8	0.10				
							Mann-Whitney U Test	
		Mean	N	SEM	Kruskal-Wallis Test	Control / LTD 10	Control / LTD 30	LTD10 / LTD 30
Bdnf Transctipt VI	Control	1.00	8	0.00	1.05E-02	1.00E+00	4.40E-04	1.99E-01
	LTD 10	1.00	6	0.12				
	LTD 30	1.25	7	0.06				
							Mann-Whitney U Test	
		Mean	N	SEM	Kruskal-Wallis Test	Control / LTD 10	Control / LTD 30	LTD10 / LTD 30
Bdnf Transctipt VI	Control	1.00	8	0.00	1.69E-04	4.72E-04	3.31E-04	1.07E-01
	LTD 10	1.28	5	0.09				
	LTD 30	1.49	8	0.10				

Supp. Table 18: Figure R18

A)

		Mean	N	SEM
H3K27Me3	*Bdnf* Promoter I	2.62	4	0.63
	Bdnf Promoter II	2.08	4	0.21
	Bdnf Promoter IV	2.09	4	0.48
	Bdnf Promoter VI	2.67	4	0.11
	ßActin	0.37	4	0.12
	hoxA1	6.43	4	1.15

		Mean	N	SEM
IgG	*Bdnf* Promoter I	0.027	4	0.010
	Bdnf Promoter II	0.042	4	0.018
	Bdnf Promoter IV	0.028	4	0.013
	Bdnf Promoter VI	0.044	4	0.008
	ßActin	0.029	4	0.008
	hoxA1	0.021	4	0.007

B)

		Mean	N	SEM
EZH2	*Bdnf* Promoter I	2.73	6	0.49
	Bdnf Promoter II	2.90	6	0.53
	Bdnf Promoter IV	2.64	6	0.46
	Bdnf Promoter VI	3.50	6	0.65
	ßActin	1.25	6	0.23
	hoxA1	5.46	6	0.53

		Mean	N	SEM
IgG	*Bdnf* Promoter I	0.034	6	0.012
	Bdnf Promoter II	0.029	6	0.008
	Bdnf Promoter IV	0.022	6	0.012
	Bdnf Promoter VI	0.034	6	0.009
	ßActin	0.025	6	0.007
	hoxA1	0.027	6	0.009

C)

		Mean	N	SEM
JMJD3	*Bdnf* Promoter I	0.47	5	0.07
	Bdnf Promoter II	0.45	5	0.06
	Bdnf Promoter IV	0.52	5	0.07
	Bdnf Promoter VI	0.59	5	0.12
	ßActin	0.40	5	0.09
	hoxA1	0.08	5	0.02

		Mean	N	SEM
IgG	*Bdnf* Promoter I	0.053	5	0.033
	Bdnf Promoter II	0.040	5	0.014
	Bdnf Promoter IV	0.079	5	0.034
	Bdnf Promoter VI	0.044	5	0.019
	ßActin	0.066	5	0.016
	hoxA1	0.070	5	0.029

D)

		Mean	N	SEM
H3K4Me3	*Bdnf* Promoter I	5.36	4	0.76
	Bdnf Promoter II	1.50	4	0.09
	Bdnf Promoter IV	1.21	4	0.17
	Bdnf Promoter VI	5.74	4	0.65
	ßActin	6.25	4	0.46
	hoxA1	2.29	4	0.22

		Mean	N	SEM
IgG	*Bdnf* Promoter I	0.027	4	0.010
	Bdnf Promoter II	0.042	4	0.018
	Bdnf Promoter IV	0.028	4	0.013
	Bdnf Promoter VI	0.044	4	0.008
	ßActin	0.029	4	0.008
	hoxA1	0.021	4	0.007

E)

		Mean	N	SEM
H3K27Ac	*Bdnf* Promoter I	0.40	4	0.05
	Bdnf Promoter II	0.11	4	0.03
	Bdnf Promoter IV	0.73	4	0.14
	Bdnf Promoter VI	0.49	4	0.06
	ßActin	1.15	4	0.16
	hoxA1	0.08	4	0.03

		Mean	N	SEM
IgG	*Bdnf* Promoter I	0.027	4	0.010
	Bdnf Promoter II	0.042	4	0.018
	Bdnf Promoter IV	0.028	4	0.013
	Bdnf Promoter VI	0.044	4	0.008
	ßActin	0.029	4	0.008
	hoxA1	0.021	4	0.007

Supp. Table 19: Figure R19

A)

		Mean	N	SEM	Mann-Whitney U Test
Bdnf Promoter I	EZH2	0.79	6	0.05	2.09E-03
	JMJD3	2.19	6	0.32	2.09E-03
	H3K4Me3	2.19	6	0.32	1.69E-02
	H3K27Ac	1.24	7	0.31	1.00E+00
	H3K27Me3	0.97	6	0.19	1.52E-01
	H3K27Me3S28p	1.46	7	0.13	7.10E-03

			Mean	N	SEM
Bdnf Promoter I	EZH2	IgG	0.012	6	0.0048
	JMJD3	IgG	0.072	6	0.0218
	H3K4Me3	IgG	0.061	6	0.0244
	H3K27Ac	IgG	0.019	7	0.0047
	H3K27Me3	IgG	0.001	6	0.0005
	H3K27Me3S28p	IgG	0.075	7	0.0202

		Mean	N	SEM	Mann-Whitney U Test
Bdnf Promoter II	EZH2	0.81	6	0.04	2.09E-03
	JMJD3	2.42	6	0.41	2.09E-03
	H3K4Me3	1.32	6	0.10	2.09E-03
	H3K27Ac	1.60	6	0.29	4.03E-02
	H3K27Me3	0.80	7	0.11	1.69E-02
	H3K27Me3S28p	1.59	7	0.33	1.69E-02

			Mean	N	SEM
Bdnf Promoter II	EZH2	IgG	0.029	6	0.0170
	JMJD3	IgG	0.061	6	0.0244
	H3K4Me3	IgG	0.001	6	0.0004
	H3K27Ac	IgG	0.068	6	0.0345
	H3K27Me3	IgG	0.001	7	0.0004
	H3K27Me3S28p	IgG	0.064	7	0.0385

		Mean	N	SEM	Mann-Whitney U Test
Bdnf Promoter IV	EZH2	0.74	6	0.06	2.09E-03
	JMJD3	2.14	6	0.30	2.09E-03
	H3K4Me3	1.32	6	0.10	2.09E-03
	H3K27Ac	1.05	6	0.25	3.05E-01
	H3K27Me3	0.70	6	0.10	2.97E-02
	H3K27Me3S28p	1.34	6	0.15	4.03E-02

			Mean	N	SEM
Bdnf Promoter IV	EZH2	IgG	0.012	6	0.0041
	JMJD3	IgG	0.158	6	0.0644
	H3K4Me3	IgG	0.001	6	0.0004
	H3K27Ac	IgG	0.029	6	0.0188
	H3K27Me3	IgG	0.001	6	0.0005
	H3K27Me3S28p	IgG	0.070	6	0.0393

		Mean	N	SEM	Mann-Whitney U Test
Bdnf Promoter VI	EZH2	0.75	6	0.05	2.09E-03
	JMJD3	2.42	6	0.49	2.09E-03
	H3K4Me3	1.36	6	0.08	2.09E-03
	H3K27Ac	1.54	7	0.24	1.69E-02
	H3K27Me3	0.68	7	0.09	1.69E-02
	H3K27Me3S28p	1.34	7	0.11	1.69E-02

			Mean	N	SEM
Bdnf Promoter VI	EZH2	IgG	0.018	6	0.0099
	JMJD3	IgG	0.057	6	0.0249
	H3K4Me3	IgG	0.000	6	0.0002
	H3K27Ac	IgG	0.013	7	0.0066
	H3K27Me3	IgG	0.001	7	0.0003
	H3K27Me3S28p	IgG	0.034	7	0.0185

B)

		Mean	N	SEM	Mann-Whitney U Test
ßActin	EZH2	0.95	6	0.11	3.05E-01
	JMJD3	1.73	6	0.21	2.82E-03
	H3K4Me3	0.91	6	0.22	6.33E-01
	H3K27Ac	1.20	7	0.39	7.27E-02
	H3K27Me3	0.88	7	0.19	6.33E-01
	H3K27Me3S28p	1.33	7	0.33	6.33E-01

			Mean	N	SEM
ßActin	EZH2	IgG	0.018	6	0.0089
	JMJD3	IgG	0.109	6	0.0639
	H3K4Me3	IgG	0.091	6	0.0330
	H3K27Ac	IgG	0.001	7	0.0004
	H3K27Me3	IgG	0.145	7	0.1397
	H3K27Me3S28p	IgG	0.401	7	0.2598

		Mean	N	SEM	Mann-Whitney U Test
hoxA1	EZH2	0.79	6	0.13	9.47E-02
	JMJD3	1.32	6	0.17	9.47E-02
	H3K4Me3	0.96	6	0.21	6.33E-01
	H3K27Ac	1.27	7	0.35	6.33E-01
	H3K27Me3	0.92	7	0.10	1.52E-01
	H3K27Me3S28p	1.09	7	0.06	2.77E-01

			Mean	N	SEM
hoxA1	EZH2	IgG	0.028	6	0.0170
	JMJD3	IgG	0.091	6	0.0330
	H3K4Me3	IgG	0.001	6	0.0005
	H3K27Ac	IgG	0.099	7	0.0237
	H3K27Me3	IgG	0.002	7	0.0008
	H3K27Me3S28p	IgG	0.137	7	0.1210

Supp. Table 20: Figure R20

		Mean	N	Error	Shapiro-Wilk	Levene	Student's *t*-Test
Bdnf Transcript II	Adult	1.00	7	0.129	5.10E-02	4.41E-01	1.30E-02
	Old	0.66	7	0.063	8.41E-01		
					Shapiro-Wilk	Levene	Mann-Whitney
Bdnf Transcript VI	Adult	1.00	7	0.222	3.75E-02	2.67E-02	1.72E-03
	Old	0.35	7	0.024	3.25E-01		

Supp. Table 21: Figure R21

A)

			Mean	N	Error	Shapiro-Wilk	Levene	Student's *t*-Test
H3K27Me3	*Bdnf* Promoter II	Adult	1.77	7	0.126	7.12E-01	5.70E-03	7.43E-03
		Old	3.13	7	0.353	1.20E-01		
	Bdnf Promoter VI	Adult	1.81	7	0.206	2.35E-01	9.57E-01	4.51E-03
		Old	2.87	7	0.222	9.64E-01		

B)

			Mean	N	Error	Shapiro-Wilk	Levene	Student's *t*-Test
H3K27Me3S28p	*Bdnf* Promoter II	Adult	0.03	3	0.010	8.61E-01	9.20E-02	1.14E-02
		Old	0.13	3	0.020	9.43E-01		
	Bdnf Promoter VI	Adult	0.03	3	0.006	1.06E-01	1.18E-01	1.63E-02
		Old	0.12	3	0.035	2.92E-01		

C)

			Mean	N	Error	Shapiro-Wilk	Levene	Student's *t*-Test
H3K27Ac	*Bdnf* Promoter II	Adult	0.23	6	0.024	1.55E-01	7.23E-02	9.65E-03
		Old	0.15	6	0.011	4.29E-01		
	Bdnf Promoter VI	Adult	0.68	6	0.092	1.86E-01	9.27E-03	1.42E-02
		Old	0.38	6	0.040	7.20E-01		

D)

			Mean	N	Error	Shapiro-Wilk	Levene	Student's *t*-Test
CBP	*Bdnf* Promoter II	Adult	0.53	7	0.162	4.26E-01	7.37E-04	2.15E-02
		Old	0.16	7	0.012	8.49E-01		
	Bdnf Promoter VI	Adult	0.76	6	0.251	3.92E-01	3.22E-04	2.96E-02
		Old	0.27	6	0.030	8.19E-01		

E)

			Mean	N	Error	Shapiro-Wilk	Levene	Student's *t*-Test
HDAC4	*Bdnf* Promoter II	Adult	0.07	6	0.016	9.87E-01	8.54E-01	3.27E-06
		Old	0.29	6	0.017	9.53E-01		
	Bdnf Promoter VI	Adult	0.11	6	0.029	5.91E-01	9.97E-02	1.20E-03
		Old	0.35	6	0.046	3.45E-01		

Supp. Table 22: Figure R22

			Mean	N	Error	Shapiro-Wilk	Levene	One way ANOVA		Games-Howell	
Bdnf Transcript II	Adult	CNT	1.00	7	0.00	-			CNT / LTD 10	CNT / LTD 30	LTD 10 / LTD30
		LTD 10	1.23	7	0.07	5.93E-01	1.55E-02	3.80E-03	3.29E-02	1.48E-02	6.65E-01
		LTD 30	1.36	7	0.08	7.57E-01					
						Shapiro-Wilk	Levene	Kruskal-Wallis		Mann-Whitney	
	Old	CNT	1.00	9	0.00	-			CNT / LTD 10	CNT / LTD 30	LTD 10 / LTD30
		LTD 10	1.06	9	0.09	2.89E-02	5.39E-03	4.14E-01	2.23E-01	2.53E-01	8.14E-01
		LTD 30	1.03	6	0.08	7.48E-01					
						Shapiro-Wilk	Levene	One way ANOVA		Games-Howell	
Bdnf Transcript VI	Adult	CNT	1.00	7	0.00	-			CNT / LTD 10	CNT / LTD 30	LTD 10 / LTD30
		LTD 10	1.41	7	0.10	2.23E-01	1.28E-02	4.15E-03	1.43E-02	2.47E-02	9.94E-01
		LTD 30	1.40	7	0.11	9.43E-01					
						Shapiro-Wilk	Levene	One way ANOVA		Games-Howell	
	Old	CNT	1.00	9	0.00	-			CNT / LTD 10	CNT / LTD 30	LTD 10 / LTD30
		LTD 10	1.03	9	0.12	2.82E-01	4.02E-03	9.18E-01	9.59E-01	9.26E-01	9.87E-01
		LTD 30	1.07	6	0.18	3.91E-01					

Supp. Table 23: Figure R23

A)

			Mean	N	Error	Shapiro-Wilk	Levene	Test
CREB	Adulr	CNT	1.00	8	0.00	-	3.82E-03	Mann-Whitney
		LTD 10	1.48	8	0.11	1.90E-02		5.83E-04
	Old	CNT	1.00	8	0.00	-	2.41E-04	One Sample *t*-Test
		LTD 10	0.99	8	0.10	2.60E-01		9.43E-01

B)

			Mean	N	Error	Shapiro-Wilk	Levene	Test
αCaMKII	Adult	CNT	1.00	9	0.00	-	8.91E-04	Mann-Whitney
		LTD 10	1.27	9	0.06	2.94E-02		1.08E-05
	Old	CNT	1.00	9	0.00	-	1.10E-04	One Sample *t*-Test
		LTD 10	0.87	9	0.08	6.86E-01		1.62E-01

C)

				Mean	N	Error	Shapiro-Wilk	Levene	Test
CBP	*Bdnf* Promoter II	Adult	CNT	1.00	5	0.00	-	1.46E-01	One Sample t-Test
			LTD 10	1.50	5	0.14	2.37E-01		2.34E-02
		Old	CNT	1.00	4	0.00	-	3.96E-02	One Sample t-Test
			LTD 10	0.85	4	0.06	1.79E-01		8.12E-02
	Bdnf Promoter VI	Adult	CNT	1.00	5	0.00	-	1.46E-01	Mann-Whitney
			LTD 10	1.53	5	0.15	2.08E-02		5.35E-03
		Old	CNT	1.00	4	0.00	-	6.65E-03	One Sample t-Test
			LTD 10	1.09	4	0.07	3.25E-01		2.96E-01

D)

				Mean	N	Error	Shapiro-Wilk	Levene	One Sample *t*-Test
H3K27Ac	*Bdnf* Promoter II	Adult	CNT	1.00	5	0.00	-	9.74E-03	3.53E-02
			LTD 10	1.53	5	0.19	5.84E-01		
		Old	CNT	1.00	7	0.00	-	9.28E-03	5.23E-01
			LTD 10	1.06	7	0.09	5.69E-01		
	Bdnf Promoter VI	Adult	CNT	1.00	5	0.00	-	8.93E-04	5.91E-03
			LTD 10	1.50	5	0.14	3.17E-01		
		Old	CNT	1.00	7	0.00	-	1.11E-03	9.34E-01
			LTD 10	1.01	7	0.13	5.95E-01		

E)

				Mean	N	Error	Shapiro-Wilk	Levene	Test
HDAC4	*Bdnf* Promoter II	Adult	CNT	1.00	4	0.00	-	1.06E-01	One Sample *t*-Test
			LTD 10	0.60	4	0.06	1.66E-01		1.91E-02
		Old	CNT	1.00	5	0.00	-	2.52E-02	One Sample *t*-Test
			LTD 10	1.01	5	0.04	6.33E-01		7.69E-01
	Bdnf Promoter VI	Adult	CNT	1.00	4	0.00	-	2.90E-03	Mann-Whitney
			LTD 10	0.49	4	0.10	4.66E-03		2.77E-02
		Old	CNT	1.00	5	0.00	-	1.07E-02	One Sample *t*-Test
			LTD 10	1.00	5	0.06	3.55E-01		9.62E-01

				Mean	N	Error
IgG	*Bdnf* Promoter II	Adult	CNT	0.029	5	0.010
			LTD 10	0.022	5	0.009
		Old	CNT	0.085	4	0.020
			LTD 10	0.060	4	0.037
	Bdnf Promoter VI	Adult	CNT	0.057	5	0.038
			LTD 10	0.083	5	0.072
		Old	CNT	0.043	4	0.014
			LTD 10	0.066	4	0.022

				Mean	N	Error
IgG	*Bdnf* Promoter II	Adult	CNT	0.150	5	0.043
			LTD 10	0.125	5	0.040
		Old	CNT	0.109	7	0.035
			LTD 10	0.261	7	0.120
	Bdnf Promoter VI	Adult	CNT	0.064	5	0.023
			LTD 10	0.042	5	0.017
		Old	CNT	0.048	7	0.022
			LTD 10	0.056	7	0.020

				Mean	N	Error
IgG	*Bdnf* Promoter II	Adult	CNT	0.248	4	0.128
			LTD 10	0.233	4	0.115
		Old	CNT	0.097	5	0.038
			LTD 10	0.092	5	0.051
	Bdnf Promoter VI	Adult	CNT	0.138	4	0.131
			LTD 10	0.075	4	0.058
		Old	CNT	0.080	5	0.026
			LTD 10	0.073	5	0.025

Supp. Table 24: Figure R24

A)

		Mean	N	Error	Shapiro-Wilk	Levene	Student's *t*-Test
Cholesterol Quantification	Adult	0.10	7	0.01	7.98E-01	7.60E-02	2.50E-02
	Old	0.08	9	0.00	2.24E-01		

B)

		Mean	N	Error	Shapiro-Wilk	Levene	Student's *t*-Test
Cholesterol Quantification	-	0.09	7	0.00	5.81E-01	8.90E-02	3.46E-04
	+ MßCD-Ch	0.13	7	0.01	2.77E-01		

C)

			Mean	N	Error	Shapiro-Wilk	Levene	Kruskal-Wallis	Mann-Whitney		
		CNT	1.00	9	0.00	-			CNT / LTD 10	CNT / LTD 30	LTD 10 / LTD30
	-	LTD 10	1.06	9	0.09	2.89E-02	5.39E-03	4.14E-01	2.23E-01	2.53E-01	8.14E-01
		LTD 30	1.03	6	0.08	7.48E-01					
Bdnf Transcript II						Shapiro-Wilk	Levene	One way ANOVA		Games-Howell	
		CNT	0.95	7	0.12	-			CNT / LTD 10	CNT / LTD 30	LTD 10 / LTD30
	+ MßCD-Ch	LTD 10	1.30	7	0.08	9.69E-01	4.21E-03	6.42E-03	2.27E-02	3.60E-02	4.87E-01
		LTD 30	1.74	6	0.14	3.00E-01					
						Shapiro-Wilk	Levene	One way ANOVA		Games-Howell	
		CNT	1.00	9	0.00	-			CNT / LTD 10	CNT / LTD 30	LTD 10 / LTD30
	-	LTD 10	1.03	9	0.12	2.82E-01	4.02E-03	9.18E-01	9.59E-01	9.26E-01	9.87E-01
		LTD 30	1.07	6	0.18	3.91E-01					
Bdnf Transcript VI						Shapiro-Wilk	Levene	One way ANOVA		Games-Howell	
		CNT	1.04	7	0.07	-			CNT / LTD 10	CNT / LTD 30	LTD 10 / LTD30
	+ MßCD-Ch	LTD 10	1.41	7	0.08	1.65E-01	1.74E-04	9.22E-05	5.00E-03	7.00E-03	3.93E-01
		LTD 30	1.59	6	0.11	4.02E-01					

Supp. Table 25: Figure R25

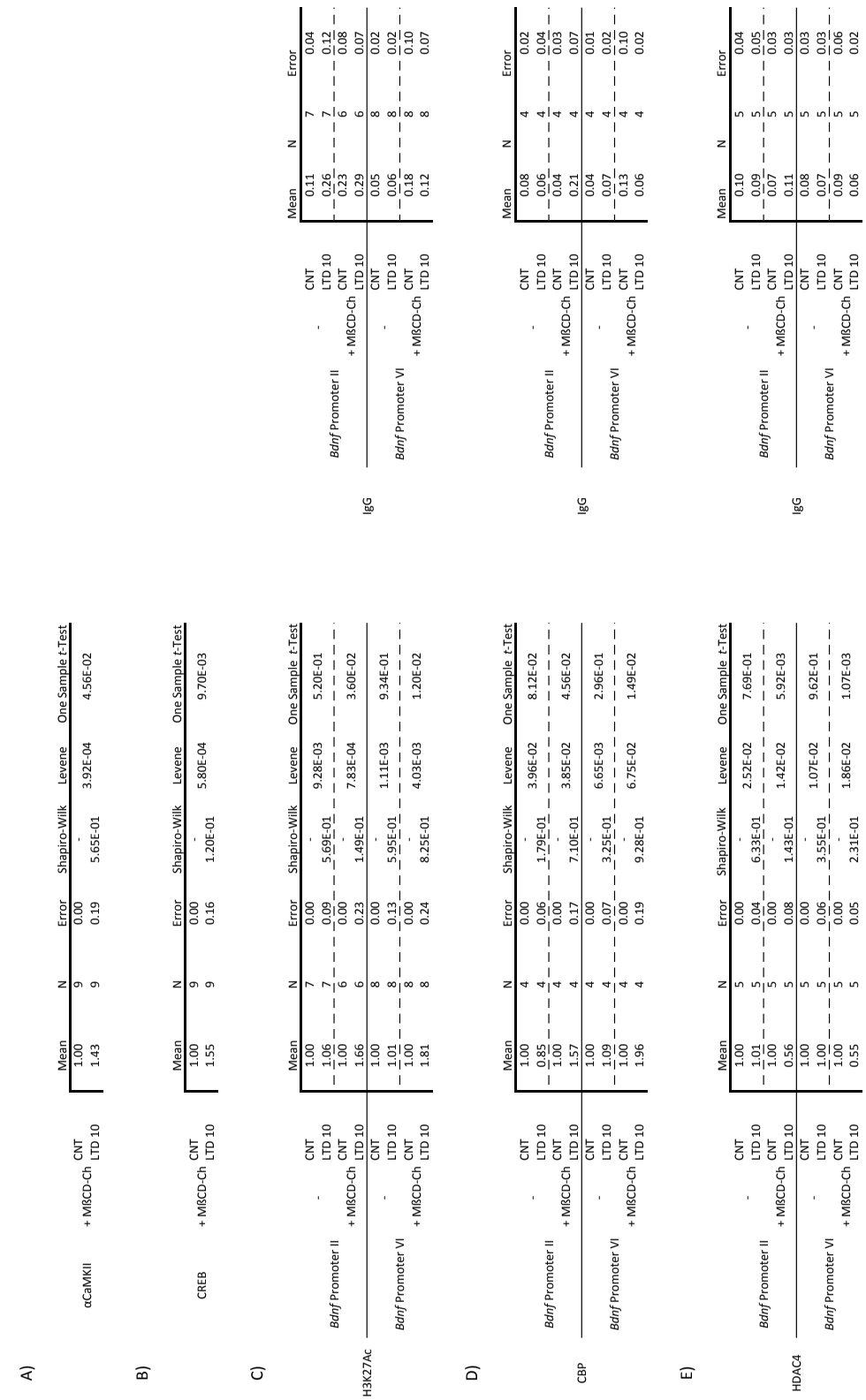

Supp. Table 26: Figure R26

A)

			Mean	N	Error	Shapiro-Wilk	Levene	Student's *t*-Test
Cholesterol Quantification	-		0.10	5	0.00	2.62E-01	8.50E-02	2.50E-05
	+ COase		0.08	5	0.00	4.54E-01		

B)

			Mean	N	Error	Shapiro-Wilk	Levene	One way ANOVA	Games-Howell		
		CNT	1.00	8	0.00	-			CNT / LTD 10	CNT / LTD 30	LTD 10 / LTD30
	-	LTD 10	1.23	8	0.07	5.93E-01	1.55E-02	3.80E-03	3.29E-02	1.48E-02	6.65E-01
		LTD 30	1.36	8	0.08	7.57E-01					
Bdnf Transcript II						Shapiro-Wilk	Levene	One way ANOVA	Games-Howell		
		CNT	1.00	8	0.00	-			CNT / LTD 10	CNT / LTD 30	LTD 10 / LTD30
	+ COase	LTD 10	0.91	8	0.07	5.40E-01	2.99E-02	8.08E-01	9.90E-01	8.54E-01	8.72E-01
		LTD 30	0.99	8	0.08	1.80E-01					
						Shapiro-Wilk	Levene	One way ANOVA	Games-Howell		
		CNT	1.00	8	0.00	-			CNT / LTD 10	CNT / LTD 30	LTD 10 / LTD30
	-	LTD 10	1.41	8	0.10	2.23E-01	1.28E-02	4.15E-03	1.43E-02	2.47E-02	9.94E-01
		LTD 30	1.40	8	0.11	9.43E-01					
Bdnf Transcript VI						Shapiro-Wilk	Levene	One way ANOVA	Games-Howell		
		CNT	1.00	8	0.00	-			CNT / LTD 10	CNT / LTD 30	LTD 10 / LTD30
	+ COase	LTD 10	0.99	8	0.09	9.00E-01	5.06E-05	2.79E-01	3.90E-01	3.01E-01	8.63E-01
		LTD 30	0.95	8	0.13	1.34E-01					

Supp. Table 27: Figure R27

A)

			Mean	N	Error	Shapiro-Wilk	Levene	One Sample *t*-Test
αCaMKII	+ Coase	CNT	1.00	8	0.00	-	8.09E-05	2.15E-01
		LTD 10	0.91	8	0.07	5.98E-01		

B)

			Mean	N	Error	Shapiro-Wilk	Levene	One Sample *t*-Test
CREB	+ Coase	CNT	1.00	8	0.00	-	2.24E-03	8.36E-01
		LTD 10	0.97	8	0.15	5.50E-01		

C)

				Mean	N	Error	Shapiro-Wilk	Levene	Test
CBP	*Bdnf* Promoter II	-	CNT	1.00	5	0.00	-	5.48E-02	One Sample *t*-Test
			LTD 10	1.50	5	0.14	2.37E-01		2.34E-02
		+ COase	CNT	1.00	5	0.00	-	1.57E-03	One Sample *t*-Test
			LTD 10	0.91	5	0.16	4.24E-01		6.10E-01
	Bdnf Promoter VI	-	CNT	1.00	5	0.00	-	4.02E-02	Mann-Whitney
			LTD 10	1.53	5	0.15	2.08E-02		5.35E-03
		+ COase	CNT	1.00	5	0.00	-	1.90E-02	One Sample *t*-Test
			LTD 10	0.91	5	0.09	8.55E-01		3.40E-01

D)

				Mean	N	Error	Shapiro-Wilk	Levene	One Sample T.Test
H3K27Ac	*Bdnf* Promoter II	-	CNT	1.00	5	0.00	-	9.74E-03	3.53E-02
			LTD 10	1.53	5	0.19	5.84E-01		
		+ COase	CNT	1.00	7	0.00	-	1.46E-04	7.55E-01
			LTD 10	0.95	7	0.16	3.37E-01		
	Bdnf Promoter VI	-	CNT	1.00	5	0.00	-	8.93E-04	5.91E-03
			LTD 10	1.50	5	0.14	3.17E-01		
		+ COase	CNT	1.00	7	0.00	-	3.81E-04	7.22E-01
			LTD 10	0.95	7	0.16	4.97E-01		

E)

				Mean	N	Error	Shapiro-Wilk	Levene	Test
HDAC4	*Bdnf* Promoter II	-	CNT	1.00	3	0.00	-	1.06E-01	One Sample *t*-Test
			LTD 10	0.60	3	0.06	1.66E-01		1.91E-02
		+ COase	CNT	1.00	3	0.00	-	3.55E-02	One Sample *t*-Test
			LTD 10	1.13	3	0.11	4.99E-01		3.34E-01
	Bdnf Promoter VI	-	CNT	1.00	4	0.00	-	2.90E-03	Mann-Whitney
			LTD 10	0.49	4	0.10	4.66E-03		2.77E-02
		+ COase	CNT	1.00	4	0.00	-	1.65E-02	One Sample *t*-Test
			LTD 10	0.78	4	0.17	7.29E-02		3.36E-01

				Mean	N	Error
IgG	*Bdnf* Promoter II	-	CNT	0.03	5	0.01
			LTD 10	0.02	5	0.01
		+ COase	CNT	0.01	5	0.01
			LTD 10	0.03	5	0.02
	Bdnf Promoter VI	-	CNT	0.06	5	0.04
			LTD 10	0.08	5	0.07
		+ COase	CNT	0.05	5	0.02
			LTD 10	0.01	5	0.00

				Mean	N	Error
IgG	*Bdnf* Promoter II	-	CNT	0.15	5	0.04
			LTD 10	0.12	5	0.04
		+ COase	CNT	0.15	7	0.05
			LTD 10	0.09	7	0.03
	Bdnf Promoter VI	-	CNT	0.06	5	0.02
			LTD 10	0.04	5	0.02
		+ COase	CNT	0.06	7	0.01
			LTD 10	0.06	7	0.03

				Mean	N	Error
IgG	*Bdnf* Promoter II	-	CNT	0.25	3	0.13
			LTD 10	0.23	3	0.11
		+ COase	CNT	0.10	3	0.08
			LTD 10	0.15	3	0.09
	Bdnf Promoter VI	-	CNT	0.14	4	0.13
			LTD 10	0.08	4	0.06
		+ COase	CNT	0.42	4	0.41
			LTD 10	0.08	4	0.08

Supp. Table 28: Figure R28

		Mean	N	Error	Shapiro-Wilk	Levene	Student's *t*-Test
Cholesterol Quantification	Veh	0.10	7	0.01	6.15E-01	2.68E-01	1.29E-03
	Vori	0.15	8	0.01	3.76E-01		

Supp. Table 29: Figure R29

A)

			Mean	N	Error	Shapiro-Wilk	Levene	One way ANOVA	Games-Howell		
Bdnf Transcript II	Veh	CNT	1.00	10	0.00	-	5.74E-04	6.66E-01	CNT / LTD 10	CNT / LTD 30	LTD 10 / LTD30
		LTD 10	0.89	10	0.12	8.57E-01			6.32E-01	6.66E-01	1.00E+00
		LTD 30	0.89	10	0.12	8.58E-01					
	Vori	CNT	1.00	10	0.00	-	1.09E-04	6.53E-04	CNT / LTD 10	CNT / LTD 30	LTD 10 / LTD30
		LTD 10	1.35	10	0.14	2.28E-01			6.54E-03	1.09E-02	3.60E-01
		LTD 30	1.68	10	0.20	3.36E-01					
Bdnf Transcript VI	Veh	CNT	1.00	10	0.00	-	3.15E-04	9.54E-01	CNT / LTD 10	CNT / LTD 30	LTD 10 / LTD30
		LTD 10	0.97	10	0.08	8.12E-01			9.48E-01	9.51E-01	1.00E+00
		LTD 30	0.97	10	0.09	5.08E-02					
	Vori	CNT	1.00	10	0.00	-	4.26E-05	8.84E-03	CNT / LTD 10	CNT / LTD 30	LTD 10 / LTD30
		LTD 10	1.49	10	0.12	5.69E-01			7.39E-03	3.46E-02	8.13E-01
		LTD 30	1.64	10	0.21	9.91E-01					

B)

			Mean	N	Error	Shapiro-Wilk	Levene	One Sample *t*-Test
H3K27Ac	*Bdnf* Promoter II	Veh CNT	1.00	5	0.00	-	1.72E-03	0.676
		Veh LTD 10	0.91	5	0.20	4.42E-01		
		Vori CNT	1.00	5	0.00	-	2.54E-04	0.046
		Vori LTD 10	2.35	5	0.49	1.94E-01		
	Bdnf Promoter VI	Veh CNT	1.00	6	0.00	-	2.24E-03	0.194
		Veh LTD 10	0.89	6	0.07	5.83E-01		
		Vori CNT	1.00	6	0.00	-	3.51E-02	0.026
		Vori LTD 10	1.64	6	0.20	8.90E-01		

				Mean	N	Error
IgG	*Bdnf* Promoter II	-	CNT	0.057	5	0.007
			LTD 10	0.060	5	0.044
		+ MßCD-Ch	CNT	0.186	5	0.073
			LTD 10	0.097	5	0.047
	Bdnf Promoter VI	-	CNT	0.026	6	0.006
			LTD 10	0.029	6	0.015
		+ MßCD-Ch	CNT	0.080	6	0.017
			LTD 10	0.036	6	0.015

Supp. Table 30: Figure R30

A)

Arc

		Mean	N	Error	Shapiro-Wilk	Levene	One way ANOVA	Games-Howell		
Adult	CNT	1.00	7	0.00	-	3.17E-07	7.21E-06	CNT / LTD 10	CNT / LTD 30	LTD 10 / LTD30
	LTD 10	1.42	7	0.12	3.56E-01			3.28E-04	6.84E-04	7.63E-01
	LTD 30	1.25	6	0.02	5.27E-01					
					Shapiro-Wilk	Levene	One way ANOVA	Games-Howell		
Old	CNT	1.00	7	0.00	-	3.16E-04	3.95E-01	CNT / LTD 10	CNT / LTD 30	LTD 10 / LTD30
	LTD 10	1.17	7	0.10	1.63E-01			5.26E-01	9.22E-01	5.36E-01
	LTD 30	0.92	6	0.12	2.91E-01					
					Shapiro-Wilk	Levene	One way ANOVA	Games-Howell		
Old + Veh	CNT	1.00	10	0.00	-	3.19E-03	9.78E-01	CNT / LTD 10	CNT / LTD 30	LTD 10 / LTD30
	LTD 10	1.01	10	0.10	3.38E-01			9.68E-01	9.86E-01	9.99E-01
	LTD 30	1.03	10	0.13	2.80E-01					
					Shapiro-Wilk	Levene	One way ANOVA	Games-Howell		
Old + Vori	CNT	1.00	10	0.00	-	1.48E-03	2.12E-02	CNT / LTD 10	CNT / LTD 30	LTD 10 / LTD30
	LTD 10	1.58	10	0.27	2.80E-01			4.69E-02	4.27E-02	9.35E-01
	LTD 30	1.73	10	0.29	1.40E-01					

B)

Ppp1cc

		Mean	N	Error	Shapiro-Wilk	Levene	One way ANOVA	Games-Howell		
Adult	CNT	1.00	7	0.00	-	2.84E-04	2.21E-05	CNT / LTD 10	CNT / LTD 30	LTD 10 / LTD30
	LTD 10	1.33	7	0.06	5.51E-01			2.72E-03	1.57E-03	9.69E-01
	LTD 30	1.32	6	0.04	4.93E-01					
					Shapiro-Wilk	Levene	One way ANOVA	Games-Howell		
Old	CNT	1.00	7	0.00	-	1.36E-03	1.79E-01	CNT / LTD 10	CNT / LTD 30	LTD 10 / LTD30
	LTD 10	1.11	7	0.08	9.93E-01			4.85E-01	6.01E-01	2.96E-01
	LTD 30	0.97	6	0.06	9.99E-01					
					Shapiro-Wilk	Levene	One way ANOVA	Games-Howell		
Old + Veh	CNT	1.00	7	0.00	-	5.20E-02	2.80E-01	CNT / LTD 10	CNT / LTD 30	LTD 10 / LTD30
	LTD 10	0.90	7	0.06	3.13E-01			2.55E-01	3.29E-01	9.81E-01
	LTD 30	0.88	7	0.07	2.35E-01					
					Shapiro-Wilk	Levene	One way ANOVA	Games-Howell		
Old + Vori	CNT	1.00	8	0.00	-	1.37E-02	1.58E-04	CNT / LTD 10	CNT / LTD 30	LTD 10 / LTD30
	LTD 10	1.21	8	0.08	4.37E-01			3.14E-02	5.30E-03	1.18E-01
	LTD 30	1.32	8	0.14	6.38E-01					

Supp. Table 31: Figure R31

A)

		Mean	N	Error	Shapiro-Wilk	Levene	Student's *t*-Test
Object location memory test	Veh	0.60	13	0.04	3.37E-01	2.90E-02	4.40E-02
	Vori	0.72	11	0.04	4.92E-01		

B)

			Mean	N	Error	Shapiro-Wilk	Levene	Friedman Tests	
Spatial learneing	Day 1	Veh	66.73	13	6.29	1.57E-01	2.68E-01	Treatments	Interaction
		Vori	68.58	11	5.36	4.16E-01			
	Day 2	Veh	62.46	13	6.99	1.90E-02	5.70E-02	Veh	
		Vori	56.55	11	5.22	7.97E-01		4.20E-02	
	Day 3	Veh	55.15	13	5.69	9.94E-01	9.60E-01		1.50E-01
		Vori	52.13	11	5.90	2.70E-02		Vori	
	Day 4	Veh	51.40	13	5.11	3.51E-01	6.50E-01	4.00E-03	
		Vori	45.00	11	6.42	5.86E-01			

C)

		Mean	N	Error	Shapiro-Wilk	Levene	Student's *t*-Test
Spatial memory test	Veh	27.13	13	3.00	6.51E-01	1.16E-01	3.46E-02
	Vori	39.53	11	4.91	8.68E-01		

D)

		Mean	N	Error	Shapiro-Wilk	Levene	Student's *t*-Test
Contextual fear conditioning test	Veh	24.35	13	4.87	5.16E-02	2.42E-01	1.14E-02
	Vori	48.28	12	7.37	8.75E-01		

E)

			Mean	N	Error	Shapiro-Wilk	Levene	Mann-Whitney
Auditory-cued fear conditioning test	pre-tone	Veh	2.18	13	0.79	2.45E-03	4.13E-01	1.64E-01
		Vori	3.88	12	0.93	2.97E-01		
			Mean	N	Error	Shapiro-Wilk	Levene	Student's *t*-Test
	post-tone	Veh	12.41	13	2.26	2.00E-01	8.59E-02	2.97E-01
		Vori	17.22	12	4.01	1.34E-01		

Supp. Table 31: Figure D2

A)

		Mean	N	SEM
CDYL	*Bdnf* Promoter I	0.05	4	0.005
	Bdnf Promoter II	0.10	4	0.005
	Bdnf Promoter IV	0.03	4	0.006
	Bdnf Promoter VI	0.03	4	0.005

		Mean	N	SEM
IgG	*Bdnf* Promoter I	0.030	4	0.008
	Bdnf Promoter II	0.013	4	0.003
	Bdnf Promoter IV	0.019	4	0.003
	Bdnf Promoter VI	0.017	4	0.005

B)

Bonferroni adjustment	95% confidence interval	99% confidence interval	99.9% confidence interval
	(*) p < 1.67E-02	(**) p < 3.33E-03	(***) p < 3.33E-04

			Mean	N	SEM	Kruskal-Wallis Test	Mann-Whitney U Test		
							Control / LTD 10	Control / LTD 30	LTD10 / LTD 30
CDYL	*Bdnf* Promoter II	CNT	1.00	4	0.00	2.18E-02	1.39E-02	1.39E-02	1.00E+00
		LTD 10	0.46	4	0.12				
		LTD 30	0.48	4	0.01				

			Mean	N	SEM
IgG	*Bdnf* Promoter II	CNT	0.14	4	0.03
		LTD 10	0.23	4	0.07
		LTD 30	0.20	4	0.08

C)

Bonferroni adjustment	95% confidence interval	99% confidence interval	99.9% confidence interval
	(*) p < 1.67E-02	(**) p < 3.33E-03	(***) p < 3.33E-04

		Mean	N	SEM	Kruskal-Wallis Test	Mann-Whitney U Test		
						Control / LTD 10	Control / LTD 30	LTD10 / LTD 30
CDYL	CNT	1.00	5	0.00	3.66E-03	5.35E-03	5.35E-03	7.58E-02
	LTD 10	0.73	5	0.09				
	LTD 30	0.50	5	0.09				

NOTES